JBC REVIEWS

⌘ Author's Choice

Role of the lipid bilayer in outer membrane protein folding in Gram-negative bacteria

Received for publication, February 4, 2020, and in revised form, June 3, 2020 Published, Papers in Press, June 4, 2020, DOI 10.1074/jbc.REV120.011473

Jim E. Horne[1,2], **David J. Brockwell**[1], **and Sheena E. Radford**[1,*]

From the [1]*Astbury Centre for Structural Molecular Biology, School of Molecular and Cellular Biology, Faculty of Biological Sciences, University of Leeds, Leeds, United Kingdom and the* [2]*Department of Biochemistry, University of Oxford, Oxford, United Kingdom*

Edited by Karen G. Fleming

β-Barrel outer membrane proteins (OMPs) represent the major proteinaceous component of the outer membrane (OM) of Gram-negative bacteria. These proteins perform key roles in cell structure and morphology, nutrient acquisition, colonization and invasion, and protection against external toxic threats such as antibiotics. To become functional, OMPs must fold and insert into a crowded and asymmetric OM that lacks much freely accessible lipid. This feat is accomplished in the absence of an external energy source and is thought to be driven by the high thermodynamic stability of folded OMPs in the OM. With such a stable fold, the challenge that bacteria face in assembling OMPs into the OM is how to overcome the initial energy barrier of membrane insertion. In this review, we highlight the roles of the lipid environment and the OM in modulating the OMP-folding landscape and discuss the factors that guide folding *in vitro* and *in vivo*. We particularly focus on the composition, architecture, and physical properties of the OM and how an understanding of the folding properties of OMPs *in vitro* can help explain the challenges they encounter during folding *in vivo*. Current models of OMP biogenesis in the cellular environment are still in flux, but the stakes for improving the accuracy of these models are high. OMP folding is an essential process in all Gram-negative bacteria, and considering the looming crisis of widespread microbial drug resistance it is an attractive target. To bring down this vital OMP-supported barrier to antibiotics, we must first understand how bacterial cells build it.

Proteins that span lipid bilayers come in two types, either α-helical or β-barrels. Whereas the cytosolic inner membranes (IMs) of bacteria and the plasma membrane of eukaryotes are comprised only of α-helical membrane proteins, β-barrel outer membrane proteins (OMPs) are found exclusively in the outer membranes (OMs) of diderm bacteria as well as in bacterially derived eukaryotic organelles, such as mitochondria and chloroplasts. The "OMPome" (the complement of OMPs encoded for by a genome) of *Escherichia coli* consists of a large number of proteins ranging in barrel size from 8 to 26 β-strands and includes monomers, small assemblies (dimers, trimers etc.), and oligomeric structures that can form up to 60-stranded pores (Fig. 1). Some OMPs comprise only the integral membrane β-barrel structure, whereas others have soluble domains in the periplasm or on the extracellular surface of the OM. Some OMPs have low copy number or can be absent in the OM under "standard" growth conditions (*e.g.* the *E. coli* porin OmpN) (1–4), and others are present in large copy number (*e.g.* OmpA is estimated to have >100,000 copies in the OM of *E. coli*, whereas OmpX, OmpC, and OmpF are estimated to have >20,000 copies each) (3–7). The functions of OMPs are also very diverse, including passive pores and ion channels (8–11), antibiotic efflux channels (12–15), nutrient uptake systems (16–18), maintenance of structural integrity (19–21), biogenesis and upkeep of the OM (22–26), host cell adhesion and invasion (27–29), biofilm formation (30–33), and cell defense (34, 35). Despite the enormous diversity of OMPs in *E. coli*, it is perhaps surprising that only two are essential: the 16-stranded BamA and 26-stranded LptD (36) (Fig. 1). This is perhaps even more remarkable considering that LptD itself relies on BamA for its assembly (37). LptD's biological role is to insert the lipid component of the outer leaflet of the OM (22, 38). BamA (part of the β-barrel assembly machinery, BAM) is required to fold and insert most (but not all) OMPs into the OM *in vivo* (39) (Table 1). The importance of BAM for the biogenesis of the OM is illustrated by the observation that despite the evolutionary distance between bacteria and eukaryotes, a homologue of BamA, Sam50, is retained in all mitochondria (70). Although only BamA and LptD are essential in *E. coli* under laboratory conditions, it is likely that many more OMPs will be necessary for bacteria to survive, invade new niches, and thrive in diverse environments. Understanding how OMPs fold has been the goal of researchers for approximately the last 3 decades, since the first observations were made that OMPs are capable of folding spontaneously into reconstituted lipid bilayers (71). Initially, the study of the structure and folding mechanisms of OMPs lagged behind those of their α-helical membrane protein counterparts, because the latter are more abundant in eukaryotes and were considered, initially at least, to be more important from the perspective of human health, as half of all approved drugs target α-helical membrane proteins (72, 73). However, in the last 15 years, it has become clear that OMPs are ubiquitous, and some are essential in bacteria (*i.e.* BamA and LptD) or in mitochondria (*i.e.* Sam50 and Tom40) (22, 23, 74–77). Furthermore, the growth in antibiotic-resistant pathogens has highlighted the importance of the OM as a formidable barrier to the entry of antibiotics into bacteria as well as a site of efflux out (78) and as a shield against recognition of surface

This article contains supporting information.

* For correspondence: Sheena E. Radford, s.e.radford@leeds.ac.uk.

epitopes by natural or designed antibodies (79–82). Hence, insights gained from studies of OMP folding and biogenesis are also vital for our understanding of human physiology (83) and will be key in guiding our choice of targets for the generation of new antibiotics and vaccines against Gram-negative bacteria (84). Consequently, a number of academic groups and drug

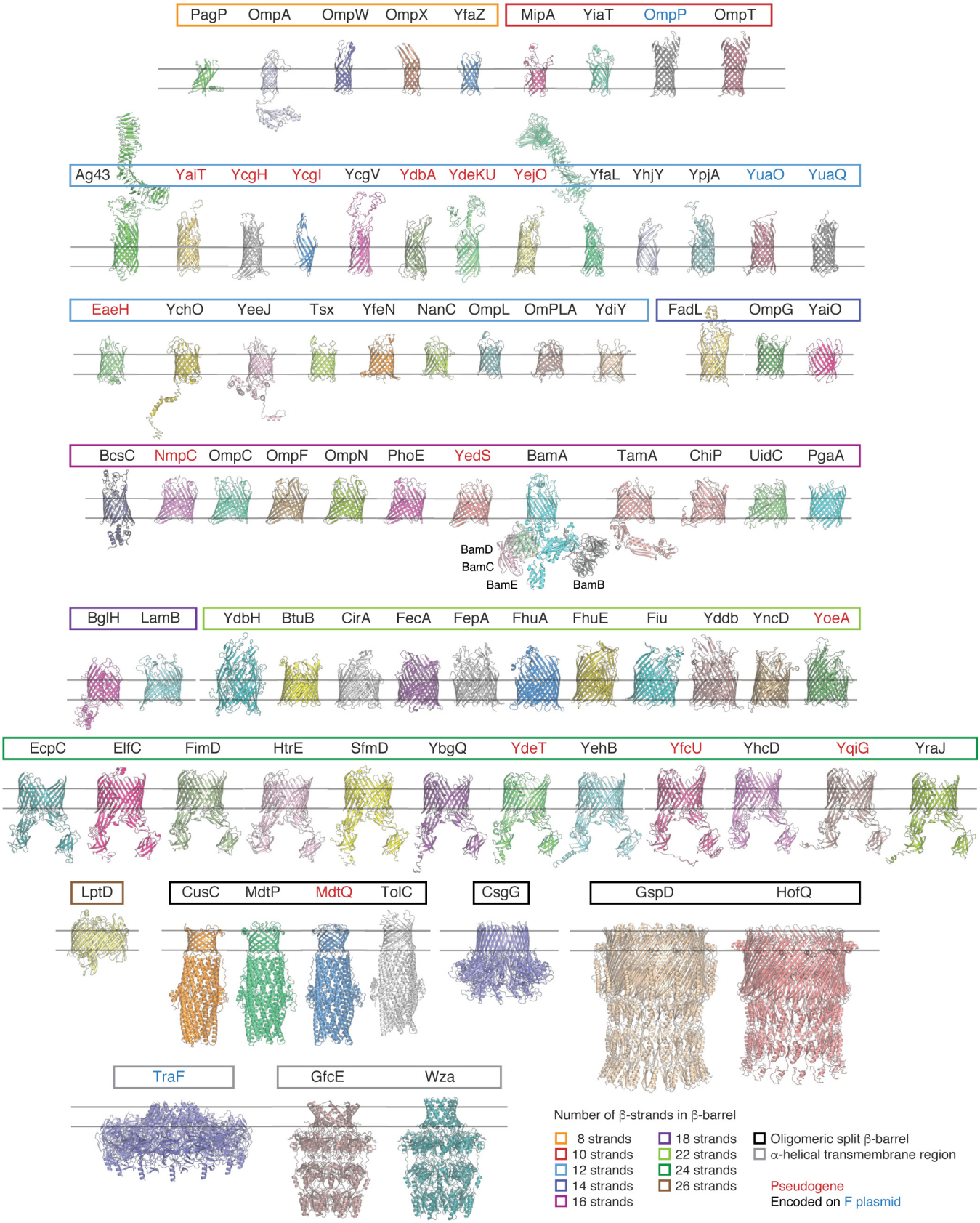

companies have ongoing research projects targeting the essential OMPs BamA (the central β-barrel-containing subunit of BAM) and LptD (80, 82, 85–92), with at least six reports of inhibitors of their function in 2018-2019 alone (93–98).

This review aims to provide a holistic view of our current understanding of the process of OMP biogenesis, including 1) the composition and physical and chemical properties of the OM *in vivo*; 2) current knowledge of the determinants of OMP folding through *in vitro* studies; and 3) how OMP folding depends on parameters such as the lipid composition, physical environment, and the presence/absence of BAM. Although information is drawn from different organisms, we focus on OMPs and the OM of *E. coli* because of the position of this bacterium as the *de facto* model organism for studying these processes.

Another brick in the wall: Building the OM

To understand OMP folding and biogenesis, it is first important to review our current understanding of the composition and architecture of the environment in which this process takes place: the complex and crowded bacterial OM.

Lipid types found in the OM

The OM of Gram-negative bacteria is unusual in that it is a highly asymmetric lipid bilayer, comprising an inner leaflet enriched in phospholipids and an outer leaflet containing lipopolysaccharide (LPS) (Fig. 2) (99). This is in contrast to the IM in Gram-negative and Gram-positive bacteria, which mostly contain phospholipids mixed between both leaflets. In Gram-negative bacteria, phospholipids in the OM generally have the canonical structure expected of a phospholipid, containing two hydrophobic acyl chains, with different length and degree of saturation. These are connected via an ester linkage to a headgroup that can be zwitterionic, or positively or negatively charged (Fig. 2). Cardiolipin (CL) is also found in the OM and has the appearance of a phospholipid dimer (Fig. 2). LPS is a much bulkier molecule, made up of a variable number of acyl chains (between 4 and 8, depending on the species) (100). The acyl chain can vary in length both within each molecule and between species (*e.g.* $C_{10:0}$–$C_{14:0}$ in *Bordetella pertussis*, $C_{12:0}$–$C_{14:0}$ in *E. coli*, $C_{14:0}$–$C_{21:0}$ in *Chlamydia trachomatis*, and $C_{14:0}$–$C_{28:0}$ in *Agrobacterium tumefaciens*) (101–104). Furthermore, the acyl chains of LPS are usually shorter than those of the average phospholipid and are almost always saturated (105) (Fig. 2). The acyl chains in LPS are connected to a disaccharide diphosphate headgroup, which in turn is connected to a conserved "core" region made up of chained sugar groups, and then finally a highly variable sugar-containing O-antigen region (Fig. 2) (106, 107). Together, these sugar regions convey a large net negative charge to the outer surface of bacteria (107).

Essentiality of specific lipids

E. coli is remarkably tolerant of modifications in its lipid biosynthesis pathways, with viable strains including bacteria in which synthesis of phosphatidylethanolamine (PE) (108, 109), phosphatidylglycerol (PG) and CL (110, 111), or CL alone (109, 112) is eliminated (see Fig. 2 for the structure of common lipid types); phosphatidylcholine (PC) synthesis is induced synthetically (*E. coli* lacks PC in its IM or OM, although this phospholipid is present in some bacterial membranes) (113, 114); gluco- or galactolipids are utilized (115); or even archaeal lipids are incorporated into the membrane (116). Although these strains are able to survive under laboratory conditions, their growth and virulence are affected (in some cases severely), stress responses are up-regulated, and defects of varying acuteness are seen in the structure and permeability of the cell envelope (109, 117). The effect of such changes in lipid composition in the OM on OMP biogenesis has not been investigated in detail for all of these strains. However, in PE-deficient strains, OmpF folding is impaired in a titratable manner, with complete lack of PE reducing folding yields from ~100% in WT to <15% (109). Lack of CL causes less severe defects but still reduces OmpF folding yields to ~25% (109) and has also been shown to cause mislocalization of the OMP IcsA, which normally resides at the cell pole in *Shigella flexneri* (117). Interestingly, in *E. coli*, lack of CL causes severe distention/detachment of the OM from the IM at the cell poles, and CL and PG have been observed to accumulate at cell poles and division sites (118), suggesting a role for CL in maintaining cell shape and integrity at sites of negative curvature (119). PG null only mutants have not been described, as CL utilizes PG for its biosynthesis. However, the creation of viable strains absent in PG synthesis also requires mutations in the major *E. coli* OM lipoprotein Lpp (Braun's lipoprotein), suggesting that lack of PG causes lethality primarily though lethal accumulation of Lpp at the IM (111, 120). The first step in lipoprotein maturation after translocation into the periplasm involves the transfer of a diacyl moiety from PG (121), and its absence presumably stalls maturation at this point. However, the OM lipoproteins LptE and BamD are essential in *E. coli*, so the viability of these *lpp* mutant strains suggests that alternate maturation pathways or sources of diacylglycerol must exist (122, 123). As BamA and LptD are essential OMPs, the fact that bacteria can still grow and divide in these strains (albeit poorly) suggests that other lipids can

Figure 1. Structures of transmembrane proteins found in the OM of *E. coli* K-12 MG1655. A list of all known and predicted transmembrane proteins in the OM of *E. coli* K-12 strain MG1655 was manually curated, creating the "OMP-ome." The Protein Data Bank was then searched for solved structures of these proteins or close homologues. Where no high-resolution solved 3D structures were available, homology models were generated using the I-TASSER server (RRID:SCR_014627) (396). For two proteins, NfrA (the N4 bacteriophage receptor), and FlgH (the flagellar L-ring protein), no homology models could be generated. Predictions for YaiO, YcgI, YdbH, and YhjY generated deformed or broken barrels (possibly due to a lack of homology to existing structures), but their predictions are displayed to indicate their approximate structure. Extracellular domains of autotransporters have only been shown where accurate models could be built or crystal structures were available. OMPs are grouped here by the number of β-strands and then by protein family. The non-OMP subunits of the BAM complex are labeled *below* the central BamA subunit. Protein names are in *red* if they represent pseudogenes (inactivated by mutation in this strain) and *blue* if they are encoded on the F plasmid. The *color* of the *box* surrounding the protein names represents the number of β-strands in the β-barrel. *Light Orange*, 8; *red*, 10; *light blue*, 12; *violet*, 14; *pink*, 16; *purple*, 18; *light green*, 22; *dark green*, 24; *brown*, 26; *black*, oligomeric split β-barrel; *gray*, α-helical transmembrane region. Structures were aligned with each other by their β-barrel domains and rendered individually in PyMOL 2.X (Schrödinger, LLC). A list of the proteins with their associated family and PDB code can be found in Table S1.

Table 1

Summary of BAM-dependent and BAM-independent OMPs in the OM of different bacteria

Listed are studies that present evidence a link is present (BAM catalysis–involved) or absent (BAM-independent folding) between the biogenesis of a particular OMP and the presence of the BAM complex. This list includes *in vivo* studies and *in vitro* folding studies performed with polar lipid extract from *E. coli*.

OMP(s)	Family	No. of β-strands	Organism	Reference
BAM catalysis–involved				
OmpA, OmpX, OmpT, OmPLA, OmpG	*Varied small barrels*	8–14	*E. coli*[a]	Refs. 40–46
Various	Autotransporters	12	*E. coli*	Refs. 46–52
OprD	Outer membrane porin	18	*P. aeruginosa*	Ref. 53
LamB	Sugar porin	18	*E. coli*	Refs. 54, 55
Various	TonB-dependent receptors	22	*Caulobacter crescentus*	Refs. 56, 57
TolC	Outer membrane factor	3 × 4 (12)	*E. coli*	Ref. 58
FimD[b]	Fimbrial usher	24	*E. coli*	Ref. 59
LptD	LPS assembly	26	*E. coli*	Refs. 37, 54, 60–62
PilQ[b]	Type IV pilus secretin	14 × 4 (56)	*Neisseria meningitidis*	Refs. 23, 63
BAM-independent folding				
PulD[b], XcpQ[b], GspD[b]	T2SS secretin	15 × 4 (60)	*Klebsiella oxytoca, P. aeruginosa, E. coli*	Refs. 64–67
pIV[b]	Phage secretin	?	Phage f1	Refs. 68, 69
CsgG[b,c]	Curli secretion	9 × 4 (36)	*E. coli*	Ref. 67

[a] These studies were all performed *in vitro*.
[b] These proteins are often assembled as part of larger protein machineries or export/import pathways and may also include their own targeting and assembly factors.
[c] Also contains an N-terminal lipid anchor.

moonlight for the loss of PE, PG, or CL or that there is no absolute need for a particular phospholipid type as a minimum requirement for OMP biogenesis in *E. coli*. Nonetheless, the severe defects observed in these strains show that outside the laboratory, all of these components are needed for bacterial viability. This highlights that whereas a stable bilayer is the minimum requirement to fold an OMP, to understand how OMP biogenesis occurs in biologically relevant environments, consideration of the complexity of the OM environment is crucial.

Organization of lipid types within the OM

The *E. coli* OM contains PE, PG, CL, and LPS (Fig. 2). These lipid types are divided asymmetrically between the inner and outer leaflets of the OM, with the outer leaflet containing almost 100% LPS and the inner leaflet containing ~80% PE, ~15% PG, and ~5% CL (Figs. 2 and 3). By contrast, the IM also contains ~5% CL with a lower ratio of PE/PG of ~70%/25% (124). Although it is physically possible for phospholipids to flip from the inner leaflet to the outer leaflet, this process is likely to be intrinsically slow (occurring on the order of hours or longer in vesicles *in vitro*) (125, 126). However, this process may be accelerated under conditions of OM/bilayer stress, such as exposure to antimicrobial peptides or detergents, in strains with truncated LPS (see Fig. 2), or after loss of OMPs (78, 127–129). This process is therefore associated with increased permeability of the OM. Regardless of such events, the asymmetry of the OM is actively maintained in *E. coli* by the maintenance of lipid asymmetry (Mla) system, which removes errant phospholipids specifically from the outer leaflet of the OM to maintain its barrier function (130–132).

The lipid acyl chain composition is diverse

The acyl chain composition of lipids in the OM of *E. coli* is more variable than that of their headgroups. The acyl chain composition of the OM depends on the growth conditions, with acyl chains varying in length from C_{12} to C_{18}, as well as in the degree of saturation or the presence of cyclopropyl modifications (Fig. 2) (133–138). Lipidomics has provided insights into the range of acyl groups found in *E. coli* membranes. Early experiments in *E. coli* K1062 reported the presence of $C_{12:0}$, $C_{14:0}$, $C_{16:0}$, $C_{16:1}$, $C_{18:1}$, and cyclo-$C_{19:0}$ acyl chains in phospholipids from the IM and OM (139). Examining total lipid content in *E. coli* K-12 strain LM3118 grown at 37 °C and harvested in stationary phase showed that the acyl chains of PE and PG lipids were comprised primarily of $C_{12:0}$, $C_{14:0}$, $C_{16:0}$, $C_{16:1}$, $C_{18:0}$, and $C_{18:1}$ (with $C_{16:0}$ being about 3 times more abundant than the other acyl chains), with a lesser contribution from $C_{15:0}$, cyclo-$C_{17:0}$, and cyclo-$C_{19:0}$ (140, 141). These acyl chains are combined to form a large variety of phospholipid types, most containing at least one unsaturated acyl bond or cyclopropyl group, although *di*$C_{16:0}$PE, *di*$C_{16:0}$PG, $C_{16:0}C_{14:0}$PG, $C_{16:0}C_{12:0}$PE, *di*$C_{14:0}$PE, and *di*$C_{12:0}$PE lipids were also observed. Despite cyclo-propyl acyl chain–containing lipids being relatively understudied, the most common lipid species detected under these conditions was $C_{16:0}$/cyclo-$C_{17:0}$ (Fig. 2). Cyclo-propyl–containing lipids are produced in large quantities in stationary phase cultures from the conversion of double bonds in unsaturated chains to cyclo-propyl groups (142, 143). Although the physiological functions of these modifications are unclear, they appear to be related to protection of the bacteria against a variety of adverse environmental conditions (143), including acid shock (144, 145), osmotic shock (146), high alcohol concentrations (147), or high temperature (148). Furthermore, OMP folding in *E. coli* occurs primarily during exponential growth (56, 149), while expression is down-regulated (150, 151) and OMPs are lost from the OM (152) when bacteria enter stationary phase. Thus, the relevance of this lipid modification for OMP biogenesis may be minor under favorable growth conditions.

Few studies have examined whether significant differences or biases exist between the acyl chain composition of phospholipids in the IM and those of the OM of Gram-negative bacteria. Some have reported an enrichment of shorter acyl chains ($C_{12:0}$ and $C_{14:0}$) (139), saturated fatty acids (153), lyso-PE lipids (154), and $C_{16:0}$ acyl chains in the OM and a depletion of polyunsaturated acyl chains (155). These biases, however, generally vary with growth conditions, and it is unclear to what extent this simply reflects the presence of the lipid A component of the outer leaflet. Regulatory systems that alter the acyl chain

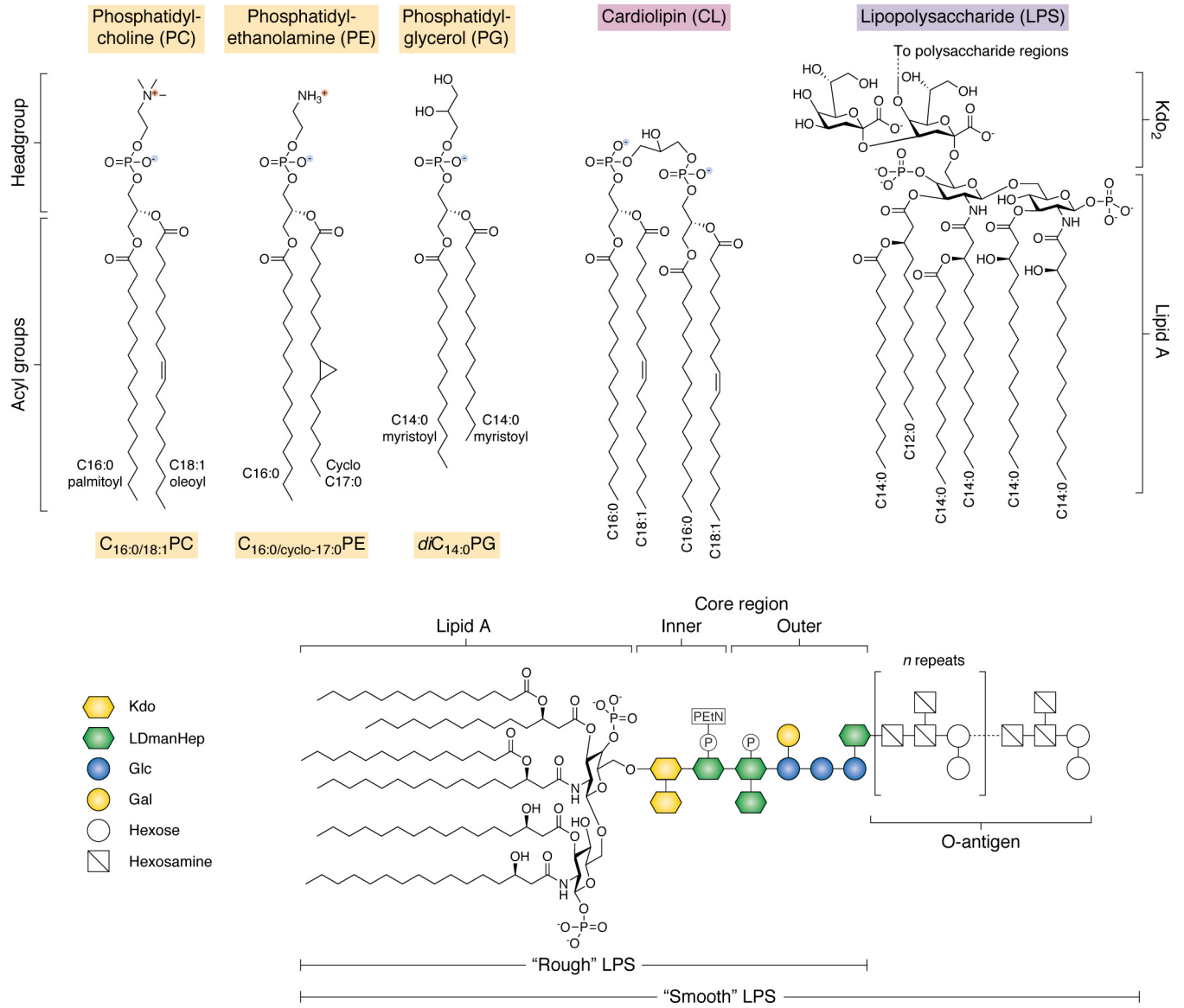

Figure 2. Common lipid types found in bacterial outer membranes and/or used in *in vitro* studies of OMP folding. *Top*, schematic of the generic structure of phospholipids and LPS. Bacterial lipids can be conceptualized as having two "domains": a polar headgroup and a hydrophobic acyl tail region. In phospholipids, the acyl tails are connected by an ester linkage to a phosphate group and a variable headgroup region. PC and PE are zwitterionic, whereas PG carries a net negative charge. Note that PC lipids are not commonly found in bacterial membranes but are often used for OMP folding-studies *in vitro* due to their net neutral charge and propensity to form bilayers. Cardiolipin comprises two acyl tail regions connected by phosphate groups via a glycerol linkage and carries a net double negative charge. LPS is found exclusively in the OM of Gram-negative bacteria and varies considerably between species in both the number and length of acyl tails in the lipid A region and the sugar composition in the polysaccharide region (shown *below*). Here the most common structure of lipid A-Kdo_2 for *E. coli* K-12 LPS is shown in full. *Bottom*, the architecture of a generic LPS is shown. The lipid A and core region are consistent with LPS found in *E. coli* K-12; however, this strain does not naturally produce an O-antigen, whereas many environmental and clinical strains do. Strains lacking the O-antigen region are said to contain "rough" LPS, and this can further be divided into subtypes dependent on truncations in the core region. The most extreme of these that is still viable at 37 °C under laboratory growth conditions is "deep rough" LPS, containing only lipid A-Kdo_2. The O-antigen region is highly variable within species and can contain as many as 40 glycan repeats. *Kdo*, keto-deoxyoctulosonate; *LDmanHep*, L-glycero-D-manno-heptose; *Glc*, glucose; *Gal*, galactose; *P*, phosphate group; *PEtN*, phosphorylethanolamine.

composition of lipids specific to the OM are known for LPS, including enzymes that alter the acyl chains attached to lipid A to modulate the endotoxicity of this lipid type during growth in a host (99). Modulation of the acyl chain content of lipid A has also been shown to occur in *E. coli* when under selective pressure from an external insult by the addition of a bactericidal BamA-specific antibody. This suggests a direct link between modulation of lipid content and a selective pressure to efficiently fold OMPs (93). However, it is not clear whether this change in lipid A reflects a need to aid the function of an essential BAM client (*e.g.* LptD), is related to conformational changes in BamA, or is simply a response to a defective permeability barrier.

This diversity of acyl chain types gives *E. coli* a wide range of lipids with which it can tailor the biophysical properties of its membranes both globally and locally. This variety may allow it to deal with local minor deformations of the membrane, due to either random thermal fluctuations or the presence of membrane-bound or embedded proteins, as acyl chains can diffuse

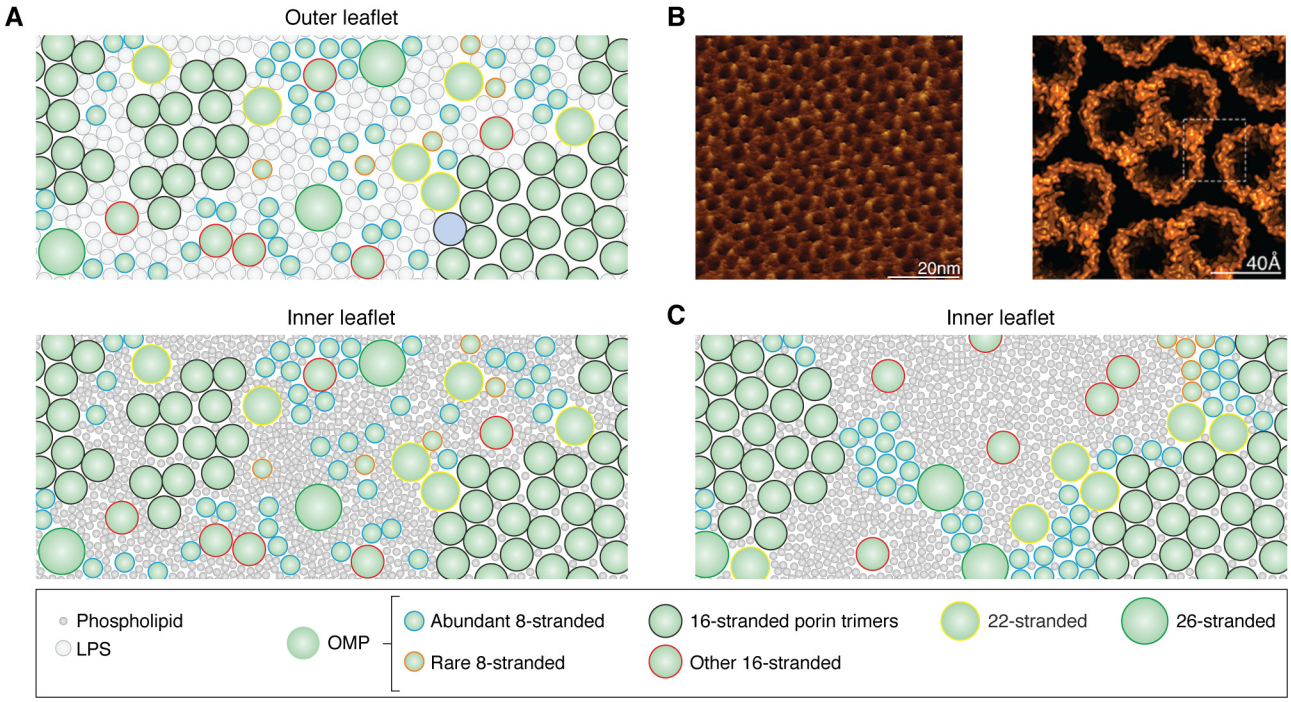

Figure 3. Model depicting the structural organization of the *E. coli* OM. A schematic displays the degree of crowding in the OM. *A*, view of an imagined OM showing the dense packing of different size OMPs in monomers, dimers, and trimers interspersed with LPS in the outer leaflet (*top*) and phospholipids in the inner leaflet (*bottom*). Phospholipids are represented as *dark gray circles* with a diameter proportional to the headgroup size of PE/PG and LPS as *light gray circles* with a diameter proportional to the size of lipid A. Different OMPs are represented as *idealized circles* with diameters proportional to their number of strands. *Blue outline*, abundant 8-stranded; *orange outline*, rare 8-stranded; *black*, 16-stranded porin trimers; *red*, other 16-stranded; *yellow*, 22-stranded; *green*, 26-stranded. The overall LPR in this schematic is ~9:1, with ~2 LPS and ~7 phospholipids per OMP, consistent with estimates for the LPR of the *E. coli* OM. *B*, *left*, high-resolution AFM image of OM extracts from *Roseobacter dentrificans* imaged from the periplasmic side showing a dense lattice of porin trimers. *Right*, atomic model of the packing of porin trimers derived from the AFM data. Reproduced with permission from Jarosøawski *et al.* (156). This research was originally published in Molecular Microbiology. Jarosøawski, S., Duquesne, K., Sturgis, J. N., and Scheuring, S. High-resolution architecture of the outer membrane of the Gram-negative bacteria *Roseobacter denitrificans*. *Molecular Microbiology* 2009; 74:1211–1222. © Wiley–Blackwell. *C*, view of an imagined OM with the same LPR as in *A* but assuming a more extreme clustering of most OMPs. Only the inner leaflet is shown. Despite having the same LPR values, the buried surface area of the clustered OMPs frees up more lipid to form larger bulk lipid domains.

laterally and occupy the most energetically favorable position, dependent on the match between their own physicochemical properties (length and saturation) and those of the membrane environment.

A crowded environment

Although the familiar fluid-mosaic model of membranes found in most textbooks depicts a biological membrane with just a few proteins floating in a "sea" of lipid, the OM is markedly different, containing instead a much higher fraction of protein by weight, with lipid/protein ratios (LPRs) (w/w) estimated to be between 0.14 and 0.36 (139, 156), corresponding to only 2–4 LPS and 4–10 phospholipid molecules per OMP (157). Estimates based on biochemical studies suggest that as much as 50% of the surface area of the OM may be occupied by OMPs (7), whereas AFM studies (156) (Fig. 3*B*), extrapolation from the copy numbers of OMPs measured by proteomics (3, 4), and the above measurements of the LPR suggest that this value may be even higher. For example, a copy number of 100,000 for OmpA would imply that ~6–20% of the surface area of *E. coli* (dependent on the size of the bacterium) would be occupied by this protein alone. Hence, the OM could be considered more like a protein-rich layer solubilized in a relatively small amount of lipid (Fig. 3, *A* and *B*). Despite the low LPR of the OM, the diffusion rates of OMPs in the OM of *E. coli* are similar to those of inner membrane proteins (IMPs) but are, on average, slower (diffusion coefficients of 0.006–0.15 $\mu m^2/s$ for OMPs *versus* 0.001–0.4 $\mu m^2/s$ for IMPs) (56, 158–170) (Fig. 4*A*). For comparison, the length elongation rate of *E. coli* alone is ~0.006 $\mu m/s$ (171), whereas the diffusion coefficients of LPS in the OM of *Salmonella typhimurium* are ~0.00005 and 0.02 $\mu m^2 s^{-1}$ (for O-antigen–containing and truncated "deep rough" LPS, respectively (Fig. 2)) (172, 173), lipid probes in the IM of *E. coli* ~0.8-1.5 $\mu m^2/s$ (162, 174, 175), and the periplasm, cytoplasm, and buffer ~3, 0.4-9, and ~87 $\mu m^2/s$, respectively (159, 168, 176–180) (Fig. 4*B*). What particularly distinguishes OMPs from IMPs is their restricted diffusion areas, with diffusion being confined within clusters in the OM, compared with free diffusion of most IMPs in the IM (56, 166, 181, 182). These observations can be explained by the propensities of OMPs to form clusters (56, 149, 156, 181–188) and/or to interact strongly with LPS or components of the cell envelope (189, 190). OMPs that have a lower tendency to cluster and/or interact with cell envelope components less strongly may exhibit higher diffusion coefficients but will ultimately become "corralled" within OMP-LPS domains. On this point, an abundance of clustered OMPs with low mobility may make the OM locally rigid. Indeed, molecular dynamics (MD) simulations have shown that membranes containing 8–12-stranded OMPs are much stiffer than membranes containing only DMPC

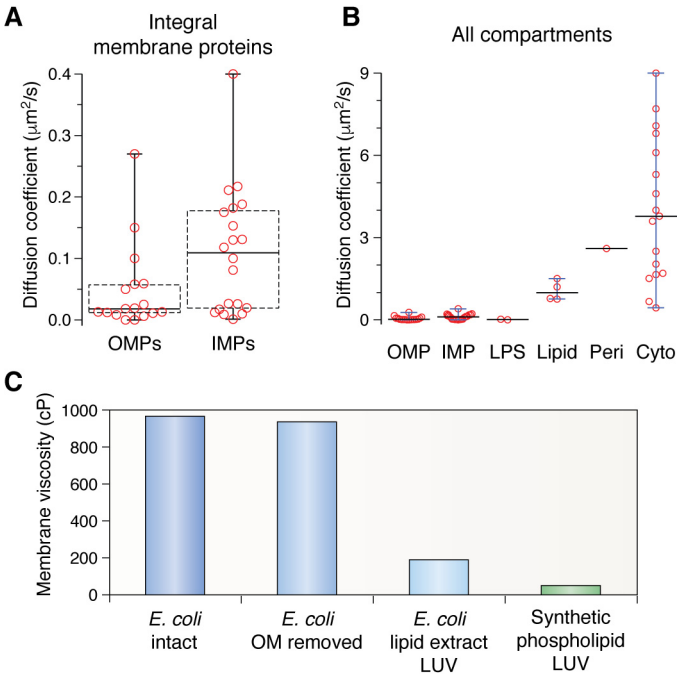

Figure 4. Comparison of physical properties of bacterial membranes. *A*, box plots showing the range of diffusion coefficients reported for OMPs and IMPs (see "*A crowded environment*"). Boxes show interquartile range calculated by the Tukey method with the median indicated as a *boldface horizontal line*. *Whiskers* show the minimum and maximum values. *B*, comparison of the diffusion coefficients of membrane proteins with other components of bacteria. *Whiskers* are only shown for components that have three or more values reported in the literature. All values are reported from *in vivo* studies. *LPS*, diffusion of LPS molecules in *S. typhimurium*. *Lipid*, diffusion rate of a fluorescent lipid reporter probe in *E. coli* membranes. *Peri*, diffusion of soluble protein in the *E. coli* periplasm. *Cyto*, diffusion of soluble protein in the *E. coli* cytoplasm. *C*, viscosities of different membrane environments as measured by the use of fluorescent BODIPY C10 lipid reporter probes. *E. coli* data are from Mika *et al.* (175), and synthetic phospholipid data are from Wu *et al.* (225). BODIPY C10 specifically incorporates into the IM of *E. coli*, and removal of the OM minimally affects the measured viscosity. Synthetic phospholipid 200 nm LUVs were comprised of DLPC, DMPC, POPC, or DOPC.

(*di*$C_{14:0}$PC) (157). However, simulations investigating larger length scales have shown that crowding a bilayer with some OMPs (*i.e.* BtuB), but not others (*i.e.* OmpF), can reduce the global bending rigidity of a POPE ($C_{16:0}C_{18:1}$PE)/POPC ($C_{16:0}C_{18:1}$PC) membrane (191)—an effect that would explain how a cell with a protein-rich OM could still maintain its shape. An interesting alternative possibility to explain the potentially incompatible concepts of OMP folding and a protein-dense, lipid-poor OM would be to consider the OM as an inhomogeneous mixture of protein and lipid (Fig. 3*C*). The view of OMP monomers or trimers, well-solubilized with lipid, would leave little bulk lipid available for nascent OMPs to fold. However, by clustering OMPs together into regions resembling two-dimensional crystals (*i.e.* forming regions highly enriched with OMPs and little to no lipid—a local LPR closer to 1:1 (mol/mol)), sufficient lipid-rich regions would be created to enable OMP folding and insertion (Fig. 3, *B* and *C*). Regardless of which model is correct, this locally stiff, crowded, and confined environment, with a relative paucity of free lipid, poses a challenging environment into which OMPs must fold.

More than a mix of lipid types

The physical properties of lipid membranes

Lipid bilayers can be characterized by a number of physical, mechanical, and chemical parameters, including stored curvature elastic stress (lateral pressure), melting temperature, the bulk lipid phase, the presence of lipid rafts, membrane viscosity, and headgroup charge (192–194) (Fig. 5). Many of these properties are interrelated and can be modulated by altering the acyl chain composition and/or the phospholipid headgroup and by altering the relative amounts of phospholipid, CL, and LPS (195–199). Stored curvature elastic stress makes membranes more rigid and less elastic in terms of their ability to deform or bend. This property can be introduced by the presence of nonbilayer-forming lipids in otherwise bilayer-forming membranes (Fig. 5). For example, PE lipids create negative curvature, whereas PG and PC lipids have zero or low spontaneous curvature, which allows them to readily form bilayers (200). Doping bilayers containing PC or PG with PE or CL generates a tension in packing of the different lipid types, creating a crowding, or pressure, near the center of the bilayer where each leaflet meets (Fig. 5), which is further altered by the length of the acyl chains (with shorter chains reducing this elastic stress) (200).

The lipid phase of a membrane is also dependent on its lipid composition and on the temperature (Fig. 5). Bilayers exist primarily in one of two major states, a solid "gel" phase in which the acyl chains are tightly packed and the mobility of lipid molecules is low, and a "liquid" phase, where lipid mobility is higher (201–203). Furthermore, analogous to the familiar phase change of ice to water, lipids in a gel-phase membrane can "melt" to become the liquid phase at a temperature characteristic of the particular lipid type—called the transition temperature, T_m. Lipid mixtures can also adopt a "liquid-ordered" phase (with the classical pure liquid phase described as "liquid-disordered"). This liquid-ordered phase contains lipids that are highly mobile but have well-ordered acyl chains and is often associated with the formation of lipid rafts in cholesterol-containing membranes in eukaryotes (204–206). Although sterol lipids are rare in bacteria, CL may play a similar role in increasing lipid order, and there is evidence that CL can participate in the formation of rafts/domains in membranes *in vitro* and *in vivo* (Fig. 5) (although it is likely this mechanism is distinct from that of cholesterol) (207, 208). *In silico*, CL has been observed to form clusters under patches of LPS in simulations of bacterial OMs in a role that may compensate for packing defects in the outer leaflet of the OM (209, 210).

The physical properties of native lipid extracts

The OM differs from the IM in its highly asymmetric structure, large fraction of proteins by weight, permeability to small molecules (<600 Da), and lack of energization across it (11, 99, 139, 156, 211). However, relatively little is known about how these unique features of the OM affect its mechanical properties and how this differs from the IM. *E. coli* is known to alter the lipid content of its membranes, particularly the length and degree of saturation of acyl chains, in response to changes in growth temperature. This process, termed "homeoviscous adaptation" (212), suggests that bacteria actively maintain their

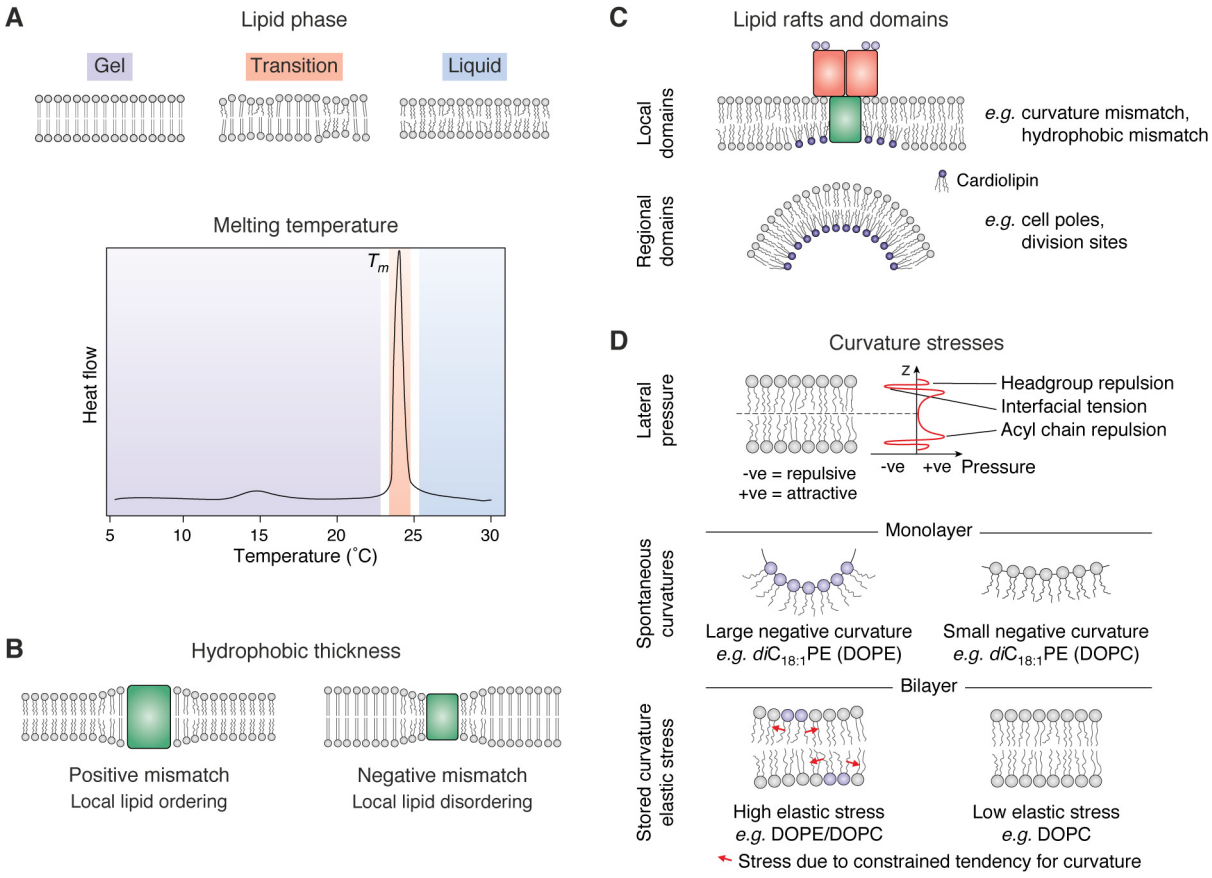

Figure 5. Physical and mechanical properties of a lipid bilayer. *A*, *top*, the phase of a lipid bilayer depends on the temperature, with the lipids being in an ordered (gel) phase below the T_m and in a (liquid) disordered phase above the T_m. At the transition temperature, frustration between packing of regions of gel and liquid phase causes defects to occur at these boundaries. *Bottom*, a typical differential scanning calorimetry curve illustrating the thermal response of a DMPC (*di*$C_{14:0}$PC) bilayer with the regions of each phase *colored* as above. *B*, the hydrophobic thickness of a membrane depends on the lipid acyl chain length. However, when an OMP becomes embedded in a lipid bilayer, the membrane responds by trying to "match" the hydrophobic thickness of the bilayer to that of the protein to minimize the energetic penalty of exposing polar lipid headgroups to a hydrophobic OMP surface or hydrophobic acyl tails to polar OMP loops. *C*, mixtures of lipids can separate, forming "rafts" or domains dependent on the physical conditions and lipid type. CL has a high propensity for negative curvature and has been shown to be enriched at cell poles and division sites where the membrane constricts. CL has also been observed to bind to membrane protein complexes such as the BAM complex (397) and cluster under patches of LPS in MD simulations (209, 210), suggesting that it may help stabilize bilayer packing defects (which might be induced by LPS) and stabilize regions of large hydrophobic mismatch (*e.g.* around embedded proteins such as BamA). *D*, schematic describing stored curvature elastic stress and how this depends on lipid type. Adapted from Booth and Curnow (398). This research was originally published in Current Opinion in Structural Biology. Booth, P. J., and Curnow, P. Folding scene investigation: membrane proteins. *Current Opinion in Structural Biology* 2009; 19:8–13. © Elsevier. Attractive and repulsive interactions driven by the packing of lipids create a pressure differential along the normal of the membrane that must be overcome to deform or alter lipid packing. Incorporation of lipids that have a tendency toward negative curvature (due to the relative size of the headgroup *versus* the acyl chain (*e.g.* PE lipids)) into a bilayer formed from lipids with a neutral or low curvature tendency (*e.g.* PC lipids) generates a stress force within the bilayer due to the opposing tendencies for bilayer formation of these lipids.

membranes at a constant level of "fluidity," or in a particular phase, that enables them to adjust to different environments. For example, whereas total lipid extract from *E. coli* K-12 W3110 showed approximately the same headgroup content (with a minor monotonic increase in CL and decrease in PG) when grown at 30, 37, 42, or 45 ℃ (213), the ratio of saturated over unsaturated acyl chains increased with temperature. This suggests a change to a more "rigid" mixture of phospholipids at higher growth temperatures to balance the increased fluidity caused by the input of thermal energy.

Membrane lipid properties can be probed using fluorescent reporter dyes that partition into membranes (either globally or into specific lipid phases) and alter their excitation or emission properties according to the local lipid environment. Hence, these dyes can be used as reporters of membrane viscosity, degree of hydration, phase, and mobility (214). The fluorophore laurdan partitions into membranes through its acyl tail, whereas its naphthalene-based headgroup resides in the interfacial region of bilayers, where its fluorescence excitation and emission spectra are sensitive to the degree of hydration of the bilayer, allowing it to report on the phase and order of lipids in a bilayer (215). Using laurdan, a T_m of *E. coli* total lipid extract of <14 ℃ was determined for bacteria grown at 30 ℃ or 37 ℃, whereas the T_m was higher (T_m ~20-22 ℃) for bacteria grown at 42 ℃ and elevated again (T_m ~27 ℃) for bacteria grown at 45 ℃ (213). This shows that the lipids in *E. coli* are natively in the liquid phase, and their T_m is as much as 20 ℃ below the growth temperature. However, when the OM and IM are considered separately, it becomes clear that "global" lipid properties do not accurately capture the differences between these two different membranes. Deuterium NMR studies, used to measure the order of acyl chains, found that lipids in an OM preparation of *E. coli* L51 were less fluid than those from the IM and that the T_m was ~7 ℃ higher than the IM (216, 217).

Electron spin resonance experiments on IMs and OMs of *E. coli* W1485 doped with a spin-labeled stearic acid probe found the T_m of the OM (26 °C) to be ~13 °C higher than the IM (13 °C) when the bacteria were grown at 37 °C (196). Fluorescence polarization studies using IM and OM extracts from *E. coli* B doped with parinaric acid also found that the phase transition of the OM was ~15 °C higher than the IM, initiating its phase transition at 40 °C (218).

E. coli membranes in situ

Few studies on the properties of bacterial membrane lipid order (or phase) *in vivo* have been reported to date, but current data suggest that the organization of the OM is more complicated than that derived using lipid extracts, as described above. Differential scanning calorimetry studies on whole cells of *E. coli* W945 grown at 20 or 37 °C observed two reversible transitions, one well below the growth temperature, which was suggested to correspond to the IM, and another slightly above the growth temperature, which was assigned to the OM (219). Experiments on fixed cells using laurdan and the dye 1,3-diphenyl-1,3,5-hexatriene as a probe of local viscosity (214) have shown that *E. coli* membranes are predominantly in the liquid phase. These experiments also revealed that these membranes are heterogeneous and contain at least two distinct phases, one more liquid and one less so, possibly indicating the presence of distinct lipid domains (220). However, an alternative explanation of these data is that they reflect a difference between the IM and the OM, because it is not clear to which membrane these probes localize. Indeed, whereas early studies suggested that these dyes (and others, including FM 4-64) localize primarily to the IM (221), it is now known that FM 4-64 partitions specifically into the OM immediately after labeling (19), and 1,3-diphenyl-1,3,5-hexatriene may equilibrate between both membranes (222, 223) or be trapped mainly in the first hydrophobic surface encountered (224). Measurements of membrane viscosity using "molecular rotor" dyes such as BODIPY C10 (viscosity alters the fluorescence lifetime of the probe) showed that the IM of *E. coli* is more viscous than previously believed, with an average viscosity of 980 cP for intact *E. coli*, 950 cP for spheroplasted cells at 37 °C, and 200 cP for large unilamellar vesicles (LUVs) of *E. coli* total lipid extract at 37 °C (175). By contrast, a lower viscosity (~60 cP) was consistently observed for 200-nm LUVs formed from DLPC ($di$$C_{12:0}$PC), DMPC ($di$$C_{14:0}$PC), POPC ($C_{16:0}C_{18:1}$PC), or DOPC ($di$$C_{18:1}$PC) in their liquid phase at 37 °C (225) (Fig. 4*C*). Although not yet measured directly, the lower diffusion coefficients of OMPs compared with IMPs (Fig. 4, *A* and *B*) suggest that the viscosity of the OM may be even higher still, and this is a characteristic that model lipid membranes commonly used for OMP-folding studies (see below) clearly cannot capture.

The influence of LPS on the mechanical properties of the OM

On the basis of the physicochemical properties of LPS extracts (which generally show T_m values at or above the growth temperature) (226–230) and those of the OM (discussed above), some authors have argued that the OM is more likely to exist in the gel phase at physiological temperatures (78). However, the exact thermotropic response of LPS in the outer leaflet may vary, depending on the composition (particularly the presence of hydrogen bond donors and acceptors) and size of the polysaccharide region of the LPS molecules incorporated (78, 229, 231, 232). *In vitro* models of the OM using an asymmetric bilayer deposited on silicon or lipid-coated gold surfaces showed that the membrane has unusual mixed characteristics with elements of both liquid- and gel-phase lipids (233, 234). The OM in these studies comprised "rough" LPS (containing the conserved polysaccharide core but lacking the O-antigen) (Fig. 2) in the outer leaflet and phospholipid (DPPC ($di$$C_{16:0}$PC)) in the inner leaflet, with lipid order parameters measured using neutron reflectometry and attenuated total reflection FTIR spectroscopy (ATR-FTIR) (233). Two transition midpoints (T_m) were observed, one just below (~36 °C) the physiological growth temperature of *E. coli* (37 °C) for the outer leaflet of LPS and the other above the T_m (~39 °C) for the inner leaflet comprising DPPC ($di$$C_{16:0}$PC) (233). Even though the composition of the inner leaflet lipids and LPS differ *in vivo* from those used in this study, the results suggest that the LPS component of the asymmetric OM may confer greater rigidity to the OM. This agrees with deuterium NMR studies of preparations of *E. coli* OM and IM, which found that at a given temperature, phospholipids were more ordered and a larger fraction were in the gel phase in the OM than the IM (217, 235). However, it should be noted that extraction of the OM likely causes mixing of the inner and outer leaflets, reducing the asymmetry (236).

The fluidity of the OM of *E. coli* may also be controlled by temperature-dependent modification of LPS in the outer leaflet. The *lpxT* gene in *E. coli* transfers a phosphate group onto lipid A, which may alter the rigidity of the OM, and expression of this gene is regulated by an mRNA thermostat (237). LpxT is an IM protein that covalently modifies LPS before it reaches the OM. The protein was shown to be stable between 28 and 42 °C; however, its mRNA levels fall dramatically across this same temperature range (237). Another LPS biosynthesis pathway gene, *lpxP*, replaces the $C_{12:0}$ chain in *E. coli* lipid A (which is normally installed by *lpxL*) with a $C_{16:1}$ chain, but expression of this protein is only induced at low temperature (12 °C) and may also be regulated by an mRNA thermostat similar to *lpxT* (238). *Francisella novicida* synthesizes lipid A with shorter acyl chains at low growth temperatures (25 °C compared with 37 °C), an effect that has been linked to both the differential expression and enzyme activity of the *lpxD2* and *lpxD1* genes (which add different length acyl chains to lipid A) at 25 and 37 °C, respectively (239). In *Yersinia pestis*, the *lpxR* gene, which is responsible for the removal of acyl chains from lipid A, is inactive at 21 °C (resulting in a hexa-acylated LPS) but functional at 37 °C, resulting in a tetra-acylated LPS in the OM of bacteria grown at this temperature (240). The deacylase enzyme and OMP, PagL, alters lipid A through the removal of acyl chains. The activity of this enzyme in *Pseudomonas aeruginosa* is also affected by growth temperature, with activity falling at low growth temperature ($\leq$ 21 °C) (241). The extent to which these temperature-dependent modifications are a mechanical response to maintain or alter membrane rigidity/fluidity or an immune-modulating response triggered by the detection of a

host environment, or both, remains unclear (242). Despite this, it is likely that the structure and mechanical properties of LPS are important for OMP folding. For example, genetic alterations to the biosynthetic pathway of LPS, which cause changes in its degree of acylation or its sugar headgroup have been shown to cause severe defects in the biogenesis of OMPs (243–245).

The effect of asymmetry

The asymmetric architecture of the OM, with an inner leaflet containing canonical phospholipids and an outer leaflet containing LPS with its highly acylated lipid A attached to large sugar groups that protrude into solution, impacts the physical properties of the OM and creates a lipid environment that is very different from that of the IM *in vivo* and vesicles of lipids commonly used in *in vitro* experiments. Representative models of the OM have been built *in silico* and studied using coarse-grained molecular dynamics (CG-MD) and atomistic molecular dynamics (A-MD). A model was built of the *P. aeruginosa* PAO1 OM, with an LPS outer leaflet and a DPPE (diC$_{16:0}$PE) inner leaflet and studied by A-MD (246). At 37 ℃, molecules of DPPE in the inner leaflet showed diffusive movement consistent with a liquid phase, whereas LPS in the outer leaflet showed an order of magnitude lower mean-square displacement. Despite this low lateral mobility, calculation of the lipid order parameters of the acyl tails of LPS indicated that they are fluid and not ordered as would be expected for lipids in the gel phase (246). Similar results have been observed in other A-MD simulations of *E. coli* and *P. aeruginosa* OMs with an outer leaflet containing LPS with a short O-antigen region (247, 248) or a "rough" LPS (248, 249) (Fig. 2) and an inner leaflet comprised of a 75:20:5 (mol/mol/mol) mix of PPPE ($C_{16:0}C_{16:1}$PE)/PVPG ($C_{16:0}C_{18:1}$PG)/CL. CG-MD simulations of the *E. coli* OM with a DPPE (diC$_{16:0}$PE) inner leaflet and an outer leaflet containing a different ratio of LPS/DPPE (diC$_{16:0}$PE) from 10:90 to 100:0 (mol/mol) showed that increasing the fraction of LPS lowered the simulated T_m from 73 to 15 ℃ (250) (for reference, a symmetric bilayer composed solely of DPPE has an experimental T_m of ~64 ℃, showing interleaflet coupling can have hard-to-predict consequences on phase behavior) (251). A-MD simulations of a model of a *P. aeruginosa* OM containing only lipid A in the outer leaflet and a mix of DPPE (diC$_{16:0}$PE), DPPG (diC$_{16:0}$PG), DOPE (diC$_{18:1}$PE), and DOPG (diC$_{18:1}$PG) in the inner leaflet showed that the acyl chains of lipid A were also consistent with a liquid phase but were overall less disordered than observed with larger sugar regions—again emphasizing the importance of the polysaccharide region of LPS in modulating its packing behavior (252). Other CG-MD experiments showed that *E. coli* asymmetric membranes with a lipid A outer leaflet and a DPPE (diC$_{16:0}$PE) inner leaflet had a lower T_m than a "rough" LPS outer leaflet and DPPE (diC$_{16:0}$PE) inner leaflet (~41-46 ℃ *versus* ~55 ℃) (253), although it is not clear why the T_m values are much higher in these simulations than observed previously from the same group (250). Preparations of the OM and IM from *E. coli* J5 doped with spin label probes showed that membrane order is higher, and lipid mobility lower, in the OM, and the magnitude of this difference decreases when a large fraction of LPS is removed (254). Furthermore, in the absence of galactose, this strain is unable to synthesize the full polysaccharide region and produces a short "rough" LPS (Fig. 2) (255). The presence of the O-antigen was shown to confer even greater rigidity to the OM extracts than when they contained only truncated "rough" LPS (254). Deuterium solid-state NMR experiments on multilamellar vesicles containing a mix of partially deuterated DPPC (diC$_{16:0}$PC) and "rough" LPS from *E. coli* J5 or *E. coli* EH100 also found an "ordering" effect on the acyl chains of DPPC conferred by LPS (256). Despite this ordering of acyl chains, experiments with SUVs composed of *E. coli* B LPS and phospholipid extract doped with spin-labeled PE and PG lipids, and *S. typhimurium* OM lipid preparations doped with a spin-labeled stearic acid probe found that phospholipids remained freely diffusive and segregated away from LPS (226, 257, 258). The slower diffusion of phospholipids in the inner leaflet of the OM observed in the previous study (which retained its complement of OMPs) (254) may therefore be due to the transient clustering and reduced diffusion of lipids around embedded OMPs (186, 259–261). These *in vitro* studies, although not on fully asymmetric membranes (236), broadly validate the observations of the above *in silico* studies.

Measurement of water permeation in *P. aeruginosa* PAO1 LPS (outer)–DPPE (diC$_{16:0}$PE) (inner), *P. aeruginosa* LPS (outer)–PPPE ($C_{16:0}C_{16:1}$PE)/PVPG ($C_{16:0}C_{18:1}$PG)/CL (inner), and *E. coli* LPS (outer)–PPPE/PVPG/CL (inner) asymmetric bilayers by A-MD showed that the outer leaflet is relatively permeable to water when compared with the inner leaflet (with water reaching the terminal methyl groups of lipid A acyl chains) with both "rough" LPS and LPS containing an O-antigen region (246, 248,249, 262). This polarity gradient is also apparent through interactions between loop regions of OMPs and charged and polar groups on LPS that have been observed by A-MD and CG-MD (79, 210, 247–249, 253, 263–274) and specific LPS-binding sites that have been validated experimentally for trimeric porins such as OmpF (6, 189, 275–278). One area that remains understudied but warrants further investigation is the effect of the acyl tails of lipoproteins in the inner leaflet of the asymmetric OM on membrane properties. The copy number of lipoproteins at the IM is small enough to, presumably, have a negligible effect on the membrane's bulk physicochemical properties. However, at the OM there may be over 1 million lipoproteins anchored to the inner leaflet, composed primarily of Lpp (Braun's lipoprotein)—one of the most abundant proteins in *E. coli*—and Pal (3, 4, 279, 280). Each lipoprotein is triacylated at an N-terminal cysteine (121), and each acyl chain can be approximated to occupy ~0.28 nm^2 in a bilayer (100, 262,263, 281–285). Assuming a lower bound on the surface area of an average *E. coli* as 3.7 μm^2 and an upper bound of 13 μm^2 (286–288), and the total area occupied by lipoprotein tails similarly bounded between 0.25 μm^2 (3×10^5 proteins) and 1.1 μm^2 (1.3×10^6 proteins) (3, 4), we come to an estimate of 2–30% of the inner leaflet of the OM occupied by these lipid anchors. Lpp and Pal both bind peptidoglycan through their protein domains. This interaction restricts their mobility (and therefore the lateral mobility of their lipid anchors) and stiffens the OM, and the protein itself physically occludes the

headgroups of the OM inner leaflet lipids (171, 289, 290). The impact that this has on the bilayer properties of the OM requires further study, but the presence of these lipoproteins would act to further reduce the "accessible" surface for OMPs to bind and initiate folding.

Just as early *in vitro* experiments on synthetic lipid vesicles allowed hypotheses to be generated about the properties of biological membranes, we can look to *in vitro* experimental models of asymmetric phospholipid membranes to infer information about how asymmetry may affect the OM. These systems remain experimentally challenging due to problems with mixing/scrambling of the inner and outer leaflets in both surface-deposited (291, 292) and liposome-based asymmetric membranes (293), as well as difficulties in accurately controlling the composition of the outer leaflet in asymmetric liposome-based studies (294, 295). Nonetheless, such studies have suggested that asymmetry results in coupling between leaflets, which alters the physical properties of the bilayer distinctly from those of the same lipid types mixed symmetrically. These include changes to the membrane potential difference, lateral pressure differential, and the packing of lipids (296–300).

Synthesizing the data described above from *in vitro* and *in silico* studies allows insights into the view of the membrane encountered by a nascent OMP as it approaches and is inserted into the OM. As the OMP approaches and moves through the membrane, it begins folding on a 'typical' liquid-disordered bilayer leaflet where phospholipids are free to diffuse before entering a region of low lateral mobility and increased hydration in the outer leaflet. These gradients of lateral mobility, lipid packing, hydration, and lipid headgroup polarity as an OMP inserts across the membrane normal could help to stabilize the tertiary structure of OMPs, particularly the hydrophilic loop regions (which can be >20 residues in length) (301), and drive the folding of the β-barrel domain to completion. Overall, therefore, the above studies have shown that the physical properties of the OM are highly complex and can vary dependent on the underlying lipid phase and the elastic stress, as well as the presence of OMPs and lipoproteins, and the LPR (175, 214, 302). These parameters, in turn, can be tuned by the lipids incorporated into each leaflet, especially by modifications to the LPS in the outer leaflet of the OM. Hence, bacteria have to be adaptable so that they can form and maintain their OM whatever the nature of their environment and the environmental stresses that they encounter.

Membrane-spanning OMPs need to insert through both leaflets of the OM to adopt their native, functional folds, yet how this unique asymmetry and changing lipid content of the OM affects the folding and function of OMPs is currently unknown. We now need to take a deeper look into what we know about OMP folding, starting with the basics and then building more complexity into experimental and theoretical models to allow us to understand how the unusual properties of the OM might influence the process of OMP biogenesis in bacteria.

How do OMPs fold?

30 years of experiments on OMP folding in vitro

Likely due their high thermodynamic stability (ΔG°_{F} = −10 to −140 kJ mol^{-1}) (303–312), relatively low hydrophobicity (by all-residue average on the Kyte–Doolittle scale most OMPs are hydrophilic due their alternating hydrophobic membrane facing/generally hydrophilic lumen facing patterning), and ease of recombinant expression and purification, OMPs are unusually tractable models for *in vitro* studies of membrane protein folding. The first published study on the successful folding of OMPs *in vitro* was carried out in 1978, when it was shown that SDS-boiled and denatured OmpA (Fig. 6) could be refolded with high yield into LPS (but not into solutions containing total *E. coli* phospholipids, DMPC (diC$_{14:0}$PC), or the sugar moiety of LPS) (313). This refolded OmpA was shown to be natively structured because it had regained function (activity in phage receptor binding assays), was protected from protease digestion, and migrated at an anomalous molecular weight in SDS-polyacrylamide gels when loaded without boiling (cold SDS-PAGE) (313). Hence, the stage was set for detailed studies of the mechanisms of OMP folding, at least for this and other small (8-stranded) OMPs.

The next major breakthroughs in our understanding of OMP folding were made in the 1990s, when it was shown that OmpA and an unnamed porin could be spontaneously refolded *in vitro* into detergent (octyl glucoside), small unilamellar vesicles (SUVs) of DMPC (diC$_{14:0}$PC), or mixed lipid-detergent micelles (octyl-poly-oxyethyleneoxide (C8POE) and soybean lecithin) in the presence of SDS without the addition of an external energy source or other proteins (314–316). Soon after, several groups began to experiment with the refolding conditions to identify the determinants that allow OMPs to attain their native structure. These studies showed that detergents are required to be above their critical micelle concentration for successful OMP folding (317, 318). This highlighted the importance of a surface to initiate folding and showed that simple binding of hydrophobic molecules around an unfolded OMP chain is insufficient to enable folding. Instead, some degree of preorganization is required. These studies also showed that folding of OMPs *in vitro* is a remarkably slow process (most OMPs taking on the order of minutes to hours to fold), too slow to be physiologically relevant (the doubling time of *E. coli* is ~20 min at 37 °C). They also showed that refolding yields are improved by the addition of urea, implying that the OMP-folding landscape contains kinetic traps and/or off-pathway intermediates or aggregates that can be suppressed by the addition of chaotrope (317, 319). These experiments also showed that the β-barrel transmembrane fold is extremely stable once formed, with native OMPs being resilient to denaturation by SDS (unless heated to high temperatures), enabling kinetic measurement of folding using cold SDS-PAGE (71, 313, 320). This is due to the high kinetic barrier to unfolding in SDS (on the order of years at 30 °C for OmpA) (314, 321).

Due to their high kinetic and thermodynamic stability, high concentrations of denaturant often fail to unfold OMPs that have been refolded into detergent micelles or lipid bilayers. For example, OmPLA remains enzymatically active in 8 M urea and in 6 M guanidine-HCl (317). Experiments measuring the activity of OmPLA following refolding into LPS and a range of detergents showed not only that the protein can reacquire a stable fold, but also that it regained its phospholipase activity, confirming reversible folding to a functional state (317). Thus,

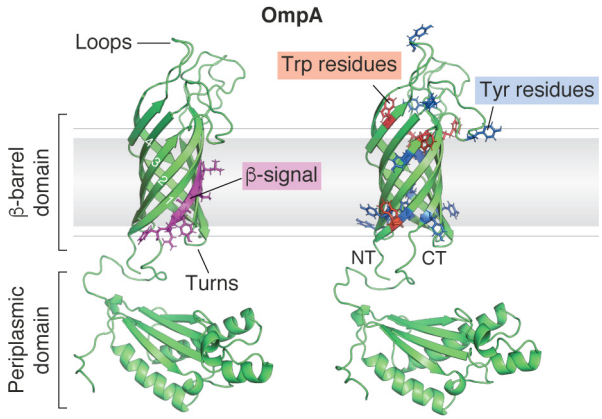

Figure 6. The structure and architecture of OmpA. The 8-stranded β-barrel OmpA has been used for many studies of OMP folding *in vitro*. It comprises a transmembrane β-barrel domain and a soluble periplasmic peptidoglycan-binding domain. Neighboring β-strands are connected on their extracellular side by a long disordered "loop" and on the periplasmic side by a short "turn." OMP β-strands are usually numbered from the N terminus (*NT*) to the C terminus (*CT*), and the C-terminal β-strand often contains a conserved motif of Gly-*X*-*X*-Ar-*X*-Ar (where Ar represents any aromatic residue), indicated in *purple* on OmpA, thought to be important for recognition by BAM (386, 399). Many OMPs contain an enrichment in aromatic Trp and Tyr residues in their β-barrel domain, particularly at the interfacial region between the lipid headgroups (approximate position indicated by the *gray line*) and acyl tails (approximate position indicated by the *gray box*) known as an "aromatic girdle." Trp (*red*) and Tyr (*blue*) residues found in the β-barrel domain of OmpA are indicated *above*. This model of OmpA was created in PyMol 2.X (Schrödinger, LLC) by fusing the NMR structures of the *E. coli* OmpA β-barrel (PDB code 1G90) (400) and its periplasmic domain (PDB code 2MQE) (401).

OMPs obey Anfinsen's dogma that all of the information for a protein to reach its thermodynamically stable native structure is contained in its amino acid sequence (322).

First glimpses of an OMP-folding mechanism

The next era of work on OMP folding focused on attempts to determine the mechanisms of folding, including why the process is so slow, whether partially folded intermediates are formed, the nature of folding transition states, and the role of the protein sequence, lipid composition, and folding factors (including BAM and molecular chaperones) in the folding process. In some of the earliest studies of this kind, Surrey *et al.* (316) measured the kinetics of OmpA folding into SUVs formed from 95% DMPC ($diC_{14:0}PC$), 5% DMPG ($diC_{14:0}PG$) (mol/mol) at a temperature above the lipid T_m by rapid dilution from urea *in vitro*. The techniques employed and optimized in these early studies of OMP folding form the toolset used for such studies to this day (323). They also reinforced the idea garnered from studies on the folding of water-soluble proteins (324–327) that insights into the mechanisms of folding can be best learned by taking a kinetic approach to dissect each step in the folding pathway. These methods include (i) monitoring the change in tryptophan (and/or tyrosine) fluorescence as an OMP folds from aqueous solution into a nonpolar membrane (Fig. 6 shows the location of aromatic residues on OmpA); (ii) measuring the formation of secondary structure using far-UV CD, and (iii) following the formation of SDS-resistant molecules (presumably containing a correctly folded β-barrel domain) using cold SDS-PAGE (316, 328). This work showed that OmpA folds into lipid bilayers *in vitro* via a multiphasic mechanism involving rapid hydrophobic collapse that occurs in the experimental dead time (~1 s), followed by two slower phases occurring in minutes (phase 1) and tens of minutes (phase 2) corresponding to structural rearrangement and concurrent formation of secondary and tertiary structure (Fig. 7*A*) (316). It was also shown that pH affects the yield and rate of OMP folding, with pH values close to the pI of OmpA (pI ~5.7) increasing the folding rate but decreasing the folding yield. The average pI of the OMPs shown in Fig. 1 is ~5.4, and the environment in which *E. coli* has evolved (the large colon) is mildly acidic (pH 5.5-7.5) (329), suggesting that *E. coli* has adapted to favor rapid folding and has systems to handle or circumvent the lower yields. Higher LPRs were also shown to increase the folding rate and yield, consistent with models suggesting that the OMP first binds to the surface of the lipid bilayer before folding and insertion are completed (316, 330–332). Indeed, refolding studies of OmpA into lipids above their T_m confirmed this membrane-binding step with elegant experiments using membranes composed of lipids that had been brominated at different positions along the acyl chain (bromination quenches fluorescence from tryptophan only when in close proximity, thereby allowing depth-dependent changes in fluorescence) (333, 334). Earlier data from ATR-FTIR studies showed that this membrane-adsorbed (but not stably integrated) folding intermediate had significant β-sheet content, with β-strands that have still to adopt the orientation found in the native β-barrel (335). Finally, the finding that tryptophan residues located in β-strands, near extracellular loops, or in intracellular turns show similar rates of membrane insertion (judged by tryptophan fluorescence quenching) suggested that folding occurs via a concerted mechanism in which all four hairpins of this 8-stranded OMP move synchronously across the bilayer (330), increasing in tilt angle as the protein becomes fully membrane embedded (335). More recent experiments employing single-Cys single-Trp variants of OmpA labeled at the Cys with Trp-quenching nitroxyl spin labels have shown that despite being concerted, OmpA's β-strands form in a particular order (336), with β-strands initially associating with each other at their "extracellular" sides like a tipi (*i.e.* before the "periplasmic" side forms) (Fig. 7*A*, step 4) and showing that the N- and C-terminal strands are already in close proximity in the membrane-adsorbed state (Fig. 7*A*, step 3), providing evidence against models invoking β-barrel closure as the last step (336). These experiments also failed to detect native β-strand association in aqueous solution, ruling out models in which the OmpA β-barrel "pre-folds" in solution before inserting as a single unit into the membrane. This complex, multistep process where formation of secondary and tertiary structure is coordinated contrasts markedly with the two-stage mechanism proposed for α-helical membrane proteins in which the formation of α-helices precedes formation of the native tertiary structure (337, 338). The overall general model for spontaneous OMP folding *in vitro* is summarized in Fig. 7*A*.

The role of the membrane in OMP folding

Studies varying the lipid headgroup, acyl chain length, lipid phase, membrane curvature, and elastic curvature stress (the

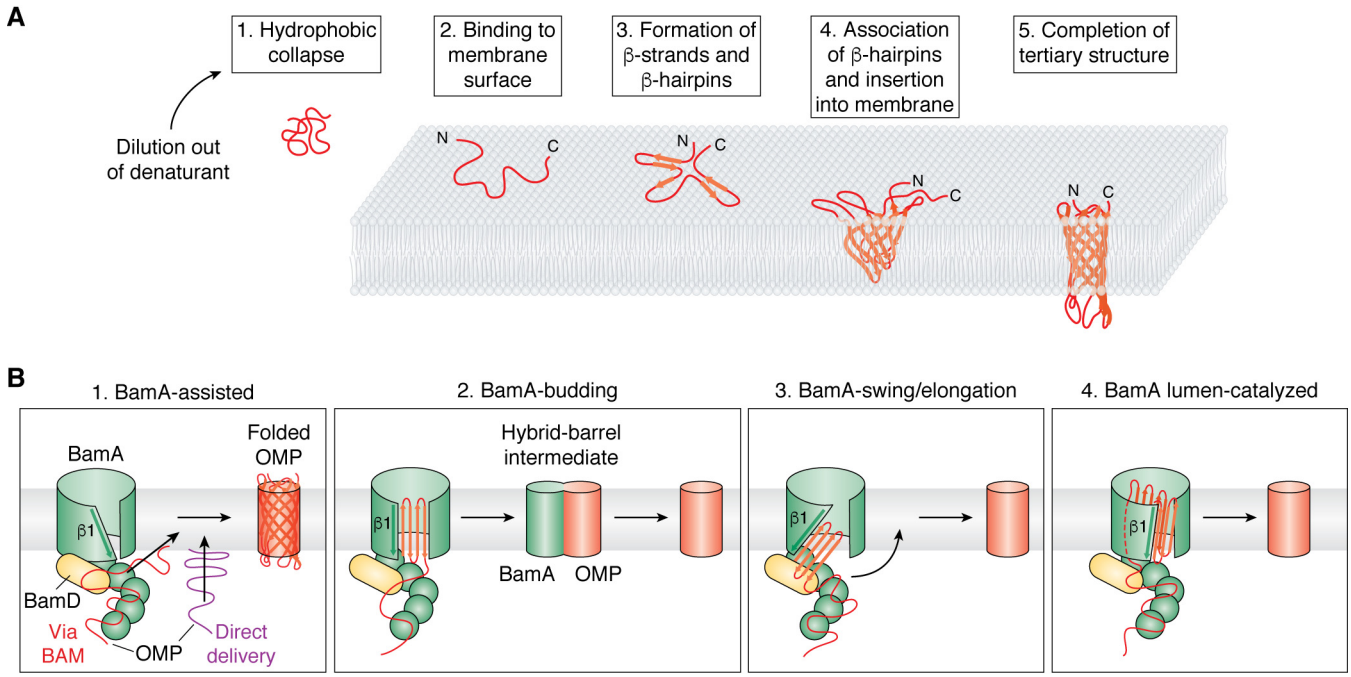

Figure 7. Mechanisms of OMP folding *in vitro* and *in vivo*. *A*, Mechanism of spontaneous OMP folding *in vitro* as described for OmpA. *In vitro* studies have shed light on the folding pathway of model OMPs, particularly OmpA, after dilution out of high concentrations of denaturant in the presence of a lipid bilayer. Adapted from Danoff and Fleming (351). This research was originally published in Biochemistry. Danoff, E. J., and Fleming, K. G. Membrane defects accelerate outer membrane β-barrel protein folding. *Biochemistry* 2015; 54:97–99. © American Chemical Society. *1*, immediately after dilution out of denaturant, the chain undergoes hydrophobic collapse; *2*, the polypeptide chain then binds to the surface of a membrane; *3*, the nascent OMP then begins to form secondary structure as it brings together neighboring β-strands to form β-hairpins while still mostly exposed to the aqueous environment; *4*, these β-hairpins associate and begin to insert into the acyl tail region of the membrane; *5*, the tertiary structure of the barrel is complete with the final step likely being a slower equilibration of side chains and extrusion of hydrophilic loops from the barrel lumen. *B*, proposed mechanisms of BAM-catalyzed folding of OMPs *in vivo*. The nascent OMP is shown in *red* or *purple*, BamA is shown in *green*, and BamD is shown in *yellow* (other subunits have been omitted for clarity). *1, BamA-assisted*. Substrate OMPs are delivered to BAM or directly to the membrane by periplasmic chaperones. These nascent OMPs then fold spontaneously into a region of destabilized membrane in front of the lateral gate of BamA, essentially following the same pathway as described in *A*. *2, BamA-budding*. Binding/recognition of the OMP occurs on BAM before β-strands are added a β-hairpin at a time between β1 and β16 of BamA, forming a semisymmetric hybrid-barrel intermediate. Once all β-hairpins are added, this folded OMP then buds off from BamA. *3, BamA-swing/elongation*. Binding/recognition of the OMP occurs on BAM and folding starts with templating of the C-terminal β-strand of a nascent OMP against β1 of BamA. Folding proceeds in the periplasm through the stepwise addition of more β-strands. Once all β-strands have been added, a conformational change in BamA "swings" the folded β-barrel into the membrane. *4, BamA lumen–catalyzed*. This model begins as described in *3* with templating against BamA β1. However, formation of further β-strands is catalyzed against the lumen wall of BamA with a conserved motif in loop 6 of BamA (not shown) possibly stabilizing this interaction. In all of these models, BamD (*yellow*) may play an important role in substrate recognition and/or the conformational cycle.

change in lateral pressure across the membrane) (Fig. 5) have shown that the properties of the membrane can have dramatic effects on the folding of OMPs. For example, whereas OMPs such as OmpA and PagP (both 8-stranded; Fig. 1) are able to fold into highly curved SUVs comprised of DOPC ($diC_{18:1}$PC) or DMPC ($diC_{14:0}$PC) in minutes, folding is slower or effectively prevented (beyond the timescale employed in the study) when these proteins are folding into LUVs formed from DOPC ($diC_{18:1}$PC) under the same experimental conditions (40). Similar studies have recapitulated these results and shown that the elastic curvature stress, hydrophobic mismatch (hydrophobic thickness of the OMP *versus* the bilayer), and membrane curvature (SUV *versus* LUV) affect OMP folding, emphasizing the importance of the physical properties of the lipid environment in determining the folding process (339, 340). The steep decrease in refolding rates observed as the acyl chain length of PC lipids increases (330) and the absence of reports of spontaneous folding into LUVs formed from pure PC lipids with saturated acyl chain lengths >14 carbon units (*i.e.* >DMPC ($diC_{14:0}$PC)) can be rationalized by the elastic free energy of the membrane, as this parameter is expected to increase to the fourth power of membrane thickness (341). Membrane thickness is also thought to relate to the incidence of packing defects and thermal fluctuations in the bilayer, with thinner membranes having more defects. Such packing defects may be responsible for the more rapid folding of OMPs into thinner bilayers (341). OMPs have also been shown to be unable to fold into some lipids, such as DMPC ($diC_{14:0}$PC) and DPPC ($diC_{16:0}$PC), in the gel phase, but they fold readily when the same lipids are in the liquid-disordered phase, suggesting a significant activation energy barrier for the protein to insert across the bilayer (333, 334). Accordingly, the folding rate and yield of tOmpA (the β-barrel domain of OmpA) and OmpX (8-stranded; Fig. 1) into micelles (or mixed micelles of different lipid/detergent types) can be increased 10−100-fold by applying a transient "heat shock" (~70 °C) during folding (342). This heat shock presumably confers enough thermal energy to rapidly take the unfolded ensemble over the activation energy barrier. It has also been shown that whereas gel-phase lipids (below their T_m) prevent or retard folding, and more rapid folding is observed into lipids in their liquid-disordered phase, folding is most rapid at the interface between these phases (*i.e.* at the T_m)

(343). At this temperature, regions of gel-phase (ordered acyl chains) and liquid-phase (disordered acyl chains) lipids coexist (344, 345), and frustration between the packing requirements of these phases is believed to generate packing defects (as shown by an increase in solute permeability) (346–350), which may be responsible for the acceleration of OMP folding. Kinetic modeling experiments have suggested that this phenomenon involves an acceleration in the formation of an early membrane-inserted folding intermediate (351).

Together, these data have established the importance of the chemical and physical properties of the membrane environment (lipid headgroup, acyl chain length, size, and curvature of the membrane vesicle) and the intimate connection between the protein sequence and membrane into which the OMP must fold.

Commonalities in the folding mechanisms of OMPs in vitro

OMP-folding intermediates formed by initial adsorption to the lipid bilayer surface have been observed for several small OMPs, including the 8-stranded OmpA (see above) and PagP (332). An extensive mutational study of the folding kinetics and equilibrium stability of single point mutants of PagP revealed the first evidence for the nature of an OMP-folding transition state (in DLPC (diC$_{12:0}$PC) LUVs), revealing that this species, which is formed subsequent to initial folding on the membrane surface, contains a partially folded β-barrel, in which the C-terminal strands have formed native-like contacts, but the N-terminal strands remain largely unstructured (352). The results from this study also suggested that PagP is tilted in the membrane in the transition state ensemble, reminiscent of CG-MD studies observing the insertion of preformed OmpA into a DPPC (diC$_{16:0}$PC) bilayer (353). Kinetic analysis of PagP folding also showed that this OMP folds via parallel pathways, with the route taken depending on the nature of the lipid employed (332). Similar results showing parallel folding pathways were also obtained for FomA (331), yet again highlighting the importance of the membrane surface and the physical state of the lipid bilayer for OMPs to fold (331, 332).

The view of OMP folding *in vitro* that emerges from these studies shows a common first step involving folding on the lipid surface followed by preorganization of the approximate structure of the OMP, with translocating aromatic residues anchoring the nascent β-barrel to the membrane, and association of neighboring β-strands causing a hydrophobic surface to be displayed toward the membrane. This would, in turn, drive the energetically favorable partitioning of the hydrophobic protein surface deeper into the acyl chains (354). At the same time, hydrogen bonding between β-strands during insertion may be driven by the energetic penalty associated with displaying the unbonded polar peptide backbone to the nonpolar membrane environment. Finally, the association of β-strands in the correct order may be a rate-limiting step for insertion into the bilayer.

BAM: Nature's answer to the challenges of OMP folding

Whereas many OMPs can be folded *in vitro* into SUVs and LUVs composed of short chain lipids, attempts to fold these proteins into liposomes comprised of *E. coli* polar lipid extract result in moderate folding yields for some OMPs (OmpA (8 strands), OmpT (10 strands), and BamA (16 strands)) and poor or no folding for others (OmpX (8 strands), PagP (8 strands), OmpW (8 strands), OmPLA (12 strands), and FadL (14 strands)) (Fig. 1) (40, 41). Spontaneous folding of OMPs of many sizes has been observed into DDPC (diC$_{10:0}$PC) LUVs (40) but has been shown to be suppressed upon incorporation of lipids with headgroups native to the *E. coli* OM that confer negative spontaneous curvature (PE) or net negative charge (PG) (41). BamA is a 16-stranded essential OMP (Fig. 1) and is the most conserved subunit of the multiprotein BAM complex, which is involved in the biogenesis of other OMPs. BamA or a BamA variant lacking most (4 of 5) of its periplasmic polypeptide transport-associated (POTRA) domains can partially rescue the poor folding efficiency of OMPs into these liposomes (41). These results highlight the vital role of BAM for OMP folding into lipids commensurate with those found *in vivo*, suggesting that spontaneous folding of OMPs into a native lipid bilayer *in vivo* is kinetically unfavorable unless BAM is present.

BAM as a modulator of the physical properties of membranes

Until recently, how BAM folds OMPs remained mysterious. The solution of several structures of BamA and BAM, as well as kinetic experiments, are now starting to provide glimpses of how this amazing machinery functions and how it might involve remodeling of the lipid bilayer. MD simulations of BamA and the full BAM complex have shown that the presence of the 16-stranded BamA β-barrel causes thinning and disordering of the membrane in the vicinity of its β1–β16 seam and that BamA can switch between conformations at this interface (355–360) (Fig. 8). Other OMPs have been shown to generate variable (*i.e.* anisotropic) membrane thickness around their circumference experimentally (*e.g.* BtuB, 22-stranded) (361), and more isotropic bilayer thinning is seen in A-MD and CG-MD simulations in the vicinity of many OMPs (OprH (8-stranded from *P. aeruginosa*), OmpA, LpxR (12-stranded from *S. typhimurium*), Hia (3 × 4 strands from *Hemophilus influenzae*), OmPLA, NanC, OmpF, LamB, and FhuA) (186, 209, 248, 249, 267, 274, 359, 362). Although the dynamics of lipids surrounding BamA have not yet been studied *in vitro* or *in vivo* (*e.g.* by using spin-labeled lipids), experiments examining the lipids directly surrounding other OMPs have found them to be motionally restricted in the vicinity of the β-barrel, as seen for FomA (8-stranded from *Fusobacterium nucleatum*), OmpA, OmpG, and FhuA (363–365). This has also been observed in CG-MD simulations of OmpA, NanC, OmpF, LamB, and FhuA in a bilayer formed from 75% POPE ($C_{16:0}C_{18:1}$PE), 25% POPG ($C_{16:0}C_{18:1}$PG) (186). It should be noted, however, that it is not certain that the two parameters of lipid order and motional restriction are always correlated—consider a situation where disordered lipids are corralled by ordered lipids. With current data, it is unclear whether the lipid disordering observed around the β1–β16 seam of BamA is purely a consequence of membrane thinning (*i.e.* a large hydrophobic mismatch) or is accentuated by some other mechanism in this OMP. Evidence for such a reaction cycle that could support a membrane-

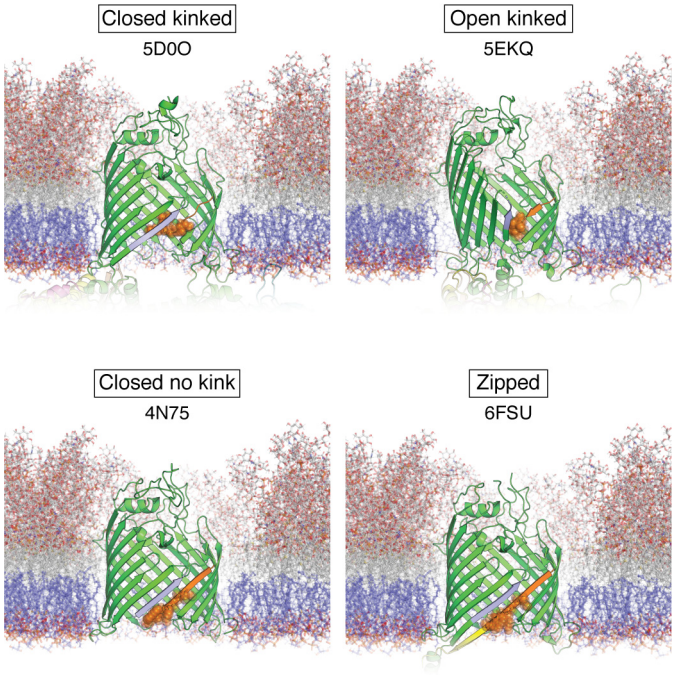

Figure 8. Conformations of the BamA lipid-facing lateral gate. Shown are example structures of *E. coli* BamA adopting different conformations around the location of the $\beta1$–$\beta16$ seam/gate. BamA has been observed in both gate open and closed states with the open state observed in the presence of other BAM subunits but not in structures of BamA in isolation. Furthermore, in all structures of the full BAM complex, $\beta16$ of BamA adopts a kinked conformation at a highly conserved glycine (Gly^{807}) in both the open (PDB code 5EKQ; BamACDE) (368) and closed (PDB code 5D0O; BamABCDE) (357) states of the gate. Residues Asn^{427}–Gly^{433} ($\beta1$) are *highlighted* in *light blue*, residues Phe^{802}–Trp^{810} ($\beta16$) are indicated in *orange*, and the kink is further highlighted with *spheres* (Ile^{806}–Trp^{810}). This kink is also observed in structures of BamA from *Salmonella enterica* (PDB code 5OR1) (370) and *Neisseria gonorrhoeae* (PDB code 4K3B) (355) (not shown) and in the BamA homologue, TamA, which also plays a role in OMP assembly (PDB codes 4N74 and 4C00) (387) (not shown). BamA with a closed gate and no kink has been observed in isolation (PDB code 4N75; BamAΔ1–427) (366) and in a hybrid BamA containing a C-terminal 9-residue extension (*colored yellow*) comprised of part of turn 3 and $\beta7$ from OmpX, which may represent a mimic of an OMP-BamA folding intermediate (PDB code 6FSU) (371). Structures are represented in an asymmetric bilayer with a mixture of phospholipids with 14-18 carbon acyl chains (shown in *violet*) in the inner leaflet and *E. coli* rough LPS in the outer leaflet (acyl chains in *white*). Note the different hydrophobic thickness between each leaflet. Asymmetric bilayer was built using the GNOMM server (402).

remodeling mechanism for BamA was suggested from crystal structures of BamA in isolation and from crystal and cryo-EM structures of BamA in the BAM complex. These studies showed that the BamA β-barrel is shorter in the $\beta1$–$\beta16$ region than in the rest of the barrel and that it can explore at least three distinct and potentially membrane-influencing conformations: a closed fully zipped (*i.e.* hydrogen-bonded along its whole seam) barrel (Fig. 8, closed no kink and zipped), a closed partially zipped barrel (Fig. 8, closed kink), and an open barrel (Fig. 8, open kinked) (42, 91, 355, 357, 366–371). This open conformation was surprising, as it would intuitively seem highly energetically unfavorable to break hydrogen bonds in a hydrophobic environment. However, WT BamA is only capable of forming at most 6-8 backbone hydrogen bonds between its first and last β-strands (Fig. 8, closed no kink). MD simulations showed that this fully hydrogen-bonded conformation is unstable and eventually forms the "partially zipped/closed kink" conformation seen in structures of the full BAM complex (Fig. 8, closed kink) where the terminal strand bends back into the barrel lumen, leaving just 2–3 hydrogen bonds (360). This partially zipped state may lower the energetic cost of fully opening the BamA barrel (360), leaving at most one hydrogen bond between $\beta1$ and the periplasmic turn between $\beta15$ and $\beta16$. This periplasmic turn is likely to be important in stabilizing this open state, as its mutation or truncation is lethal *in vivo* (370). This still requires the breaking of 5–7 hydrogen bonds, but some of this may be compensated by the kinked residues hydrogen-bonding to water within the lumen of the BamA barrel. Furthermore, the cost for OMPs to break hydrogen bonds in the membrane may be lower than previously assumed (372), and the outer leaflet of the OM may be more hydrated than a symmetric phospholipid bilayer. These effects could help stabilize the structure of BamA while effecting local changes in packing or stability of the membrane. The importance of this BamA barrel opening was highlighted by the lethality of disulfide bonds engineered to lock the barrel closed (356) or open (357). Interestingly, folding of OmpT and OmpX via BamA or the full BAM complex *in vitro* is still catalyzed in the locked closed state (42, 373). This implies that the structure of BamA alone, with its reduced hydrophobic thickness around $\beta1$–$\beta16$, may intrinsically accelerate OMP folding by distorting the membrane—even in the absence of the open state. *In vitro*, BamA has been shown to have a greater catalytic effect on tOmpA folding (higher catalytic fold rate enhancement) as the hydrophobic thickness of a bilayer is increased from ~19.5 Å in DLPC ($diC_{12:0}PC$) LUVs to ~23.0 Å in DMPC ($diC_{14:0}PC$) LUVs, showing that hydrophobic mismatch and/or lipid disordering plays an important role in the mechanism of BamA-assisted folding (359). These data illustrate how both structural and biochemical approaches will be required to fully understand the function of the BAM complex.

Recent studies have also shown the importance of BAM and membrane fluidity in folding OMPs *in vivo.* These studies exploited a mAb that was found to be bactericidal, binding to extracellular loop 6 of BamA (93). Interestingly, bacteria showing spontaneous resistance to this BAM-mediated toxicity were found to have mutations in the *lpxM* gene. This protein transfers a C14 (myristoyl) chain to penta-acylated LPS, creating hexa-acylated LPS (93). Antibody sensitivity was restored (*i.e.* bactericidal effects of the antibody were reinstated) when *lpxM* was expressed from a plasmid. Assays of membrane fluidity using a pyrene-based probe showed that membrane fluidity decreased in the resistant strains, and this effect was recapitulated in other conditions that decrease membrane fluidity (high salt, longer LPS sugar region, lower temperature) (80, 93). The levels of OMPs were not reduced in Δ*lpxM* strains in the absence of the antibody. This suggests that there is a mechanistic link between BamA/BAM and membrane fluidity, as BAM is most sensitive to inhibition when the membrane is more fluid. Hence BamA activity (as part of the BAM complex) may be lower when the OM is excessively fluid, confirming a link between OMP-folding efficiency, BAM activity, and membrane fluidity *in vivo.* More generally, it is interesting to consider the role of the lipids that directly surround BAM and how they might interact with it. Most MD studies on BamA have utilized

simple lipid mixtures (355–360). However, it is known that membrane proteins can enrich lipids or other proteins around them that match their hydrophobic thickness (374–376). In the context of BAM, this may have two consequences. First, shorter-chain lipids may be enriched around the β1–β16 seam to reduce the energetic penalty of membrane thinning, with $C_{12:0}$ and $C_{14:0}$ acyl tails found in *E. coli* and also reported to be more abundant in the OM than the IM (139). Second, the hydrophobic thickness of substrate OMPs is generally greater than that of BamA. This means immediately after insertion into the region surrounding the BamA β1–β16 seam, the newly folded or folding OMPs will encounter a region of positive hydrophobic mismatch (Fig. 5), and it may be energetically favorable for them to diffuse away to regions of greater hydrophobic thickness with a more optimal match to their size (376). This could provide a mechanism for release and local clearance of newly folded OMPs from BAM. Furthermore, although substrate binding to BAM subunits or the POTRA domains of BamA is likely to be important in conformational cycling (60, 377–382), the lateral pressure or fluidity (Fig. 5) within the OM might also play a role in controlling opening and closing of the BamA barrel. These dynamics are thought to be essential for its role in catalyzing OMP folding *in vivo* (356, 383), so modulation of the BamA barrel dynamics by the lipid environment may also provide a secondary mechanism of controlling the function of BAM.

A multifaceted mechanism for the BAM complex

Growing evidence points to a mechanism of BAM function in catalyzing OMP folding and membrane insertion that involves the templating of C-terminal β-strands of the nascent substrate OMPs onto the β1 strand of BamA (Figs. 6–8) (47, 61, 384). The C-terminal strands of OMPs in bacteria and mitochondria contain a conserved aromatic-rich motif termed the β-signal (Fig. 6), which may be important in the recognition of OMP clients by the BAM complex (385, 386). The initial recognition of the OMP's C-terminal strand is thought to then trigger nucleation of further β-hairpins to the growing β-barrel, perhaps favored by the reduced entropic penalty of folding (as the degrees of freedom of the unfolded chain are reduced). However, the steps following this initial binding event, particularly how the β-barrel of the newly forming OMP folds and inserts into the membrane, remain unclear. A role for the lateral gate of BamA in this process was proposed after the first structures of this family of proteins were solved (355, 387, 388). Further experimental evidence suggests four possible models for how this is achieved (Fig. 7*B*). 1) BamA plays a passive role in OMP folding/insertion and merely targets nascent OMPs to a destabilized bilayer in front of its β1–β16 seam. Substrate binding possibly initiates a conformational change in BamA, increasing its "lipid disorderase" activity, but folding otherwise proceeds as in the *in vitro* pathway (Fig. 7*A*) (the assisted model) (388). 2) The β-barrel grows laterally into the membrane after templating onto the BamA gate (the budding model) (384, 388). 3) Prefolding/elongation of the OMP occurs in the periplasm after binding to β1 of BamA. A conformational change in BAM then inserts the already-folded β-barrel (the swing/elongation models) (47, 389). 4) Substrates fold against the interior wall of BamA while keeping their N and C termini in close proximity ready for β-barrel closure and release into the membrane (the lumen-catalyzed model) (61). The last two models are particularly intriguing as they suggest that the hydrophobic surface of the folding OMP is partially exposed to an aqueous or polar environment. How this step could be energetically favorable is not yet clear, but some authors have proposed that the cradle created by the BamA lumen and POTRA domains may aid folding by acting like an entropic cage, analogous to chaperonins such as GroEL/ES (61, 389). This may drive folding by reducing the conformational entropy of the unfolded state but may also restrict the mobility of water, perhaps offsetting some of the cost of exposing hydrophobic residues.

Through its mechanism of β-strand capture, the BAM complex may also act to suppress the reversible off-pathway intermediates in OMP folding that cause kinetic retardation of folding *in vitro* and which may be related to both misfolded monomeric intermediates and aberrant transient intermolecular interactions (351). Furthermore, these aberrant multimers (so called "elusive" states as they are not easily observed by SDS-PAGE) are not observed in the absence of a lipid bilayer (351), implicating the OMP-membrane interaction as an important control point where these states could form. The nature of the terminal stages of folding, including how the OMP is able to partition rapidly into the OM and how it overcomes the activation energy barrier associated with membrane insertion, remain unresolved. Finally, the enrichment of shorter-chain phospholipids and depletion of OMPs around BamA proposed above would essentially "clear some space" for folding to proceed (*e.g.* see Fig. 3*C*), providing a mechanism that could overcome the remarkably low LPR of the OM and an inner leaflet crowded with OMPs and lipoproteins. The proposed formation of "supercomplexes" that span the periplasm linking the IM SecYEG translocon and the BAM complex at the OM could also provide a direct conduit for OMP biogenesis (390–392). If only limited patches of free lipid exist, it would be important to direct OMPs to these regions of the OM before they misfold or aggregate.

Comparison of folding *in vitro* and *in vivo*

Our current knowledge about the physical constraints of OMP folding into lipid bilayers, the properties of the OM, the folding of OMPs *in vitro*, and the mechanism of BAM action all point to the membrane as an important interface for preorganization of OMPs into an insertion-competent state. Despite clear evidence for the importance of this early folding step, the unusually low LPR of the OM of *E. coli* (which may be as low as 6–14:1) (139, 156, 157) calls into question the direct interaction of the OMP and the OM during folding *in vivo*. Given this dearth of lipid surface and the observation that the rate of OMP folding falls dramatically with decreasing LPR (316, 331, 332), how do OMPs insert into the OM on a biologically meaningful timescale? Large lipid-rich patches could exist in the OM, but *in vivo* imaging studies have shown that BAM and newly inserted OMPs appear together in protein-rich clusters (56,

149, 181). This means that there are either very few free lipids (Fig. 3*A*) or only small, local, lipid-enriched domains (Fig. 3*C*). Hence, BAM may have evolved to provide an initial nucleation site for OMP folding in a generally lipid-poor environment and to accelerate this process, particularly for rapidly growing organisms such as *E. coli*. This would also be necessary to pack the OM to the high protein density that is observed *in vivo*. Although the recognition of nascent OMPs and the nucleation of β-barrel formation through templating/recognition of the newly folding OMP's β-strands on BamA would provide a rate enhancement in folding, the dramatic differences of folding rates into detergent micelles (fast) *versus* LUVs (slow) suggest that the ability of an OMP to navigate its folding pathway to find the native fold is not necessarily a major rate-limiting factor. Instead, it appears that membrane insertion and disruption of lipid packing could play a more significant role in controlling the rate of folding. *In vitro* experiments have shown that the greater the lateral pressure, lipid order, and packing of lipids within a bilayer, the greater the activation energy barrier for folding (41, 339, 340). However, local or transient defects in the packing of lipids in a membrane can allow OMPs to bypass a slower folding pathway and instead fold more rapidly (as shown by studies on the propensity of thinner bilayers and lipids at their T_m to accelerate OMP folding) (40, 343). The physical structure of the OM remains poorly defined, but what we know is this: already-folded OMPs are resistant to deformation in the OM, LPS can rigidify the outer leaflet, and *in vivo* measurements suggest that at least some proportion of lipids in the OM are relatively ordered and less mobile. BAM may introduce local defects into this environment (by thinning of the membrane and causing local disorder of the lipids) to lower the energy barrier to insertion and thus accelerate OMP folding into this otherwise impenetrable membrane barrier.

Concluding remarks and open questions

The OMP-folding problem *in vivo* can be simplified as the interplay between three factors: enzyme (BAM), substrate (OMP), and solvent (lipid). To fully understand OMP folding *in vivo*, it is necessary to characterize the relationships between these three dominating factors to understand their holistic function. BAM acts to catalyze the folding of OMPs into a lipid bilayer, and it may do this by nucleating the folding of the unfolded OMP substrate (BAM-OMP interaction) and/or by locally disrupting the packing of lipids (BAM-lipid interaction) to lower the activation energy of folding (OMP-lipid interaction). The evidence for the action of BAM on lipids is currently restricted to *in silico* experiments, although we can imply its importance from *in vitro* studies of the effect of the physical and chemical properties of the bilayer on OMP folding. More studies are now needed to determine the relative importance of this "disorderase" activity of BAM in ensuring that OMPs can gain access to the highly crowded and lipid-poor OM.

Our current lack of understanding of the physical properties of the OM prevents the generation of accurate models for the mechanism(s) of BAM in the OM, the effect of BAM on the structure and dynamics of the OM lipids (and vice versa), and how these changes impact OMP folding. Although levels of OMPs fall upon depletion of BAM *in vivo*, and OMP insertion kinetics are slowed in the absence of BAM *in vitro*, which OMPs require BAM for folding into the OM *in vivo* is still not known unequivocally. Indeed, some OMPs have been shown to be capable of folding without the aid of BAM, and others are aided by other proteins such as those of the localization of lipoproteins (Lol) machinery (Table 1). The asymmetry of the OM, combined with the mixture of lipid types, high fraction of proteins, and tethering to the peptidoglycan layer, makes the journey taken by a nascent OMP to the OM and its insertion *in vivo* an immensely challenging task to replicate *in vitro*. Future *in vitro* work should focus on understanding the OM and OMP folding in a context closer to that found *in vivo* and also on better understanding the effects of suppressor variants on the catalytic activity of BAM, so as to narrow the gap between *in vivo* and *in vitro* insights. At the same time, modern biophysical and biochemical tools are also needed to make these same measurements directly on OMPs in their native context within bacteria. *En route* to this, the use of outer membrane vesicles directly derived from bacteria may provide an excellent stepping stone (393–395).

In summary, despite enormous progress in our understanding of how OMPs fold *in vitro* and in dissecting the interactions and mechanisms of BAM, we still do not fully understand how BAM folds OMPs of different size and sequence; nor do we understand fully the role of the asymmetric OM lipid bilayer in defining this process. OMP folding has moved in the last few years from a question of fundamental importance and interest to one having direct implications for the development of new antibiotics targeting OM biogenesis. The challenge has thus been set to define how OMPs fold *in vivo* and to solve the remaining mysteries, so that BAM can be targeted to break the OM barrier and render pathogenic bacteria susceptible to attack by new antimicrobial agents.

Acknowledgments—We thank members of the S. E. R. and D. J. B. laboratories and our collaborators for many helpful discussions, particularly the OMP team, including Bob Schiffrin, Anna Higgins, Paul White, Anton Calabrese, James Whitehouse, Sam Haysom, Matt Iadanza, Matt Watson, Roman Tuma, and Neil Ranson.

Funding and additional information—J. E. H. was supported by Biological and Biotechnology Research Council (BBSRC) Grant BB/M01151/1. Work on BAM and OMPs by S. E. R. and D. J. B. was supported by BBSRC Grants BB/K000659/1, BB/T000635/1, and BB/N007603/1 and Medical Research Council Grant MR/P018491/1.

Conflict of interest—The authors declare that they have no conflicts of interest with the contents of this article.

Abbreviations—The abbreviations used are: IM, inner membrane; A-MD, atomistic molecular dynamics; BAM, β-barrel assembly infection with five pathogenic microbes whichmachinery; CG-MD, coarse-grained molecular dynamics; CL, cardiolipin; DDPC, 1,2-didecanoyl-*sn*-glycero-3-phosphocholine; DLPC, 1,2-dilauroyl-*sn*-glycero-3-phosphocholine; DMPC, 1,2-dimyristoyl-*sn*-of C. elegansglycero-3-phosphocholine; DMPG, 1,2-dimyristoyl-*sn*-glycero-3-phosphoglycerol; DOPC, 1,2-dioleoyl-*sn*-glycero-3-phosphocholine; DOPE, 1,2-

dioleoyl-*sn*-glycero-3-phosphoetha-nolamine; DOPG, 1,2-dioleoyl-*sn*-glycero-3-phosphoglycerol; DPPC, 1,2-dipalmitoyl-*sn*-glycero-3-phosphocholine; DPPE, 1,2-dipalmitoyl-*sn*-glycero-3-phosphoethanolamine; DPPG, 1,2-dipalmitoyl-*sn*-glycero-3-phosphoglycerol; IMP, inner membrane protein; LPR, lipid-to-protein ratio; LPS, lipopolysaccharide; LUV, large unilamellar vesicle; MD, molecular dynamics; OM, outer membrane; OMP, outer membrane protein ; PC, phosphatidylcholine; PE, phosphatidylethanolamine; PG, phosphatidylglycerol; POPC, 1-palmitoyl-2-oleoyl-*sn*-glycero-3-phosphocholine; POPE, 1-palmitoyl-2-oleoyl-*sn*-glycero-3-phosphoethanolamine; POPG, 1-palmitoyl-2-oleoyl-*sn*-glycero-3-phosphoglycerol; POTRA domain polypeptide transport–associated domain; PPPE, 1-palmitoyl-2-palmitoleoyl-*sn*-glycero-3-phosphoethanolamine; PVPG, 1-palmitoyl-2-vacenoyl-*sn*-glycero-3-phosphoglycerol; SUV, small unilamellar vesicle; T_m, transition temperature; tOmpA, the β-barrel domain of OmpA; cP, centipoise; AFM, atomic force microscopy; ATR, attenuated total reflection; PDB, Protein Data Bank.

Note added in proof—After this manuscript was accepted for publication, a cryo-EM structure of a substrate-engaged BAM complex purified after stalling *in vivo* was reported supported by *in vivo* cross-linking. This structure shows a late-stage assembly intermediate and, along with the cross-linking data, appears to support model 3 (BamA-swing/elongation) or 4 (BamA lumen-catalyzed) of BAM-catalyzed OMP folding shown in Fig. 7 (403).

References

1. Prilipov, A., Phale, P. S., Koebnik, R., Widmer, C., and Rosenbusch, J. P. (1998) Identification and characterization of two quiescent porin genes, *nmpC* and *ompN*, in *Escherichia coli* BE. *J. Bacteriol.* **180,** 3388–3392 CrossRef Medline
2. Fàbrega, A., Rosner, J. L., Martin, R. G., Solé, M., and Vila, J. (2012) SoxS-dependent coregulation of *ompN* and *ydbK* in a multidrug-resistant *Escherichia coli* strain. *FEMS Microbiol. Lett.* **332,** 61–67 CrossRef Medline
3. Li, G.-W., Burkhardt, D., Gross, C., and Weissman, J. S. (2014) Quantifying absolute protein synthesis rates reveals principles underlying allocation of cellular resources. *Cell* **157,** 624–635 CrossRef Medline
4. Soufi, B., Krug, K., Harst, A., and Macek, B. (2015) Characterization of the *E. coli* proteome and its modifications during growth and ethanol stress. *Front. Microbiol.* **6,** 103 CrossRef Medline
5. Henning, U., Höhn, B., and Sonntag, I. (1973) Cell envelope and shape of *Escherichia coli* K12: the ghost membrane. *Eur. J. Biochem.* **39,** 27–36 CrossRef Medline
6. Rosenbusch, J. P. (1974) Characterization of the major envelope protein from *Escherichia coli*. Regular arrangement on the peptidoglycan and unusual dodecyl sulfate binding. *J. Biol. Chem.* **249,** 8019–8029 Medline
7. Lugtenberg, B., and Van Alphen, L. (1983) Molecular architecture and functioning of the outer membrane of *Escherichia coli* and other Gram-negative bacteria. *Biochim. Biophys. Acta* **737,** 51–115 CrossRef Medline
8. Ye, J., and van den Berg, B. (2004) Crystal structure of the bacterial nucleoside transporter Tsx. *EMBO J.* **23,** 3187–3195 CrossRef Medline
9. Subbarao, G. V., and van den Berg, B. (2006) Crystal structure of the monomeric porin OmpG. *J. Mol. Biol.* **360,** 750–759 CrossRef Medline
10. Wirth, C., Condemine, G., Boiteux, C., Bernèche, S., Schirmer, T., and Peneff, C. M. (2009) NanC crystal structure, a model for outer-membrane channels of the acidic sugar-specific KdgM porin family. *J. Mol. Biol.* **394,** 718–731 CrossRef Medline
11. Vergalli, J., Bodrenko, I. V., Masi, M., Moynié, L., Acosta-Gutiérrez, S., Naismith, J. H., Davin-Regli, A., Ceccarelli, M., van den Berg, B., Winterhalter, M., and Pagès, J.-M. (2019) Porins and small-molecule translocation across the outer membrane of Gram-negative bacteria. *Nat. Rev. Microbiol.* **18,** 164–176 CrossRef Medline
12. Xu, C., Lin, X., Ren, H., Zhang, Y., Wang, S., and Peng, X. (2006) Analysis of outer membrane proteome of *Escherichia coli* related to resistance to ampicillin and tetracycline. *Proteomics* **6,** 462–473 CrossRef Medline
13. Beketskaia, M. S., Bay, D. C., and Turner, R. J. (2014) Outer membrane protein OmpW participates with small multidrug resistance protein member EmrE in quaternary cationic compound efflux. *J. Bacteriol.* **196,** 1908–1914 CrossRef Medline
14. Wang, Z., Fan, G., Hryc, C. F., Blaza, J. N., Serysheva, I. I., Schmid, M. F., Chiu, W., Luisi, B. F., and Du, D. (2017) An allosteric transport mechanism for the AcrAB-TolC multidrug efflux pump. *Elife* **6,** e24905 CrossRef Medline
15. Fitzpatrick, A. W. P., Llabrés, S., Neuberger, A., Blaza, J. N., Bai, X.-C., Okada, U., Murakami, S., van Veen, H. W., Zachariae, U., Scheres, S. H. W., Luisi, B. F., and Du, D. (2017) Structure of the MacAB-TolC ABC-type tripartite multidrug efflux pump. *Nat. Microbiol.* **2,** 17070 CrossRef Medline
16. Noinaj, N., Guillier, M., Barnard, T. J., and Buchanan, S. K. (2010) TonB-dependent transporters: regulation, structure, and function. *Annu. Rev. Microbiol.* **64,** 43–60 CrossRef Medline
17. Lepore, B. W., Indic, M., Pham, H., Hearn, E. M., Patel, D. R., and van den Berg, B. (2011) Ligand-gated diffusion across the bacterial outer membrane. *Proc. Natl. Acad. Sci. U. S. A.* **108,** 10121–10126 CrossRef Medline
18. Aunkham, A., Zahn, M., Kesireddy, A., Pothula, K. R., Schulte, A., Baslé, A., Kleinekathöfer, U., Suginta, W., and van den Berg, B. (2018) Structural basis for chitin acquisition by marine *Vibrio* species. *Nat. Commun.* **9,** 220 CrossRef Medline
19. Rojas, E. R., Billings, G., Odermatt, P. D., Auer, G. K., Zhu, L., Miguel, A., Chang, F., Weibel, D. B., Theriot, J. A., and Huang, K. C. (2018) The outer membrane is an essential load-bearing element in Gram-negative bacteria. *Nature* **559,** 617–621 CrossRef Medline
20. Samsudin, F., Ortiz-Suarez, M. L., Piggot, T. J., Bond, P. J., and Khalid, S. (2016) OmpA: a flexible clamp for bacterial cell wall attachment. *Structure* **24,** 2227–2235 CrossRef Medline
21. Vollmer, W., Von Rechenberg, M., and Höltje, J. V. (1999) Demonstration of molecular interactions between the murein polymerase PBP1B, the lytic transglycosylase MltA, and the scaffolding protein MipA of *Escherichia coli*. *J. Biol. Chem.* **274,** 6726–6734 CrossRef Medline
22. Braun, M., and Silhavy, T. J. (2002) Imp/OstA is required for cell envelope biogenesis in *Escherichia coli*. *Mol. Microbiol.* **45,** 1289–1302 CrossRef Medline
23. Voulhoux, R., Bos, M. P., Geurtsen, J., Mols, M., and Tommassen, J. (2003) Role of a highly conserved bacterial protein in outer membrane protein assembly. *Science* **299,** 262–265 CrossRef Medline
24. Bishop, R. E., Gibbons, H. S., Guina, T., Trent, M. S., Miller, S. I., and Raetz, C. R. H. (2000) Transfer of palmitate from phospholipids to lipid A in outer membranes of Gram-negative bacteria. *EMBO J.* **19,** 5071–5080 CrossRef Medline
25. May, K. L., and Silhavy, T. J. (2018) The *Escherichia coli* phospholipase PldA regulates outer membrane homeostasis via lipid signaling. *MBio* **9,** 11325–11340 CrossRef Medline
26. Stubenrauch, C. J., and Lithgow, T. (2019) The TAM: a translocation and assembly module of the β-barrel assembly machinery in bacterial outer membranes. *EcoSal Plus* **8,** CrossRef Medline
27. Mecsas, J., Welch, R., Erickson, J. W., and Gross, C. A. (1995) Identification and characterization of an outer membrane protein, OmpX, in *Escherichia coli* that is homologous to a family of outer membrane proteins including Ail of *Yersinia enterocolitica*. *J. Bacteriol.* **177,** 799–804 CrossRef Medline
28. Mulvey, M. A., Lopez-Boado, Y. S., Wilson, C. L., Roth, R., Parks, W. C., Heuser, J., and Hultgren, S. J. (1998) Induction and evasion of host defenses by type 1-piliated uropathogenic *Escherichia coli*. *Science* **282,** 1494–1497 CrossRef Medline
29. Du, M., Yuan, Z., Yu, H., Henderson, N., Sarowar, S., Zhao, G., Werneburg, G. T., Thanassi, D. G., and Li, H. (2018) Handover mechanism of the growing pilus by the bacterial outer-membrane usher FimD. *Nature* **562,** 444–447 CrossRef Medline
30. Henderson, I. R., and Owen, P. (1999) The major phase-variable outer membrane protein of *Escherichia coli* structurally resembles

the immunoglobulin A1 protease class of exported protein and is regulated by a novel mechanism involving Dam and oxyR. *J. Bacteriol.* **181,** 2132–2141 CrossRef Medline
31. de Luna, M., das, G., Scott-Tucker, A., Desvaux, M., Ferguson, P., Morin, N. P., Dudley, E. G., Turner, S., Nataro, J. P., Owen, P., and Henderson, I. R. (2008) The *Escherichia coli* biofilm-promoting protein Antigen 43 does not contribute to intestinal colonization. *FEMS Microbiol. Lett.* **284,** 237–246 CrossRef Medline
32. Wang, Y., Andole Pannuri, A., Ni, D., Zhou, H., Cao, X., Lu, X., Romeo, T., and Huang, Y. (2016) Structural basis for translocation of a biofilm-supporting exopolysaccharide across the bacterial outer membrane. *J. Biol. Chem.* **291,** 10046–10057 CrossRef Medline
33. Acheson, J. F., Derewenda, Z. S., and Zimmer, J. (2019) Architecture of the cellulose synthase outer membrane channel and its association with the periplasmic TPR domain. *Structure* **27,** 1855–1861.e3 CrossRef Medline
34. Stumpe, S., Schmid, R., Stephens, D. L., Georgiou, G., and Bakker, E. P. (1998) Identification of OmpT as the protease that hydrolyzes the antimicrobial peptide protamine before it enters growing cells of *Escherichia coli*. *J. Bacteriol.* **180,** 4002–4006 CrossRef Medline
35. Hwang, B.-Y., Varadarajan, N., Li, H., Rodriguez, S., Iverson, B. L., and Georgiou, G. (2007) Substrate specificity of the *Escherichia coli* outer membrane protease OmpP. *J. Bacteriol.* **189,** 522–530 CrossRef Medline
36. Ruiz, N., Kahne, D., and Silhavy, T. J. (2006) Advances in understanding bacterial outer-membrane biogenesis. *Nat. Rev. Microbiol.* **4,** 57–66 CrossRef Medline
37. Lee, J., Xue, M., Wzorek, J. S., Wu, T., Grabowicz, M., Gronenberg, L. S., Sutterlin, H. A., Davis, R. M., Ruiz, N., Silhavy, T. J., and Kahne, D. E. (2016) Characterization of a stalled complex on the β-barrel assembly machine. *Proc. Natl. Acad. Sci. U. S. A.* **113,** 8717–8722 CrossRef Medline
38. Gu, Y., Stansfeld, P. J., Zeng, Y., Dong, H., Wang, W., and Dong, C. (2015) Lipopolysaccharide is inserted into the outer membrane through an intramembrane hole, a lumen gate, and the lateral opening of LptD. *Structure* **23,** 496–504 CrossRef Medline
39. Ricci, D. P., and Silhavy, T. J. (2019) Outer membrane protein insertion by the β-barrel assembly machine. *EcoSal Plus* **8,** CrossRef Medline
40. Burgess, N. K., Dao, T. P., Stanley, A. M., and Fleming, K. G. (2008) β-Barrel proteins that reside in the *Escherichia coli* outer membrane *in vivo* demonstrate varied folding behavior *in vitro*. *J. Biol. Chem.* **283,** 26748–26758 CrossRef Medline
41. Gessmann, D., Chung, Y. H., Danoff, E. J., Plummer, A. M., Sandlin, C. W., Zaccai, N. R., and Fleming, K. G. (2014) Outer membrane β-barrel protein folding is physically controlled by periplasmic lipid head groups and BamA. *Proc. Natl. Acad. Sci. U. S. A.* **111,** 5878–5883 CrossRef Medline
42. Iadanza, M. G., Higgins, A. J., Schiffrin, B., Calabrese, A. N., Brockwell, D. J., Ashcroft, A. E., Radford, S. E., and Ranson, N. A. (2016) Lateral opening in the intact β-barrel assembly machinery captured by cryo-EM. *Nat. Commun.* **7,** 12865 CrossRef Medline
43. Hagan, C. L., Kim, S., and Kahne, D. (2010) Reconstitution of outer membrane protein assembly from purified components. *Science* **328,** 890–892 CrossRef Medline
44. Hagan, C. L., Westwood, D. B., and Kahne, D. (2013) Bam lipoproteins assemble BamA *in vitro*. *Biochemistry* **52,** 6108–6113 CrossRef Medline
45. Patel, G. J., and Kleinschmidt, J. H. (2013) The lipid bilayer-inserted membrane protein BamA of *Escherichia coli* facilitates insertion and folding of outer membrane protein A from its complex with Skp. *Biochemistry* **52,** 3974–3986 CrossRef Medline
46. Hussain, S., and Bernstein, H. D. (2018) The Bam complex catalyzes efficient insertion of bacterial outer membrane proteins into membrane vesicles of variable lipid composition. *J. Biol. Chem.* **293,** 2959–2973 CrossRef Medline
47. Doyle, M. T., and Bernstein, H. D. (2019) Bacterial outer membrane proteins assemble via asymmetric interactions with the BamA β-barrel. *Nat. Commun.* **10,** 3358 CrossRef Medline
48. Ieva, R., and Bernstein, H. D. (2009) Interaction of an autotransporter passenger domain with BamA during its translocation across the bacterial outer membrane. *Proc. Natl. Acad. Sci. U. S. A.* **106,** 19120–19125 CrossRef Medline
49. Sauri, A., Soprova, Z., Wickström, D., de Gier, J.-W., Van der Schors, R. C., Smit, A. B., Jong, W. S. P., and Luirink, J. (2009) The Bam (Omp85) complex is involved in secretion of the autotransporter haemoglobin protease. *Microbiology* **155,** 3982–3991 CrossRef Medline
50. Bodelón, G., Marín, E., and Fernández, L. A. (2009) Role of periplasmic chaperones and BamA (YaeT/Omp85) in folding and secretion of intimin from enteropathogenic *Escherichia coli* strains. *J. Bacteriol.* **191,** 5169–5179 CrossRef Medline
51. Norell, D., Heuck, A., Tran-Thi, T.-A., Götzke, H., Jacob-Dubuisson, F., Clausen, T., Daley, D. O., Braun, V., Müller, M., and Fan, E. (2014) Versatile *in vitro* system to study translocation and functional integration of bacterial outer membrane proteins. *Nat. Commun.* **5,** 5396 CrossRef Medline
52. Roman-Hernandez, G., Peterson, J. H., and Bernstein, H. D. (2014) Reconstitution of bacterial autotransporter assembly using purified components. *Elife* **3,** e04234 CrossRef Medline
53. Klein, K., Sonnabend, M. S., Frank, L., Leibiger, K., Franz-Wachtel, M., Macek, B., Trunk, T., Leo, J. C., Autenrieth, I. B., Schütz, M., and Bohn, E. (2019) Deprivation of the periplasmic chaperone SurA reduces virulence and restores antibiotic susceptibility of multidrug-resistant *Pseudomonas aeruginosa*. *Front. Microbiol.* **10,** 100 CrossRef Medline
54. Ruiz, N., Falcone, B., Kahne, D., and Silhavy, T. J. (2005) Chemical conditionality: a genetic strategy to probe organelle assembly. *Cell* **121,** 307–317 CrossRef Medline
55. Wu, T., Malinverni, J., Ruiz, N., Kim, S., Silhavy, T. J., and Kahne, D. (2005) Identification of a multicomponent complex required for outer membrane biogenesis in *Escherichia coli*. *Cell* **121,** 235–245 CrossRef Medline
56. Rassam, P., Copeland, N. A., Birkholz, O., Tóth, C., Chavent, M., Duncan, A. L., Cross, S. J., Housden, N. G., Kaminska, R., Seger, U., Quinn, D. M., Garrod, T. J., Sansom, M. S. P., Piehler, J., Baumann, C. G., *et al.* (2015) Supramolecular assemblies underpin turnover of outer membrane proteins in bacteria. *Nature* **523,** 333–336 CrossRef Medline
57. Ryan, K. R., Taylor, J. A., and Bowers, L. M. (2010) The BAM complex subunit BamE (SmpA) is required for membrane integrity, stalk growth and normal levels of outer membrane β-barrel proteins in *Caulobacter crescentus*. *Microbiology* **156,** 742–756 CrossRef Medline
58. Werner, J., and Misra, R. (2005) YaeT (Omp85) affects the assembly of lipid-dependent and lipid-independent outer membrane proteins of *Escherichia coli*. *Mol. Microbiol.* **57,** 1450–1459 CrossRef Medline
59. Palomino, C., Marín, E., and Fernández, L. Á. (2011) The fimbrial usher FimD follows the SurA-BamB pathway for its assembly in the outer membrane of *Escherichia coli*. *J. Bacteriol.* **193,** 5222–5230 CrossRef Medline
60. Lee, J., Sutterlin, H. A., Wzorek, J. S., Mandler, M. D., Hagan, C. L., Grabowicz, M., Tomasek, D., May, M. D., Hart, E. M., Silhavy, T. J., and Kahne, D. (2018) Substrate binding to BamD triggers a conformational change in BamA to control membrane insertion. *Proc. Natl. Acad. Sci. U. S. A.* **115,** 2359–2364 CrossRef Medline
61. Lee, J., Tomasek, D., Santos, T. M., May, M. D., Meuskens, I., and Kahne, D. (2019) Formation of a β-barrel membrane protein is catalyzed by the interior surface of the assembly machine protein BamA. *Elife* e49787 CrossRef Medline
62. Chimalakonda, G., Ruiz, N., Chng, S.-S., Garner, R. A., Kahne, D., and Silhavy, T. J. (2011) Lipoprotein LptE is required for the assembly of LptD by the β-barrel assembly machine in the outer membrane of *Escherichia coli*. *Proc. Natl. Acad. Sci. U. S. A.* **108,** 2492–2497 CrossRef Medline
63. Volokhina, E. B., Beckers, F., Tommassen, J., and Bos, M. P. (2009) The β-barrel outer membrane protein assembly complex of *Neisseria meningitidis*. *J. Bacteriol.* **191,** 7074–7085 CrossRef Medline
64. Collin, S., Guilvout, I., Chami, M., and Pugsley, A. P. (2007) YaeT-independent multimerization and outer membrane association of secretin PulD. *Mol. Microbiol.* **64,** 1350–1357 CrossRef Medline
65. Hoang, H. H., Nickerson, N. N., Lee, V. T., Kazimirova, A., Chami, M., Pugsley, A. P., and Lory, S. (2011) Outer membrane targeting of *Pseudomonas aeruginosa* proteins shows variable dependence on the

components of Bam and Lol machineries. *MBio*. **2,** e00246-11 CrossRef Medline
66. Huysmans, G. H. M., Guilvout, I., Chami, M., Nickerson, N. N., and Pugsley, A. P. (2015) Lipids assist the membrane insertion of a BAM-independent outer membrane protein. *Sci. Rep*. **5,** 1–15 CrossRef Medline
67. Dunstan, R. A., Hay, I. D., Wilksch, J. J., Schittenhelm, R. B., Purcell, A. W., Clark, J., Costin, A., Ramm, G., Strugnell, R. A., and Lithgow, T. (2015) Assembly of the secretion pores GspD, Wza and CsgG into bacterial outer membranes does not require the Omp85 proteins BamA or TamA. *Mol. Microbiol*. **97,** 616–629 CrossRef Medline
68. Kazmierczak, B. I., Mielke, D. L., Russel, M., and Model, P. (1994) pIV, a filamentous phage protein that mediates phage export across the bacterial cell envelope, forms a multimer. *J. Mol. Biol*. **238,** 187–198 CrossRef Medline
69. Nickerson, N. N., Abby, S. S., Rocha, E. P. C., Chami, M., and Pugsley, A. P. (2012) A single amino acid substitution changes the self-assembly status of a Type IV piliation secretin. *J. Bacteriol*. **194,** 4951–4958 CrossRef Medline
70. Paschen, S. A., Neupert, W., and Rapaport, D. (2005) Biogenesis of β-barrel membrane proteins of mitochondria. *Trends Biochem. Sci*. **30,** 575–582 CrossRef Medline
71. Surrey, T., and Jähnig, F. (1992) Refolding and oriented insertion of a membrane protein into a lipid bilayer. *Proc. Natl. Acad. Sci. U. S. A*. **89,** 7457–7461 CrossRef Medline
72. Yildirim, M. A., Goh, K.-I., Cusick, M. E., Barabási, A.-L., and Vidal, M. (2007) Drug-target network. *Nat. Biotechnol*. **25,** 1119–1126 CrossRef Medline
73. Yin, H., and Flynn, A. D. (2016) Drugging membrane protein interactions. *Annu. Rev. Biomed. Eng*. **18,** 51–76 CrossRef Medline
74. Genevrois, S., Steeghs, L., Roholl, P., Letesson, J.-J., and van der Ley, P. (2003) The Omp85 protein of *Neisseria meningitidis* is required for lipid export to the outer membrane. *EMBO J*. **22,** 1780–1789 CrossRef Medline
75. Wiedemann, N., Kozjak, V., Chacinska, A., Schönfisch, B., Rospert, S., Ryan, M. T., Pfanner, N., and Meisinger, C. (2003) Machinery for protein sorting and assembly in the mitochondrial outer membrane. *Nature* **424,** 565–571 CrossRef Medline
76. Paschen, S. A., Waizenegger, T., Stan, T., Preuss, M., Cyrklaff, M., Hell, K., Rapaport, D., and Neupert, W. (2003) Evolutionary conservation of biogenesis of β-barrel membrane proteins. *Nature* **426,** 862–866 CrossRef Medline
77. Kozjak, V., Wiedemann, N., Milenkovic, D., Lohaus, C., Meyer, H. E., Guiard, B., Meisinger, C., and Pfanner, N. (2003) An essential role of Sam50 in the protein sorting and assembly machinery of the mitochondrial outer membrane. *J. Biol. Chem*. **278,** 48520–48523 CrossRef Medline
78. Nikaido, H. (2003) Molecular basis of bacterial outer membrane permeability revisited. *Microbiol. Mol. Biol. Rev*. **67,** 593–656 CrossRef Medline
79. Domínguez-Medina, C. C., Pérez-Toledo, M., Schager, A. E., Marshall, J. L., Cook, C. N., Bobat, S., Hwang, H., Chun, B. J., Logan, E., Bryant, J. A., Channell, W. M., Morris, F. C., Jossi, S. E., Alshayea, A., Rossiter, A. E., *et al*. (2020) Outer membrane protein size and LPS O-antigen define protective antibody targeting to the *Salmonella* surface. *Nat. Commun*. **11,** 851 CrossRef Medline
80. Storek, K. M., Vij, R., Sun, D., Smith, P. A., Koerber, J. T., and Rutherford, S. T. (2018) The *Escherichia coli* β-barrel assembly machinery is sensitized to perturbations under high membrane fluidity. *J. Bacteriol*. **201,** 1–15 CrossRef Medline
81. Bentley, A. T., and Klebba, P. E. (1988) Effect of lipopolysaccharide structure on reactivity of antiporin monoclonal antibodies with the bacterial cell surface. *J. Bacteriol*. **170,** 1063–1068 CrossRef Medline
82. Storek, K. M., Chan, J., Vij, R., Chiang, N., Lin, Z., Bevers, J., Koth, C. M., Vernes, J.-M., Meng, Y. G., Yin, J., Wallweber, H., Dalmas, O., Shriver, S., Tam, C., Schneider, K., *et al*. (2019) Massive antibody discovery used to probe structure-function relationships of the essential outer membrane protein LptD. *Elife* **8,** e46258 CrossRef Medline
83. Ellenrieder, L., Mårtensson, C. U., and Becker, T. (2015) Biogenesis of mitochondrial outer membrane proteins, problems and diseases. *Biol. Chem*. **396,** 1199–1213 CrossRef Medline
84. Tacconelli, E., Carrara, E., Savoldi, A., Harbarth, S., Mendelson, M., Monnet, D. L., Pulcini, C., Kahlmeter, G., Kluytmans, J., Carmeli, Y., Ouellette, M., Outterson, K., Patel, J., Cavaleri, M., Cox, E. M., *et al*. (2018) Discovery, research, and development of new antibiotics: the WHO priority list of antibiotic-resistant bacteria and tuberculosis. *Lancet Infect. Dis*. **18,** 318–327 CrossRef Medline
85. Srinivas, N., Jetter, P., Ueberbacher, B. J., Werneburg, M., Zerbe, K., Steinmann, J., Van der Meijden, B., Bernardini, F., Lederer, A., Dias, R. L. A., Misson, P. E., Henze, H., Zumbrunn, J., Gombert, F. O., Obrecht, D., *et al*. (2010) Peptidomimetic antibiotics target outer-membrane biogenesis in *Pseudomonas aeruginosa*. *Science* **327,** 1010–1013 CrossRef Medline
86. Wedege, E., Lie, K., Bolstad, K., Weynants, V. E., Halstensen, A., Herstad, T. K., Kreutzberger, J., Nome, L., Naess, L. M., and Aase, A. (2013) Meningococcal *omp85* in detergent-extracted outer membrane vesicle vaccines induces high levels of non-functional antibodies in mice. *Scand. J. Immunol*. **77,** 452–459 CrossRef Medline
87. Vetterli, S. U., Moehle, K., and Robinson, J. A. (2016) Synthesis and antimicrobial activity against *Pseudomonas aeruginosa* of macrocyclic β-hairpin peptidomimetic antibiotics containing *N*-methylated amino acids. *Bioorg. Med. Chem*. **24,** 6332–6339 CrossRef Medline
88. Machutta, C. A., Kollmann, C. S., Lind, K. E., Bai, X., Chan, P. F., Huang, J., Ballell, L., Belyanskaya, S., Besra, G. S., Barros-Aguirre, D., Bates, R. H., Centrella, P. A., Chang, S. S., Chai, J., Choudhry, A. E., *et al*. (2017) Prioritizing multiple therapeutic targets in parallel using automated DNA-encoded library screening. *Nat. Commun*. **8,** 16081 CrossRef Medline
89. Vij, R., Lin, Z., Chiang, N., Vernes, J.-M., Storek, K. M., Park, S., Chan, J., Meng, Y. G., Comps-Agrar, L., Luan, P., Lee, S., Schneider, K., Bevers, J., Zilberleyb, I., Tam, C., *et al*. (2018) A targeted boost-and-sort immunization strategy using *Escherichia coli*: BamA identifies rare growth inhibitory antibodies. *Sci. Rep*. **8,** 7136 CrossRef Medline
90. Ghequire, M. G. K., Swings, T., Michiels, J., Buchanan, S. K., and De Mot, R. (2018) Hitting with a BAM: selective killing by lectin-like bacteriocins. *MBio* **9,** e02138-17 CrossRef Medline
91. Kaur, H., Hartmann, J.-B., Jakob, R. P., Zahn, M., Zimmermann, I., Maier, T., Seeger, M. A., and Hiller, S. (2019) Identification of conformation-selective nanobodies against the membrane protein insertase BamA by an integrated structural biology approach. *J. Biomol. NMR* **73,** 375–384 CrossRef Medline
92. Ghequire, M. G. K., and De Mot, R. (2019) LlpB represents a second subclass of lectin-like bacteriocins. *Microb. Biotechnol*. **12,** 567–573 CrossRef Medline
93. Storek, K. M., Auerbach, M. R., Shi, H., Garcia, N. K., Sun, D., Nickerson, N. N., Vij, R., Lin, Z., Chiang, N., Schneider, K., Wecksler, A. T., Skippington, E., Nakamura, G., Seshasayee, D., Koerber, J. T., *et al*. (2018) Monoclonal antibody targeting the β-barrel assembly machine of *Escherichia coli* is bactericidal. *Proc. Natl. Acad. Sci. U. S. A*. **115,** 3692–3697 CrossRef Medline
94. Psonis, J. J., Chahales, P., Henderson, N. S., Rigel, N. W., Hoffman, P. S., and Thanassi, D. G. (2019) The small molecule nitazoxanide selectively disrupts BAM-mediated folding of the outer membrane usher protein. *J. Biol. Chem*. **294,** 14357–14369 CrossRef Medline
95. Steenhuis, M., Abdallah, A. M., de Munnik, S. M., Kuhne, S., Sterk, G.-J., van den Berg van Saparoea, B., Westerhausen, S., Wagner, S., van der Wel, N. N., Wijtmans, M., van Ulsen, P., Jong, W. S. P., and Luirink, J. (2019) Inhibition of autotransporter biogenesis by small molecules. *Mol. Microbiol*. **112,** 81–98 CrossRef Medline
96. Luther, A., Urfer, M., Zahn, M., Müller, M., Wang, S., Mondal, M., Vitale, A., Hartmann, J., Sharpe, T., Monte, F. L., Kocherla, H., Cline, E., Pessi, G., Rath, P., Modaresi, S. M., *et al*. (2019) Chimeric peptidomimetic antibiotics against Gram-negative bacteria. *Nature* **576,** 452–458 CrossRef Medline
97. Imai, Y., Meyer, K. J., Iinishi, A., Favre-Godal, Q., Green, R., Manuse, S., Caboni, M., Mori, M., Niles, S., Ghiglieri, M., Honrao, C., Ma, X., Guo, J. J., Makriyannis, A., Linares-Otoya, L., *et al*. (2019) A new

antibiotic selectively kills Gram-negative pathogens. *Nature* **576,** 459–464 CrossRef Medline
98. Hart, E. M., Mitchell, A. M., Konovalova, A., Grabowicz, M., Sheng, J., Han, X., Rodriguez-Rivera, F. P., Schwaid, A. G., Malinverni, J. C., Balibar, C. J., Bodea, S., Si, Q., Wang, H., Homsher, M. F., Painter, R. E., *et al.* (2019) A small-molecule inhibitor of BamA impervious to efflux and the outer membrane permeability barrier. *Proc. Natl. Acad. Sci. U. S. A.* **116,** 21748–21757 CrossRef Medline
99. Henderson, J. C., Zimmerman, S. M., Crofts, A. A., Boll, J. M., Kuhns, L. G., Herrera, C. M., and Trent, M. S. (2016) The power of asymmetry: architecture and assembly of the Gram-negative outer membrane lipid bilayer. *Annu. Rev. Microbiol.* **70,** 255–278 CrossRef Medline
100. Kim, S., Patel, D. S., Park, S., Slusky, J., Klauda, J. B., Widmalm, G., and Im, W. (2016) Bilayer properties of lipid A from various Gram-negative bacteria. *Biophys. J.* **111,** 1750–1760 CrossRef Medline
101. Kosma, P. (1999) Chlamydial lipopolysaccharide. *Biochim. Biophys. Acta* **1455,** 387–402 CrossRef Medline
102. Raetz, C. R. H., and Whitfield, C. (2002) Lipopolysaccharide endotoxins. *Annu. Rev. Biochem.* **71,** 635–700 CrossRef Medline
103. Silipo, A., De Castro, C., Lanzetta, R., Molinaro, A., and Parrilli, M. (2004) Full structural characterization of the lipid A components from the *Agrobacterium tumefaciens* strain C58 lipopolysaccharide fraction. *Glycobiology* **14,** 805–815 CrossRef Medline
104. Albitar-Nehme, S., Basheer, S. M., Njamkepo, E., Brisson, J.-R., Guiso, N., and Caroff, M. (2013) Comparison of lipopolysaccharide structures of *Bordetella pertussis* clinical isolates from pre- and post-vaccine era. *Carbohydr. Res.* **378,** 56–62 CrossRef Medline
105. Zähringer, U., Lindner, B., and Rietschel, E. T. (1994) Molecular structure of lipid A, the endotoxic center of bacterial lipopolysaccharides. *Adv. Carbohydr. Chem. Biochem.* **50,** 211–276 Medline
106. Miller, S. I., Ernst, R. K., and Bader, M. W. (2005) LPS, TLR4 and infectious disease diversity. *Nat. Rev. Microbiol.* **3,** 36–46 CrossRef Medline
107. Steimle, A., Autenrieth, I. B., and Frick, J.-S. (2016) Structure and function: lipid A modifications in commensals and pathogens. *Int. J. Med. Microbiol.* **306,** 290–301 CrossRef Medline
108. DeChavigny, A., Heacock, P. N., and Dowhan, W. (1991) Sequence and inactivation of the *pss* gene of *Escherichia coli*: phosphatidylethanolamine may not be essential for cell viability. *J. Biol. Chem.* **266,** 5323–5332 Medline
109. Rowlett, V. W., Mallampalli, V. K. P. S., Karlstaedt, A., Dowhan, W., Taegtmeyer, H., Margolin, W., and Vitrac, H. (2017) Impact of membrane phospholipid alterations in *Escherichia coli* on cellular function and bacterial stress adaptation. *J. Bacteriol.* **199,** 1–22 CrossRef Medline
110. Kikuchi, S., Shibuya, I., and Matsumoto, K. (2000) Viability of an *Escherichia coli pgsA* null mutant lacking detectable phosphatidylglycerol and cardiolipin. *J. Bacteriol.* **182,** 371–376 CrossRef Medline
111. Matsumoto, K. (2001) Dispensable nature of phosphatidylglycerol in *Escherichia coli*: dual roles of anionic phospholipids. *Mol. Microbiol.* **39,** 1427–1433 CrossRef Medline
112. Tan, B. K., Bogdanov, M., Zhao, J., Dowhan, W., Raetz, C. R. H., and Guan, Z. (2012) Discovery of a cardiolipin synthase utilizing phosphatidylethanolamine and phosphatidylglycerol as substrates. *Proc. Natl. Acad. Sci. U. S. A.* **109,** 16504–16509 CrossRef Medline
113. Chen, F., Zhao, Q., Cai, X., Lv, L., Lin, W., Yu, X., Li, C., Li, Y., Xiong, M., and Wang, X.-G. (2009) Phosphatidylcholine in membrane of *Escherichia coli* changes bacterial antigenicity. *Can. J. Microbiol.* **55,** 1328–1334 CrossRef Medline
114. Geiger, O., López-Lara, I. M., and Sohlenkamp, C. (2013) Phosphatidylcholine biosynthesis and function in bacteria. *Biochim. Biophys. Acta* **1831,** 503–513 CrossRef Medline
115. Wikström, M., Kelly, A. A., Georgiev, A., Eriksson, H. M., Klement, M. R., Bogdanov, M., Dowhan, W., and Wieslander, A. (2009) Lipid-engineered *Escherichia coli* membranes reveal critical lipid headgroup size for protein function. *J. Biol. Chem.* **284,** 954–965 CrossRef Medline
116. Caforio, A., Siliakus, M. F., Exterkate, M., Jain, S., Jumde, V. R., Andringa, R. L. H., Kengen, S. W. M., Minnaard, A. J., Driessen, A. J. M., and van der Oost, J. (2018) Converting *Escherichia coli* into an archaebacterium with a hybrid heterochiral membrane. *Proc. Natl. Acad. Sci. U. S. A.* **115,** 3704–3709 CrossRef Medline
117. Rossi, R. M., Yum, L., Agaisse, H., and Payne, S. M. (2017) Cardiolipin synthesis and outer membrane localization are required for *Shigella flexneri* virulence. *MBio* **8,** e01199-17 CrossRef Medline
118. Oliver, P. M., Crooks, J. A., Leidl, M., Yoon, E. J., Saghatelian, A., and Weibel, D. B. (2014) Localization of anionic phospholipids in *Escherichia coli* cells. *J. Bacteriol.* **196,** 3386–3398 CrossRef Medline
119. Koppelman, C. M., Den Blaauwen, T., Duursma, M. C., Heeren, R. M., and Nanninga, N. (2001) *Escherichia coli* minicell membranes are enriched in cardiolipin. *J. Bacteriol.* **183,** 6144–6147 CrossRef Medline
120. Suzuki, M., Hara, H., and Matsumoto, K. (2002) Envelope disorder of *Escherichia coli* cells lacking phosphatidylglycerol. *J. Bacteriol.* **184,** 5418–5425 CrossRef Medline
121. Nakayama, H., Kurokawa, K., and Lee, B. L. (2012) Lipoproteins in bacteria: structures and biosynthetic pathways. *FEBS J.* **279,** 4247–4268 CrossRef Medline
122. Grabowicz, M., and Silhavy, T. J. (2017) Redefining the essential trafficking pathway for outer membrane lipoproteins. *Proc. Natl. Acad. Sci. U. S. A.* **114,** 4769–4774 CrossRef Medline
123. Grabowicz, M. (2018) Lipoprotein transport: greasing the machines of outer membrane biogenesis: re-examining lipoprotein transport mechanisms among diverse Gram-negative bacteria while exploring new discoveries and questions. *Bioessays* **40,** e1700187 CrossRef Medline
124. McMorran, L. M., Brockwell, D. J., and Radford, S. E. (2014) Mechanistic studies of the biogenesis and folding of outer membrane proteins *in vitro* and *in vivo*: what have we learned to date? *Arch. Biochem. Biophys.* **564,** 265–280 CrossRef Medline
125. Bai, J., and Pagano, R. E. (1997) Measurement of spontaneous transfer and transbilayer movement of BODIPY-labeled lipids in lipid vesicles. *Biochemistry* **36,** 8840–8848 CrossRef Medline
126. Nakano, M., Fukuda, M., Kudo, T., Matsuzaki, N., Azuma, T., Sekine, K., Endo, H., and Handa, T. (2009) Flip-flop of phospholipids in vesicles: kinetic analysis with time-resolved small-angle neutron scattering. *J. Phys. Chem. B* **113,** 6745–6748 CrossRef Medline
127. Vaara, M., and Vaara, T. (1983) Polycations as outer membrane-disorganizing agents. *Antimicrob. Agents Chemother.* **24,** 114–122 CrossRef Medline
128. Paul, S., Chaudhuri, K., Chatterjee, A. N., and Das, J. (1992) Presence of exposed phospholipids in the outer membrane of *Vibrio cholerae*. *J. Gen. Microbiol.* **138,** 755–761 CrossRef Medline
129. Contreras, F.-X., Sánchez-Magraner, L., Alonso, A., and Goñi, F. M. (2010) Transbilayer (flip-flop) lipid motion and lipid scrambling in membranes. *FEBS Lett.* **584,** 1779–1786 CrossRef Medline
130. Malinverni, J. C., and Silhavy, T. J. (2009) An ABC transport system that maintains lipid asymmetry in the Gram-negative outer membrane. *Proc. Natl. Acad. Sci. U. S. A.* **106,** 8009–8014 CrossRef Medline
131. Abellón-Ruiz, J., Kaptan, S. S., Baslé, A., Claudi, B., Bumann, D., Kleinekathöfer, U., and van den Berg, B. (2017) Structural basis for maintenance of bacterial outer membrane lipid asymmetry. *Nat. Microbiol.* **2,** 1616–1623 CrossRef Medline
132. Powers, M. J., and Trent, M. S. (2019) Intermembrane transport: glycerophospholipid homeostasis of the Gram-negative cell envelope. *Proc. Natl. Acad. Sci. U. S. A.* **116,** 17147–17155 CrossRef Medline
133. Ingram, L. O. (1977) Changes in lipid composition of *Escherichia coli* resulting from growth with organic solvents and with food additives. *Appl. Environ. Microbiol.* **33,** 1233–1236 CrossRef Medline
134. McGarrity, J. T., and Armstrong, J. B. (1981) The effect of temperature and other growth conditions on the fatty acid composition of *Escherichia coli*. *Can. J. Microbiol.* **27,** 835–840 CrossRef Medline
135. Ingram, L. O. (1982) Regulation of fatty acid composition in *Escherichia coli*: a proposed common mechanism for changes induced by ethanol, chaotropic agents, and a reduction of growth temperature. *J. Bacteriol.* **149,** 166–172 CrossRef
136. Arneborg, N., Salskov-Iversen, A., and Mathiasen, T. (1993) The effect of growth rate and other growth conditions on the lipid composition of *Escherichia coli*. *Appl. Microbiol. Biotechnol.* **39,** 353–357 CrossRef

137. Gidden, J., Denson, J., Liyanage, R., Ivey, D. M., and Lay, J. O. (2009) Lipid compositions in *Escherichia coli* and *Bacillus subtilis* during growth as determined by MALDI-TOF and TOF/TOF mass spectrometry. *Int. J. Mass Spectrom.* **283,** 178–184 CrossRef Medline
138. Jeucken, A., Molenaar, M. R., van de Lest, C. H. A., Jansen, J. W. A., Helms, J. B., and Brouwers, J. F. (2019) A comprehensive functional characterization of *Escherichia coli* lipid genes. *Cell Rep.* **27,** 1597–1606.e2 CrossRef Medline
139. Overath, P., Brenner, M., Gulik-Krzywicki, T., Shechter, E., and Letellier, L. (1975) Lipid phase transitions in cytoplasmic and outer membranes of *Escherichia coli*. *Biochim. Biophys. Acta* **389,** 358–369 CrossRef Medline
140. Oursel, D., Loutelier-Bourhis, C., Orange, N., Chevalier, S., Norris, V., and Lange, C. M. (2007) Identification and relative quantification of fatty acids in *Escherichia coli* membranes by gas chromatography/mass spectrometry. *Rapid Commun. Mass Spectrom.* **21,** 3229–3233 CrossRef Medline
141. Oursel, D., Loutelier-Bourhis, C., Orange, N., Chevalier, S., Norris, V., and Lange, C. M. (2007) Lipid composition of membranes of *Escherichia coli* by liquid chromatography/tandem mass spectrometry using negative electrospray ionization. *Rapid Commun. Mass Spectrom.* **21,** 1721–1728 CrossRef Medline
142. Wang, A. -Y., and Cronan, J. E. (1994) The growth phase-dependent synthesis of cyclopropane fatty acids in *Escherichia coli* is the result of an RpoS(KatF)-dependent promoter plus enzyme instability. *Mol. Microbiol.* **11,** 1009–1017 CrossRef Medline
143. Grogan, D. W., and Cronan, J. E. (1997) Cyclopropane ring formation in membrane lipids of bacteria. *Microbiol. Mol. Biol. Rev.* **61,** 429–441 CrossRef Medline
144. Chang, Y. Y., and Cronan, J. E. (1999) Membrane cyclopropane fatty acid content is a major factor in acid resistance of *Escherichia coli*. *Mol. Microbiol.* **33,** 249–259 CrossRef Medline
145. Kim, B. H., Kim, S., Kim, H. G., Lee, J., Lee, I. S., and Park, Y. K. (2005) The formation of cyclopropane fatty acids in *Salmonella enterica* serovar Typhimurium. *Microbiology* **151,** 209–218 CrossRef Medline
146. Asakura, H., Ekawa, T., Sugimoto, N., Momose, Y., Kawamoto, K., Makino, S.-I., Igimi, S., and Yamamoto, S. (2012) Membrane topology of *Salmonella* invasion protein SipB confers osmotolerance. *Biochem. Biophys. Res. Commun.* **426,** 654–658 CrossRef Medline
147. Grandvalet, C., Assad-García, J. S., Chu-Ky, S., Tollot, M., Guzzo, J., Gresti, J., and Tourdot-Maréchal, R. (2008) Changes in membrane lipid composition in ethanol- and acid-adapted *Oenococcus oeni* cells: characterization of the cfa gene by heterologous complementation. *Microbiology* **154,** 2611–2619 CrossRef Medline
148. Annous, B. A., Kozempel, M. F., and Kurantz, M. J. (1999) Changes in membrane fatty acid composition of *Pediococcus* sp. strain NRRL B-2354 in response to growth conditions and its effect on thermal resistance. *Appl. Environ. Microbiol.* **65,** 2857–2862 CrossRef Medline
149. Ursell, T. S., Trepagnier, E. H., Huang, K. C., and Theriot, J. A. (2012) Analysis of surface protein expression reveals the growth pattern of the Gram-negative outer membrane. *PLoS Comput. Biol.* **8,** e1002680 CrossRef Medline
150. Johansen, J., Rasmussen, A. A., Overgaard, M., and Valentin-Hansen, P. (2006) Conserved small non-coding RNAs that belong to the sigmaE regulon: role in down-regulation of outer membrane proteins. *J. Mol. Biol.* **364,** 1–8 CrossRef Medline
151. Guillier, M., Gottesman, S., and Storz, G. (2006) Modulating the outer membrane with small RNAs. *Genes Dev.* **20,** 2338–2348 CrossRef Medline
152. Allen, R. J., and Scott, G. K. (1979) Biosynthesis and turnover of outer-membrane proteins in *Escherichia coli* ML308-225. *Biochem. J.* **182,** 407–412 CrossRef Medline
153. Lugtenberg, E. J. J., and Peters, R. (1976) Distribution of lipids in cytoplasmic and outer membranes of *Escherichia coli* K12. *Biochim. Biophys. Acta* **441,** 38–47 CrossRef Medline
154. White, D. A., Lennarz, W. J., and Schnaitman, C. A. (1972) Distribution of lipids in the wall and cytoplasmic membrane subfractions of the cell envelope of *Escherichia coli*. *J. Bacteriol.* **109,** 686–690 CrossRef
155. Ishinaga, M., Kanamoto, R., and Kito, M. (1979) Distribution of phospholipid molecular species in outer and cytoplasmic membrane of *Escherichia coli*. *J. Biochem.* **86,** 161–165 CrossRef Medline
156. Jarosøawski, S., Duquesne, K., Sturgis, J. N., and Scheuring, S. (2009) High-resolution architecture of the outer membrane of the Gram-negative bacteria *Roseobacter denitrificans*. *Mol. Microbiol.* **74,** 1211–1222 CrossRef Medline
157. Lessen, H. J., Fleming, P. J., Fleming, K. G., and Sodt, A. J. (2018) Building blocks of the outer membrane: calculating a general elastic energy model for β-barrel membrane proteins. *J. Chem. Theory Comput.* **14,** 4487–4497 CrossRef Medline
158. Oddershede, L., Dreyer, J. K., Grego, S., Brown, S., and Berg-Sørensen, K. (2002) The motion of a single molecule, the λ-receptor, in the bacterial outer membrane. *Biophys. J.* **83,** 3152–3161 CrossRef Medline
159. Kumar, M., Mommer, M. S., and Sourjik, V. (2010) Mobility of cytoplasmic, membrane, and DNA-binding proteins in *Escherichia coli*. *Biophys. J.* **98,** 552–559 CrossRef Medline
160. Ritchie, K., Lill, Y., Sood, C., Lee, H., and Zhang, S. (2013) Single-molecule imaging in live bacteria cells. *Philos. Trans. R. Soc. Lond. B. Biol. Sci.* **368,** 20120355 CrossRef Medline
161. Oh, D., Yu, Y., Lee, H., Wanner, B. L., and Ritchie, K. (2014) Dynamics of the serine chemoreceptor in the *Escherichia coli* inner membrane: a high-speed single-molecule tracking study. *Biophys. J.* **106,** 145–153 CrossRef Medline
162. Oswald, F., Varadarajan, A., Lill, H., Peterman, E. J. G., and Bollen, Y. J. M. (2016) MreB-dependent organization of the *E. coli* cytoplasmic membrane controls membrane protein diffusion. *Biophys. J.* **110,** 1139–1149 CrossRef Medline
163. Gibbs, K. A., Isaac, D. D., Xu, J., Hendrix, R. W., Silhavy, T. J., and Theriot, J. A. (2004) Complex spatial distribution and dynamics of an abundant *Escherichia coli* outer membrane protein, LamB. *Mol. Microbiol.* **53,** 1771–1783 CrossRef Medline
164. Spector, J., Zakharov, S., Lill, Y., Sharma, O., Cramer, W. A., and Ritchie, K. (2010) Mobility of BtuB and OmpF in the *Escherichia coli* outer membrane: implications for dynamic formation of a translocon complex. *Biophys. J.* **99,** 3880–3886 CrossRef Medline
165. Rothenberg, E., Sepúlveda, L. A., Skinner, S. O., Zeng, L., Selvin, P. R., and Golding, I. (2011) Single-virus tracking reveals a spatial receptor-dependent search mechanism. *Biophys. J.* **100,** 2875–2882 CrossRef Medline
166. Kleanthous, C., Rassam, P., and Baumann, C. G. (2015) Protein-protein interactions and the spatiotemporal dynamics of bacterial outer membrane proteins. *Curr. Opin. Struct. Biol.* **35,** 109–115 CrossRef Medline
167. Deich, J., Judd, E. M., McAdams, H. H., and Moerner, W. E. (2004) Visualization of the movement of single histidine kinase molecules in live *Caulobacter* cells. *Proc. Natl. Acad. Sci. U. S. A.* **101,** 15921–15926 CrossRef Medline
168. Mullineaux, C. W., Nenninger, A., Ray, N., and Robinson, C. (2006) Diffusion of green fluorescent protein in three cell environments in *Escherichia coli*. *J. Bacteriol.* **188,** 3442–3448 CrossRef Medline
169. Leake, M. C., Chandler, J. H., Wadhams, G. H., Bai, F., Berry, R. M., and Armitage, J. P. (2006) Stoichiometry and turnover in single, functioning membrane protein complexes. *Nature* **443,** 355–358 CrossRef Medline
170. Leake, M. C., Greene, N. P., Godun, R. M., Granjon, T., Buchanan, G., Chen, S., Berry, R. M., Palmer, T., and Berks, B. C. (2008) Variable stoichiometry of the TatA component of the twin-arginine protein transport system observed by *in vivo* single-molecule imaging. *Proc. Natl. Acad. Sci. U. S. A.* **105,** 15376–15381 CrossRef Medline
171. Szczepaniak, J., Holmes, P., Rajasekar, K., Kaminska, R., Samsudin, F., Inns, P. G., Rassam, P., Khalid, S., Murray, S. M., Redfield, C., and Kleanthous, C. (2020) The lipoprotein Pal stabilises the bacterial outer membrane during constriction by a mobilisation-and-capture mechanism. *Nat. Commun.* **11,** 1305 CrossRef Medline
172. Mühlradt, P. F., Menzel, J., Golecki, J. R., and Speth, V. (1974) Lateral mobility and surface density of lipopolysaccharide in the outer membrane of *Salmonella typhimurium*. *Eur. J. Biochem.* **43,** 533–539 CrossRef Medline

173. Schindler, M., Osborn, M. J., and Koppel, D. E. (1980) Lateral diffusion of lipopolysaccharide in the outer membrane of *Salmonella typhimurium*. *Nature* **285,** 261–263 CrossRef Medline
174. Nenninger, A., Mastroianni, G., Robson, A., Lenn, T., Xue, Q., Leake, M. C., and Mullineaux, C. W. (2014) Independent mobility of proteins and lipids in the plasma membrane of *Escherichia coli*. *Mol. Microbiol.* **92,** 1142–1153 CrossRef Medline
175. Mika, J. T., Thompson, A. J., Dent, M. R., Brooks, N. J., Michiels, J., Hofkens, J., and Kuimova, M. K. (2016) Measuring the viscosity of the *Escherichia coli* plasma membrane using molecular rotors. *Biophys. J.* **111,** 1528–1540 CrossRef Medline
176. Elowitz, M. B., Surette, M. G., Wolf, P. E., Stock, J. B., and Leibler, S. (1999) Protein mobility in the cytoplasm of *Escherichia coli*. *J. Bacteriol.* **181,** 197–203 CrossRef Medline
177. Cluzel, P., Surette, M., and Leibler, S. (2000) An ultrasensitive bacterial motor revealed by monitoring signaling proteins in single cells. *Science* **287,** 1652–1655 CrossRef Medline
178. Konopka, M. C., Shkel, I. A., Cayley, S., Record, M. T., and Weisshaar, J. C. (2006) Crowding and confinement effects on protein diffusion *in vivo*. *J. Bacteriol.* **188,** 6115–6123 CrossRef Medline
179. Potma, E. O., de Boeij, W. P., Bosgraaf, L., Roelofs, J., van Haastert, P. J., and Wiersma, D. A. (2001) Reduced protein diffusion rate by cytoskeleton in vegetative and polarized dictyostelium cells. *Biophys. J.* **81,** 2010–2019 CrossRef Medline
180. Terry, B. R., Matthews, E. K., and Haseloff, J. (1995) Molecular characterisation of recombinant green fluorescent protein by fluorescence correlation microscopy. *Biochem. Biophys. Res. Commun.* **217,** 21–27 CrossRef Medline
181. Gunasinghe, S. D., Shiota, T., Stubenrauch, C. J., Schulze, K. E., Webb, C. T., Fulcher, A. J., Dunstan, R. A., Hay, I. D., Naderer, T., Whelan, D. R., Bell, T. D. M., Elgass, K. D., Strugnell, R. A., and Lithgow, T. (2018) The WD40 protein BamB mediates coupling of BAM complexes into assembly precincts in the bacterial outer membrane. *Cell Rep.* **23,** 2782–2794 CrossRef Medline
182. Lill, Y., Jordan, L. D., Smallwood, C. R., Newton, S. M., Lill, M. A., Klebba, P. E., and Ritchie, K. (2016) Confined mobility of TonB and FepA in *Escherichia coli* membranes. *PLoS ONE* **11,** e0160862 CrossRef Medline
183. Gold, V. A. M., Ieva, R., Walter, A., Pfanner, N., van der Laan, M., and Kühlbrandt, W. (2014) Visualizing active membrane protein complexes by electron cryotomography. *Nat. Commun.* **5,** 4129 CrossRef Medline
184. Casuso, I., Khao, J., Chami, M., Paul-Gilloteaux, P., Husain, M., Duneau, J.-P., Stahlberg, H., Sturgis, J. N., and Scheuring, S. (2012) Characterization of the motion of membrane proteins using high-speed atomic force microscopy. *Nat. Nanotechnol.* **7,** 525–529 CrossRef Medline
185. Yamashita, H., Taoka, A., Uchihashi, T., Asano, T., Ando, T., and Fukumori, Y. (2012) Single-molecule imaging on living bacterial cell surface by high-speed AFM. *J. Mol. Biol.* **422,** 300–309 CrossRef Medline
186. Goose, J. E., and Sansom, M. S. P (2013) Reduced lateral mobility of lipids and proteins in crowded membranes. *PLoS Comput. Biol.* **9,** e1003033 CrossRef Medline
187. Chavent, M., Duncan, A. L., Rassam, P., Birkholz, O., Hélie, J., Reddy, T., Beliaev, D., Hambly, B., Piehler, J., Kleanthous, C., and Sansom, M. S. P. (2018) How nanoscale protein interactions determine the mesoscale dynamic organisation of bacterial outer membrane proteins. *Nat. Commun.* **9,** 2846 CrossRef Medline
188. Smit, J., and Nikaido, H. (1978) Outer membrane of Gram-negative bacteria. XVIII. Electron microscopic studies on porin insertion sites and growth of cell surface of *Salmonella typhimurium*. *J. Bacteriol.* **135,** 687–702 CrossRef Medline
189. Arunmanee, W., Pathania, M., Solovyova, A. S., Le Brun, A. P., Ridley, H., Baslé, A., van den Berg, B., and Lakey, J. H. (2016) Gram-negative trimeric porins have specific LPS binding sites that are essential for porin biogenesis. *Proc. Natl. Acad. Sci. U. S. A.* **113,** E5034–E5043 CrossRef Medline
190. Verhoeven, G. S., Dogterom, M., and den Blaauwen, T. (2013) Absence of long-range diffusion of OmpA in *E. coli* is not caused by its peptidoglycan binding domain. *BMC Microbiol.* **13,** 66 CrossRef Medline
191. Fowler, P. W., Hélie, J., Duncan, A., Chavent, M., Koldsø, H., and Sansom, M. S. P. (2016) Membrane stiffness is modified by integral membrane proteins. *Soft Matter* **12,** 7792–7803 CrossRef Medline
192. Heberle, F. A., and Feigenson, G. W. (2011) Phase separation in lipid membranes. *Cold Spring Harb. Perspect. Biol.* **3,** a004630 CrossRef Medline
193. Bigay, J., and Antonny, B. (2012) Curvature, lipid packing, and electrostatics of membrane organelles: defining cellular territories in determining specificity. *Dev. Cell* **23,** 886–895 CrossRef Medline
194. Budin, I., de Rond, T., Chen, Y., Chan, L. J. G., Petzold, C. J., and Keasling, J. D. (2018) Viscous control of cellular respiration by membrane lipid composition. *Science* **362,** 1186–1189 CrossRef Medline
195. Jackson, M. B., and Cronan, J. E. (1978) An estimate of the minimum amount of fluid lipid required for the growth of *Escherichia coli*. *Biochim. Biophys. Acta* **512,** 472–479 CrossRef Medline
196. Janoff, A. S., Haug, A., and McGroarty, E. J. (1979) Relationship of growth temperature and thermotropic lipid phase changes in cytoplasmic and outer membranes from *Escherichia coli* K12. *Biochim. Biophys. Acta* **555,** 56–66 CrossRef Medline
197. Nakayama, H., Mitsui, T., Nishihara, M., and Kito, M. (1980) Relation between growth temperature of *E. coli* and phase transition temperatures of its cytoplasmic and outer membranes. *Biochim. Biophys. Acta* **601,** 1–10 CrossRef Medline
198. Janoff, A. S., Gupte, S., and McGroarty, E. J. (1980) Correlation between temperature range of growth and structural transitions in membranes and lipids of *Escherichia coli* K12. *Biochim. Biophys. Acta* **598,** 641–646 CrossRef Medline
199. Souzu, H. (1982) *Escherichia coli* B membrane stability related to cell growth phase. Measurement of temperature dependent physical state change of the membrane over a wide range. *Biochim. Biophys. Acta* **691,** 161–170 CrossRef Medline
200. van den Brink-van der Laan, E., Killian, J. A., and de Kruijff, B. (2004) Nonbilayer lipids affect peripheral and integral membrane proteins via changes in the lateral pressure profile. *Biochim. Biophys. Acta* **1666,** 275–288 CrossRef Medline
201. Kranenburg, M., and Smit, B. (2005) Phase behavior of model lipid bilayers. *J. Phys. Chem. B* **109,** 6553–6563 CrossRef Medline
202. Brown, D. A., and London, E. (1998) Structure and origin of ordered lipid domains in biological membranes. *J. Membr. Biol.* **164,** 103–114 CrossRef Medline
203. M'Baye, G., Mély, Y., Duportail, G., and Klymchenko, A. S. (2008) Liquid ordered and gel phases of lipid bilayers: fluorescent probes reveal close fluidity but different hydration. *Biophys. J.* **95,** 1217–1225 CrossRef
204. Quinn, P. J., and Wolf, C. (2009) The liquid-ordered phase in membranes. *Biochim. Biophys. Acta* **1788,** 33–46 CrossRef Medline
205. Mouritsen, O. G. (2010) The liquid-ordered state comes of age. *Biochim. Biophys. Acta* **1798,** 1286–1288 CrossRef Medline
206. Sodt, A. J., Sandar, M. L., Gawrisch, K., Pastor, R. W., and Lyman, E. (2014) The molecular structure of the liquid-ordered phase of lipid bilayers. *J. Am. Chem. Soc.* **136,** 725–732 CrossRef Medline
207. Boscia, A. L., Treece, B. W., Mohammadyani, D., Klein-Seetharaman, J., Braun, A. R., Wassenaar, T. A., Klösgen, B., and Tristram-Nagle, S. (2014) X-ray structure, thermodynamics, elastic properties and MD simulations of cardiolipin/dimyristoylphosphatidylcholine mixed membranes. *Chem. Phys. Lipids* **178,** 1–10 CrossRef Medline
208. Bramkamp, M., and Lopez, D. (2015) Exploring the existence of lipid rafts in bacteria. *Microbiol. Mol. Biol. Rev.* **79,** 81–100 CrossRef Medline
209. Shearer, J., and Khalid, S. (2018) Communication between the leaflets of asymmetric membranes revealed from coarse-grain molecular dynamics simulations. *Sci. Rep.* **8,** 1805 CrossRef Medline
210. Shearer, J., Jefferies, D., and Khalid, S. (2019) Outer membrane proteins OmpA, FhuA, OmpF, EstA, BtuB, and OmpX have unique lipopolysaccharide fingerprints. *J. Chem. Theory Comput.* **15,** 2608–2619 CrossRef Medline
211. Thanassi, D. G., Stathopoulos, C., Karkal, A., and Li, H. (2005) Protein secretion in the absence of ATP: the autotransporter, two-partner secretion and chaperone/usher pathways of Gram-negative bacteria (review). *Mol. Membr. Biol.* **22,** 63–72 CrossRef Medline

212. Sinensky, M. (1974) Homeoviscous adaptation—a homeostatic process that regulates the viscosity of membrane lipids in *Escherichia coli*. *Proc. Natl. Acad. Sci. U. S. A.* **71,** 522–525 CrossRef Medline
213. Velázquez, J. B., and Fernández, M. S. (2006) GPS, the slope of Laurdan generalized polarization spectra, in the study of phospholipid lateral organization and *Escherichia coli* lipid phases. *Arch. Biochem. Biophys.* **455,** 163–174 CrossRef Medline
214. Demchenko, A. P., Mély, Y., Duportail, G., and Klymchenko, A. S. (2009) Monitoring biophysical properties of lipid membranes by environment-sensitive fluorescent probes. *Biophys. J.* **96,** 3461–3470 CrossRef Medline
215. Leung, S. S. W., Brewer, J., Bagatolli, L. A., and Thewalt, J. L. (2019) Measuring molecular order for lipid membrane phase studies: linear relationship between Laurdan generalized polarization and deuterium NMR order parameter. *Biochim. Biophys. Acta. Biomembr.* **1861,** 183053 CrossRef Medline
216. Davis, J. H., Nichol, C. P., Weeks, G., and Bloom, M. (1979) Study of the cytoplasmic and outer membranes of *Escherichia coli* by deuterium magnetic resonance. *Biochemistry* **18,** 2103–2112 CrossRef Medline
217. Nichol, C. P., Davis, J. H., Weeks, G., and Bloom, M. (1980) Quantitative study of the fluidity of *Escherichia coli* membranes using deuterium magnetic resonance. *Biochemistry* **19,** 451–457 CrossRef Medline
218. Souzu, H. (1986) Fluorescence polarization studies on *Escherichia coli* membrane stability and its relation to the resistance of the cell to freeze-thawing. I. Membrane stability in cells of differing growth phase. *Biochim. Biophys. Acta* **861,** 353–360 CrossRef Medline
219. Melchior, D. L., and Steim, J. M. (1976) Thermotropic transitions in biomembranes. *Annu. Rev. Biophys. Bioeng.* **5,** 205–238 CrossRef Medline
220. Vanounou, S., Pines, D., Pines, E., Parola, A. H., and Fishov, I. (2002) Coexistence of domains with distinct order and polarity in fluid bacterial membranes. *Photochem. Photobiol.* **76,** 1–11 CrossRef Medline
221. Fishov, I., and Woldringh, C. L. (1999) Visualization of membrane domains in *Escherichia coli*. *Mol. Microbiol.* **32,** 1166–1172 CrossRef Medline
222. Sperka-Gottlieb, C. D. M., Hermetter, A., Paltauf, F., and Daum, G. (1988) Lipid topology and physical properties of the outer mitochondrial membrane of the yeast, *Saccharomyces cerevisiae*. *Biochim. Biophys. Acta* **946,** 227–234 CrossRef Medline
223. Liu, P., Duan, W., Wang, Q., and Li, X. (2010) The damage of outer membrane of *Escherichia coli* in the presence of TiO2 combined with UV light. *Colloids Surf. B Biointerfaces* **78,** 171–176 CrossRef Medline
224. Wu, C.-H., Bialecka-Fornal, M., and Newman, D. K. (2015) Methylation at the C-2 position of hopanoids increases rigidity in native bacterial membranes. *Elife* **4,** e05663 CrossRef Medline
225. Wu, Y., Stefl, M., Olzyńska, A., Hof, M., Yahioglu, G., Yip, P., Casey, D. R., Ces, O., Humpolíčková, J., and Kuimova, M. K. (2013) Molecular rheometry: direct determination of viscosity in Lo and Ld lipid phases via fluorescence lifetime imaging. *Phys. Chem. Chem. Phys.* **15,** 14986–14993 CrossRef Medline
226. Nikaido, H., Takeuchi, Y., Ohnishi, S. I., and Nakae, T. (1977) Outer membrane of *Salmonella typhimurium*: electron spin resonance studies. *Biochim. Biophys. Acta* **465,** 152–164 CrossRef Medline
227. Labischinski, H., Barnickel, G., Bradaczek, H., Naumann, D., Rietschel, E. T., and Giesbrecht, P. (1985) High state of order of isolated bacterial lipopolysaccharide and its possible contribution to the permeation barrier property of the outer membrane. *J. Bacteriol.* **162,** 9–20 CrossRef Medline
228. Brandenburg, K., and Blume, A. (1987) Investigations into the thermotropic phase behaviour of natural membranes extracted from Gram-negative bacteria and artificial membrane systems made from lipopolysaccharides and free lipid A. *Thermochim. Acta* **119,** 127–142 CrossRef
229. Brandenburg, K., and Seydel, U. (1990) Investigation into the fluidity of lipopolysaccharide and free lipid A membrane systems by Fourier-transform infrared spectroscopy and differential scanning calorimetry. *Eur. J. Biochem.* **191,** 229–236 CrossRef Medline
230. Conde-Álvarez, R., Arce-Gorvel, V., Iriarte, M., Manček-Keber, M., Barquero-Calvo, E., Palacios-Chaves, L., Chacón-Díaz, C., Chaves-Olarte, E., Martirosyan, A., von Bargen, K., Grilló, M.-J., Jerala, R., Brandenburg, K., Llobet, E., Bengoechea, J. A., *et al.* (2012) The lipopolysaccharide core of *Brucella abortus* acts as a shield against innate immunity recognition. *PLoS Pathog.* **8,** e1002675 CrossRef Medline
231. Brandenburg, K., and Seydel, U. (1984) Physical aspects of structure and function of membranes made from lipopolysaccharides and free lipid A. *Biochim. Biophys. Acta Biomembr.* **775,** 225–238 CrossRef
232. Seydel, U., Koch, M. H. J., and Brandenburg, K. (1993) Structural polymorphisms of rough mutant lipopolysaccharides Rd to Ra from *Salmonella minnesota*. *J. Struct. Biol.* **110,** 232–243 CrossRef Medline
233. Paracini, N., Clifton, L. A., Skoda, M. W. A., and Lakey, J. H. (2018) Liquid crystalline bacterial outer membranes are critical for antibiotic susceptibility. *Proc. Natl. Acad. Sci. U. S. A.* **115,** E7587–E7594 CrossRef Medline
234. Hughes, A. V., Patel, D. S., Widmalm, G., Klauda, J. B., Clifton, L. A., and Im, W. (2019) Physical properties of bacterial outer membrane models: neutron reflectometry & molecular simulation. *Biophys. J.* **116,** 1095–1104 CrossRef Medline
235. Gally, H. U., Pluschke, G., Overath, P., and Seelig, J. (1980) Structure of *Escherichia coli* membranes: fatty acyl chain order parameters of inner and outer membranes and derived liposomes. *Biochemistry* **19,** 1638–1643 CrossRef Medline
236. Mühlradt, P. F., and Golecki, J. R. (1975) Asymmetrical distribution and artifactual reorientation of lipopolysaccharide in the outer membrane bilayer of *Salmonella typhimurium*. *Eur. J. Biochem.* **51,** 343–352 CrossRef Medline
237. Sciandrone, B., Forti, F., Perego, S., Falchi, F., and Briani, F. (2019) Temperature-dependent regulation of the *Escherichia coli lpxT* gene. *Biochim. Biophys. Acta Gene Regul. Mech.* **1862,** 786–795 CrossRef Medline
238. Carty, S. M., Sreekumar, K. R., and Raetz, C. R. H. (1999) Effect of cold shock on lipid A biosynthesis in *Escherichia coli*: induction at 12 °C of an acyltransferase specific for palmitoleoyl-acyl carrier protein. *J. Biol. Chem.* **274,** 9677–9685 CrossRef Medline
239. Li, Y., Powell, D. A., Shaffer, S. A., Rasko, D. A., Pelletier, M. R., Leszyk, J. D., Scott, A. J., Masoudi, A., Goodlett, D. R., Wang, X., Raetz, C. R. H., and Ernst, R. K. (2012) LPS remodeling is an evolved survival strategy for bacteria. *Proc. Natl. Acad. Sci. U. S. A.* **109,** 8716–8721 CrossRef Medline
240. Reinés, M., Llobet, E., Dahlström, K. M., Pérez-Gutiérrez, C., Llompart, C. M., Torrecabota, N., Salminen, T. A., and Bengoechea, J. A. (2012) Deciphering the acylation pattern of *Yersinia enterocolitica* lipid A. *PLoS Pathog.* **8,** e1002978 CrossRef Medline
241. Ernst, R. K., Adams, K. N., Moskowitz, S. M., Kraig, G. M., Kawasaki, K., Stead, C. M., Trent, M. S., and Miller, S. I. (2006) The *Pseudomonas aeruginosa* lipid A deacylase: selection for expression and loss within the cystic fibrosis airway. *J. Bacteriol.* **188,** 191–201 CrossRef Medline
242. Needham, B. D., and Trent, M. S. (2013) Fortifying the barrier: the impact of lipid A remodelling on bacterial pathogenesis. *Nat. Rev. Microbiol.* **11,** 467–481 CrossRef Medline
243. Schnaitman, C. A., and Klena, J. D. (1993) Genetics of lipopolysaccharide biosynthesis in enteric bacteria. *Microbiol. Rev.* **57,** 655–682 CrossRef Medline
244. Missiakas, D., Betton, J. M., and Raina, S. (1996) New components of protein folding in extracytoplasmic compartments of *Escherichia coli* SurA, FkpA and Skp/OmpH. *Mol. Microbiol.* **21,** 871–884 CrossRef Medline
245. Klein, G., Lindner, B., Brabetz, W., Brade, H., and Raina, S. (2009) *Escherichia coli* K-12 suppressor-free mutants lacking early glycosyltransferases and late acyltransferases: minimal lipopolysaccharide structure and induction of envelope stress response. *J. Biol. Chem.* **284,** 15369–15389 CrossRef Medline
246. López, C. A., Zgurskaya, H., and Gnanakaran, S. (2020) Molecular characterization of the outer membrane of *Pseudomonas aeruginosa*. *Biochim. Biophys. Acta Biomembr.* **1862,** 183151 CrossRef Medline
247. Patel, D. S., Re, S., Wu, E. L., Qi, Y., Klebba, P. E., Widmalm, G., Yeom, M. S., Sugita, Y., and Im, W. (2016) Dynamics and interactions of OmpF and LPS: influence on pore accessibility and ion permeability. *Biophys. J.* **110,** 930–938 CrossRef Medline
248. Lee, J., Patel, D. S., Kucharska, I., Tamm, L. K., and Im, W. (2017) Refinement of OprH-LPS interactions by molecular simulations. *Biophys. J.* **112,** 346–355 CrossRef Medline

249. Wu, E. L., Fleming, P. J., Yeom, M. S., Widmalm, G., Klauda, J. B., Fleming, K. G., and Im, W. (2014) *E. coli* outer membrane and interactions with OmpLA. *Biophys. J.* **106,** 2493–2502 CrossRef Medline
250. Ma, H., Irudayanathan, F. J., Jiang, W., and Nangia, S. (2015) Simulating Gram-negative bacterial outer membrane: a coarse grain model. *J. Phys. Chem. B* **119,** 14668–14682 CrossRef Medline
251. Petrov, A. G., Gawrisch, K., Brezesinski, G., Klose, G., and Möps, A. (1982) Optical detection of phase transitions in simple and mixed lipid-water phases. *Biochim. Biophys. Acta* **690,** 1–7 CrossRef Medline
252. Li, A., Schertzer, J. W., and Yong, X. (2018) Molecular dynamics modeling of *Pseudomonas aeruginosa* outer membranes. *Phys. Chem. Chem. Phys.* **20,** 23635–23648 CrossRef Medline
253. Ma, H., Khan, A., and Nangia, S. (2018) Dynamics of OmpF trimer formation in the bacterial outer membrane of *Escherichia coli*. *Langmuir* **34,** 5623–5634 CrossRef Medline
254. Rottem, S., and Leive, L. (1977) Effect of variations in lipopolysaccharide on the fluidity of the outer membrane of *Escherichia coli*. *J. Biol. Chem.* **252,** 2077–2081 Medline
255. Müller-Loennies, S., Holst, O., and Brade, H. (1994) Chemical structure of the core region of *Escherichia coli* J-5 lipopolysaccharide. *Eur. J. Biochem.* **224,** 751–760 CrossRef Medline
256. Bello, G., Bodin, A., Lawrence, M. J., Barlow, D., Mason, A. J., Barker, R. D., and Harvey, R. D. (2016) The influence of rough lipopolysaccharide structure on molecular interactions with mammalian antimicrobial peptides. *Biochim. Biophys. Acta* **1858,** 197–209 CrossRef Medline
257. Takeuchi, Y., and Nikaido, H. (1981) Persistence of segregated phospholipid domains in phospholipid-lipopolysaccharide mixed bilayers: studies with spin-labeled phospholipids. *Biochemistry* **20,** 523–529 CrossRef Medline
258. Takeuchi, Y., and Nikaido, H. (1984) Physical interaction between lipid A and phospholipids: a study with spin-labeled phospholipids. *Rev. Infect. Dis.* **6,** 488–492 CrossRef Medline
259. Niemelä, P. S., Miettinen, M. S., Monticelli, L., Hammaren, H., Bjelkmar, P., Murtola, T., Lindahl, E., and Vattulainen, I. (2010) Membrane proteins diffuse as dynamic complexes with lipids. *J. Am. Chem. Soc.* **132,** 7574–7575 CrossRef Medline
260. Javanainen, M., Hammaren, H., Monticelli, L., Jeon, J., Miettinen, M. S., Martinez-Seara, H., Metzler, R., and Vattulainen, I. (2013) Anomalous and normal diffusion of proteins and lipids in crowded lipid membranes. *Faraday Discuss.* **161,** 397–417, discussion 419–459 CrossRef Medline
261. Guigas, G., and Weiss, M. (2016) Effects of protein crowding on membrane systems. *Biochim. Biophys. Acta* **1858,** 2441–2450 CrossRef Medline
262. Kirschner, K. N., Lins, R. D., Maass, A., and Soares, T. A. (2012) A glycam-based force field for simulations of lipopolysaccharide membranes: Parametrization and validation. *J. Chem. Theory Comput.* **8,** 4719–4731 CrossRef Medline
263. Ortiz-Suarez, M. L., Samsudin, F., Piggot, T. J., Bond, P. J., and Khalid, S. (2016) Full-length OmpA: structure, function, and membrane interactions predicted by molecular dynamics simulations. *Biophys. J.* **111,** 1692–1702 CrossRef Medline
264. Balusek, C., and Gumbart, J. C. (2016) Role of the native outer-membrane environment on the transporter BtuB. *Biophys. J.* **111,** 1409–1417 CrossRef Medline
265. Matthias, K. A., Strader, M. B., Nawar, H. F., Gao, Y. S., Lee, J., Patel, D. S., Im, W., and Bash, M. C. (2017) Heterogeneity in non-epitope loop sequence and outer membrane protein complexes alters antibody binding to the major porin protein PorB in serogroup B *Neisseria meningitidis*. *Mol. Microbiol.* **105,** 934–953 CrossRef Medline
266. Lee, J., Pothula, K. R., Kleinekathöfer, U., and Im, W. (2018) Simulation study of Occk5 functional properties in *Pseudomonas aeruginosa* outer membranes. *J. Phys. Chem. B* **122,** 8185–8192 CrossRef Medline
267. Saunders, G. M., Bruce Macdonald, H. E., Essex, J. W., and Khalid, S. (2018) Prediction of the closed conformation and insights into the mechanism of the membrane enzyme LpxR. *Biophys. J.* **115,** 1445–1456 CrossRef Medline
268. Kesireddy, A., Pothula, K. R., Lee, J., Patel, D. S., Pathania, M., van den Berg, B., Im, W., and Kleinekathöfer, U. (2019) Modeling of specific lipopolysaccharide binding sites on a Gram-negative porin. *J. Phys. Chem. B* **123,** 5700–5708 CrossRef Medline
269. Samsudin, F., and Khalid, S. (2019) Movement of arginine through OprD: the energetics of permeation and the role of lipopolysaccharide in directing arginine to the protein. *J. Phys. Chem. B* **123,** 2824–2832 CrossRef Medline
270. Lundquist, K. P., and Gumbart, J. C. (2020) Presence of substrate aids lateral gate separation in LptD. *Biochim. Biophys. Acta Biomembr.* **1862,** 183025 CrossRef Medline
271. Kurisu, G., Zakharov, S. D., Zhalnina, M. V., Bano, S., Eroukova, V. Y., Rokitskaya, T. I., Antonenko, Y. N., Wiener, M. C., and Cramer, W. A. (2003) The structure of BtuB with bound colicin E3 R-domain implies a translocon. *Nat. Struct. Biol.* **10,** 948–954 CrossRef Medline
272. Straatsma, T. P., and Soares, T. A. (2009) Characterization of the outer membrane protein OprF of *Pseudomonas aeruginosa* in a lipopolysaccharide membrane by computer simulation. *Proteins* **74,** 475–488 CrossRef Medline
273. Piggot, T. J., Holdbrook, D. A., and Khalid, S. (2013) Conformational dynamics and membrane interactions of the *E. coli* outer membrane protein FecA: a molecular dynamics simulation study. *Biochim. Biophys. Acta* **1828,** 284–293 CrossRef Medline
274. Holdbrook, D. A., Piggot, T. J., Sansom, M. S. P., and Khalid, S. (2013) Stability and membrane interactions of an autotransport protein: MD simulations of the Hia translocator domain in a complex membrane environment. *Biochim. Biophys. Acta* **1828,** 715–723 CrossRef Medline
275. Schindler, H., and Rosenbusch, J. P. (1978) Matrix protein from *Escherichia coli* outer membranes forms voltage-controlled channels in lipid bilayers. *Proc. Natl. Acad. Sci. U. S. A.* **75,** 3751–3755 CrossRef Medline
276. Rocque, W. J., Coughlin, R. T., and McGroarty, E. J. (1987) Lipopolysaccharide tightly bound to porin monomers and trimers from *Escherichia coli* K-12. *J. Bacteriol.* **169,** 4003–4010 CrossRef Medline
277. Holzenburg, A., Engel, A., Kessler, R., Manz, H. J., Lustig, A., and Aebi, U. (1989) Rapid isolation of OmpF porin-LPS complexes suitable for structure-function studies. *Biochemistry* **28,** 4187–4193 CrossRef Medline
278. Ferguson, A. D., Welte, W., Hofmann, E., Lindner, B., Holst, O., Coulton, J. W., and Diederichs, K. (2000) A conserved structural motif for lipopolysaccharide recognition by procaryotic and eucaryotic proteins. *Structure* **8,** 585–592 CrossRef Medline
279. DiRienzo, J. M., Nakamura, K., and Inouye, M. (1978) The outer membrane proteins of Gram-negative bacteria: biosynthesis, assembly, and functions. *Annu. Rev. Biochem.* **47,** 481–532 CrossRef Medline
280. Loos, M. S., Ramakrishnan, R., Vranken, W., Tsirigotaki, A., Tsare, E.-P., Zorzini, V., Geyter, J. D., Yuan, B., Tsamardinos, I., Klappa, M., Schymkowitz, J., Rousseau, F., Karamanou, S., and Economou, A. (2019) Structural basis of the subcellular topology landscape of *Escherichia coli*. *Front. Microbiol.* **10,** 1670–1622 CrossRef Medline
281. Rand, R. P., Fuller, N., Parsegian, V. A., and Rau, D. C. (1988) Variation in hydration forces between neutral phospholipid bilayers: evidence for hydration attraction. *Biochemistry* **27,** 7711–7722 CrossRef Medline
282. Petrache, H. I., Dodd, S. W., and Brown, M. F. (2000) Area per lipid and acyl length distributions in fluid phosphatidylcholines determined by (2) H NMR spectroscopy. *Biophys. J.* **79,** 3172–3192 CrossRef Medline
283. Rappolt, M., Hickel, A., Bringezu, F., and Lohner, K. (2003) Mechanism of the lamellar/inverse hexagonal phase transition examined by high resolution x-ray diffraction. *Biophys. J.* **84,** 3111–3122 CrossRef Medline
284. Leekumjorn, S., and Sum, A. K. (2007) Molecular studies of the gel to liquid-crystalline phase transition for fully hydrated DPPC and DPPE bilayers. *Biochim. Biophys. Acta* **1768,** 354–365 CrossRef Medline
285. Piggot, T. J., Holdbrook, D. A., and Khalid, S. (2011) Electroporation of the *E. coli* and *S. aureus* membranes: molecular dynamics simulations of complex bacterial membranes. *J. Phys. Chem. B* **115,** 13381–13388 CrossRef Medline
286. Pierucci, O. (1978) Dimensions of *Escherichia coli* at various growth rates: model for envelope growth. *J. Bacteriol.* **135,** 559–574 CrossRef Medline
287. Trueba, F. J., and Woldringh, C. L. (1980) Changes in cell diameter during the division cycle of *Escherichia coli*. *J. Bacteriol.* **142,** 869–878 CrossRef Medline

288. Reshes, G., Vanounou, S., Fishov, I., and Feingold, M. (2008) Timing the start of division in *E. coli*: a single-cell study. *Phys. Biol.* **5,** 046001 CrossRef Medline
289. Mathelié-Guinlet, M., Asmar, A. T., Collet, J., and Dufrêne, Y. F. (2020) Lipoprotein Lpp regulates the mechanical properties of the *E. coli* cell envelope. *Nat. Commun.* **11,** 1789 CrossRef Medline
290. Rao, S., Bates, G. T., Matthews, C. R., Newport, T. D., Vickery, O. N., and Stansfeld, P. J. (2020) Characterizing membrane association and periplasmic transfer of bacterial lipoproteins through molecular dynamics simulations. *Structure* **28,** 475–487.e3 CrossRef Medline
291. Clifton, L. A., Skoda, M. W. A., Daulton, E. L., Hughes, A. V., Le Brun, A. P., Lakey, J. H., and Holt, S. A. (2013) Asymmetric phospholipid: lipopolysaccharide bilayers; a Gram-negative bacterial outer membrane mimic. *J. R. Soc. Interface* **10,** 20130810 CrossRef Medline
292. Clifton, L. A., Skoda, M. W. A., Le Brun, A. P., Ciesielski, F., Kuzmenko, I., Holt, S. A., and Lakey, J. H. (2015) Effect of divalent cation removal on the structure of Gram-negative bacterial outer membrane models. *Langmuir* **31,** 404–412 CrossRef Medline
293. Markones, M., Fippel, A., Kaiser, M., Drechsler, C., Hunte, C., and Heerklotz, H. (2020) Stairway to asymmetry: five steps to lipid-asymmetric proteoliposomes. *Biophys. J.* **118,** 294–302 CrossRef Medline
294. Markones, M., Drechsler, C., Kaiser, M., Kalie, L., Heerklotz, H., and Fiedler, S. (2018) Engineering asymmetric lipid vesicles: Accurate and convenient control of the outer leaflet lipid composition. *Langmuir* **34,** 1999–2005 CrossRef Medline
295. Drechsler, C., Markones, M., Choi, J.-Y., Frieling, N., Fiedler, S., Voelker, D. R., Schubert, R., and Heerklotz, H. (2018) Preparation of asymmetric liposomes using a phosphatidylserine decarboxylase. *Biophys. J.* **115,** 1509–1517 CrossRef Medline
296. Gurtovenko, A. A., and Vattulainen, I. (2008) Membrane potential and electrostatics of phospholipid bilayers with asymmetric transmembrane distribution of anionic lipids. *J. Phys. Chem. B* **112,** 4629–4634 CrossRef Medline
297. Esteban-Martín, S., Risselada, H. J., Salgado, J., and Marrink, S. J. (2009) Stability of asymmetric lipid bilayers assessed by molecular dynamics simulations. *J. Am. Chem. Soc.* **131,** 15194–15202 CrossRef Medline
298. Park, S., Beaven, A. H., Klauda, J. B., and Im, W. (2015) How tolerant are membrane simulations with mismatch in area per lipid between leaflets? *J. Chem. Theory Comput.* **11,** 3466–3477 CrossRef Medline
299. Heberle, F. A., Marquardt, D., Doktorova, M., Geier, B., Standaert, R. F., Heftberger, P., Kollmitzer, B., Nickels, J. D., Dick, R. A., Feigenson, G. W., Katsaras, J., London, E., and Pabst, G. (2016) Subnanometer structure of an asymmetric model membrane: interleaflet coupling influences domain properties. *Langmuir* **32,** 5195–5200 CrossRef Medline
300. Doktorova, M., and Weinstein, H. (2018) Accurate *in silico* modeling of asymmetric bilayers based on biophysical principles. *Biophys. J.* **115,** 1638–1643 CrossRef Medline
301. Franklin, M. W., and Slusky, J. S. G. (2018) Tight turns of outer membrane proteins: an analysis of sequence, structure, and hydrogen bonding. *J. Mol. Biol.* **430,** 3251–3265 CrossRef Medline
302. Steinkühler, J., Sezgin, E., Urbančič, I., Eggeling, C., and Dimova, R. (2019) Mechanical properties of plasma membrane vesicles correlate with lipid order, viscosity and cell density. *Commun. Biol.* **2,** 337 CrossRef Medline
303. Mogensen, J. E., Kleinschmidt, J. H., Schmidt, M. A., and Otzen, D. E. (2005) Misfolding of a bacterial autotransporter. *Protein Sci.* **14,** 2814–2827 CrossRef Medline
304. Chaturvedi, D., and Mahalakshmi, R. (2018) Folding determinants of transmembrane β-barrels using engineered OMP chimeras. *Biochemistry* **57,** 1987–1996 CrossRef Medline
305. Hong, H., Park, S., Jiménez, R. H. F., Rinehart, D., and Tamm, L. K. (2007) Role of aromatic side chains in the folding and thermodynamic stability of integral membrane proteins. *J. Am. Chem. Soc.* **129,** 8320–8327 CrossRef Medline
306. Sanchez, K. M., Gable, J. E., Schlamadinger, D. E., and Kim, J. E. (2008) Effects of tryptophan microenvironment, soluble domain, and vesicle size on the thermodynamics of membrane protein folding: lessons from the transmembrane protein OmpA. *Biochemistry* **47,** 12844–12852 CrossRef Medline
307. Andersen, K. K., Wang, H., and Otzen, D. E. (2012) A kinetic analysis of the folding and unfolding of OmpA in urea and guanidinium chloride: single and parallel pathways. *Biochemistry* **51,** 8371–8383 CrossRef Medline
308. Pocanschi, C. L., Popot, J.-L., and Kleinschmidt, J. H. (2013) Folding and stability of outer membrane protein A (OmpA) from *Escherichia coli* in an amphipathic polymer, amphipol A8-35. *Eur. Biophys. J.* **42,** 103–118 CrossRef Medline
309. Moon, C. P., and Fleming, K. G. (2011) Side-chain hydrophobicity scale derived from transmembrane protein folding into lipid bilayers. *Proc. Natl. Acad. Sci. U. S. A.* **108,** 10174–10177 CrossRef Medline
310. Moon, C. P., Kwon, S., and Fleming, K. G. (2011) Overcoming hysteresis to attain reversible equilibrium folding for outer membrane phospholipase A in phospholipid bilayers. *J. Mol. Biol.* **413,** 484–494 CrossRef Medline
311. McDonald, S. K., and Fleming, K. G. (2016) Aromatic side chain water-to-lipid transfer free energies show a depth dependence across the membrane normal. *J. Am. Chem. Soc.* **138,** 7946–7950 CrossRef Medline
312. Chaturvedi, D., and Mahalakshmi, R. (2013) Methionine mutations of outer membrane protein X influence structural stability and β-barrel unfolding. *PLoS ONE* **8,** e79351 CrossRef Medline
313. Schweizer, M., Hindennach, I., Garten, W., and Henning, U. (1978) Major proteins of the *Escherichia coli* outer cell envelope membrane. Interaction of protein II with lipopolysaccharide. *Eur. J. Biochem.* **82,** 211–217 CrossRef Medline
314. Dornmair, K., Kiefer, H., and Jähnig, F. (1990) Refolding of an integral membrane protein. OmpA of *Escherichia coli*. *J. Biol. Chem.* **265,** 18907–18911 Medline
315. Garavito, R. M., and Rosenbusch, J. P. (1986) Isolation and crystallization of bacterial porin. *Methods Enzymol.* **125,** 309–328 CrossRef Medline
316. Surrey, T., and Jähnig, F. (1995) Kinetics of folding and membrane insertion of a β-barrel membrane protein. *J. Biol. Chem.* **270,** 28199–28203 CrossRef Medline
317. Dekker, N., Merck, K., Tommassen, J., and Verheij, H. M. (1995) *In vitro* folding of *Escherichia coli* outer-membrane phospholipase A. *Eur. J. Biochem.* **232,** 214–219 CrossRef Medline
318. Kleinschmidt, J. H., Wiener, M. C., and Tamm, L. K. (1999) Outer membrane protein A of *E. coli* folds into detergent micelles, but not in the presence of monomeric detergent. *Protein Sci.* **8,** 2065–2071 CrossRef Medline
319. Ebie Tan, A., Burgess, N. K., DeAndrade, D. S., Marold, J. D., and Fleming, K. G. (2010) Self-association of unfolded outer membrane proteins. *Macromol. Biosci.* **10,** 763–767 CrossRef Medline
320. Schnaitman, C. A. (1973) Outer membrane proteins of *Escherichia coli*. I. Effect of preparative conditions on the migration of protein in polyacrylamide gels. *Arch. Biochem. Biophys.* **157,** 541–552 CrossRef Medline
321. Ohnishi, S., and Kameyama, K. (2001) *Escherichia coli* OmpA retains a folded structure in the presence of sodium dodecyl sulfate due to a high kinetic barrier to unfolding. *Biochim. Biophys. Acta* **1515,** 159–166 CrossRef Medline
322. Anfinsen, C. B. (1973) Principles that govern the folding of protein chains. *Science* **181,** 223–230 CrossRef Medline
323. Horne, J. E., and Radford, S. E. (2016) A growing toolbox of techniques for studying β-barrel outer membrane protein folding and biogenesis. *Biochem. Soc. Trans.* **44,** 802–809 CrossRef Medline
324. Clark, A. C. (2008) Protein folding: are we there yet?. *Arch. Biochem. Biophys.* **469,** 1–3 CrossRef Medline
325. Bartlett, A. I., and Radford, S. E. (2009) An expanding arsenal of experimental methods yields an explosion of insights into protein folding mechanisms. *Nat. Struct. Mol. Biol.* **16,** 582–588 CrossRef Medline
326. Gruebele, M., Dave, K., and Sukenik, S. (2016) Globular protein folding *in vitro* and *in vivo*. *Annu. Rev. Biophys.* **45,** 233–251 CrossRef Medline
327. Muñoz, V., and Cerminara, M. (2016) When fast is better: protein folding fundamentals and mechanisms from ultrafast approaches. *Biochem. J.* **473,** 2545–2559 CrossRef Medline

328. Kleinschmidt, J. H., and Tamm, L. K. (1996) Folding intermediates of a β-barrel membrane protein: kinetic evidence for a multi-step membrane insertion mechanism. *Biochemistry* **35,** 12993–13000 CrossRef Medline
329. Nugent, S. G., Kumar, D., Rampton, D. S., and Evans, D. F. (2001) Intestinal luminal pH in inflammatory bowel disease: possible determinants and implications for therapy with aminosalicylates and other drugs. *Gut* **48,** 571–577 CrossRef Medline
330. Kleinschmidt, J. H., and Tamm, L. K. (2002) Secondary and tertiary structure formation of the β-barrel membrane protein OmpA is synchronized and depends on membrane thickness. *J. Mol. Biol.* **324,** 319–330 CrossRef Medline
331. Pocanschi, C. L., Apell, H.-J., Puntervoll, P., Høgh, B., Jensen, H. B., Welte, W., and Kleinschmidt, J. H. (2006) The major outer membrane protein of *Fusobacterium nucleatum* (FomA) folds and inserts into lipid bilayers via parallel folding pathways. *J. Mol. Biol.* **355,** 548–561 CrossRef Medline
332. Huysmans, G. H. M., Radford, S. E., Baldwin, S. A., and Brockwell, D. J. (2012) Malleability of the folding mechanism of the outer membrane protein PagP: parallel pathways and the effect of membrane elasticity. *J. Mol. Biol.* **416,** 453–464 CrossRef Medline
333. Kleinschmidt, J. H., and Tamm, L. K. (1999) Time-resolved distance determination by tryptophan fluorescence quenching: probing intermediates in membrane protein folding. *Biochemistry* **38,** 4996–5005 CrossRef Medline
334. Kleinschmidt, J. H., den Blaauwen, T., Driessen, A. J., and Tamm, L. K. (1999) Outer membrane protein A of *Escherichia coli* inserts and folds into lipid bilayers by a concerted mechanism. *Biochemistry* **38,** 5006–5016 CrossRef Medline
335. Rodionova, N. A., Tatulian, S. A., Surrey, T., Jähnig, F., and Tamm, L. K. (1995) Characterization of two membrane-bound forms of OmpA. *Biochemistry* **34,** 1921–1929 CrossRef Medline
336. Kleinschmidt, J. H., Bulieris, P. V., Qu, J., Dogterom, M., and den Blaauwen, T. (2011) Association of neighboring β-strands of outer membrane protein A in lipid bilayers revealed by site-directed fluorescence quenching. *J. Mol. Biol.* **407,** 316–332 CrossRef Medline
337. Popot, J. L., and Engelman, D. M. (2000) Helical membrane protein folding, stability, and evolution. *Annu. Rev. Biochem.* **69,** 881–922 CrossRef Medline
338. Engelman, D. M., Chen, Y., Chin, C.-N., Curran, A. R., Dixon, A. M., Dupuy, A. D., Lee, A. S., Lehnert, U., Matthews, E. E., Reshetnyak, Y. K., Senes, A., and Popot, J.-L. (2003) Membrane protein folding: beyond the two stage model. *FEBS Lett.* **555,** 122–125 CrossRef Medline
339. Hong, H., and Tamm, L. K. (2004) Elastic coupling of integral membrane protein stability to lipid bilayer forces. *Proc. Natl. Acad. Sci. U. S. A.* **101,** 4065–4070 CrossRef Medline
340. Pocanschi, C. L., Patel, G. J., Marsh, D., and Kleinschmidt, J. H. (2006) Curvature elasticity and refolding of OmpA in large unilamellar vesicles. *Biophys. J.* **91,** L75–7 CrossRef Medline
341. Marsh, D., Shanmugavadivu, B., and Kleinschmidt, J. H. (2006) Membrane elastic fluctuations and the insertion and tilt of β-barrel proteins. *Biophys. J.* **91,** 227–232 CrossRef Medline
342. Maurya, S. R., Chaturvedi, D., and Mahalakshmi, R. (2013) Modulating lipid dynamics and membrane fluidity to drive rapid folding of a transmembrane barrel. *Sci. Rep.* **3,** 1989 CrossRef Medline
343. Danoff, E. J., and Fleming, K. G. (2015) Membrane defects accelerate outer membrane β-barrel protein folding. *Biochemistry* **54,** 97–99 CrossRef Medline
344. Nielsen, L. K., Bjørnholm, T., and Mouritsen, O. G. (2000) Fluctuations caught in the act. *Nature* **404,** 352 CrossRef Medline
345. Enders, O., Ngezahayo, A., Wiechmann, M., Leisten, F., and Kolb, H.-A. (2004) Structural calorimetry of main transition of supported DMPC bilayers by temperature-controlled AFM. *Biophys. J.* **87,** 2522–2531 CrossRef Medline
346. Blok, M. C., van der Neut-Kok, E. C., van Deenen, L. L., and de Gier, J. (1975) The effect of chain length and lipid phase transitions on the selective permeability properties of liposomes. *Biochim. Biophys. Acta* **406,** 187–196 CrossRef Medline
347. Blok, M. C., van Deenen, L. L., and De Gier, J. (1976) Effect of the gel to liquid crystalline phase transition on the osmotic behaviour of phosphatidylcholine liposomes. *Biochim. Biophys. Acta* **433,** 1–12 CrossRef Medline
348. van Hoogevest, P., de Gier, J., and de Kruijff, B. (1984) Determination of the size of the packing defects in dimyristoylphosphatidylcholine bilayers, present at the phase transition temperature. *FEBS Lett.* **171,** 160–164 CrossRef
349. Hays, L. M., Crowe, J. H., Wolkers, W., and Rudenko, S. (2001) Factors affecting leakage of trapped solutes from phospholipid vesicles during thermotropic phase transitions. *Cryobiology* **42,** 88–102 CrossRef Medline
350. Heimburg, T. (2007) *Thermal Biophysics of Membranes*, pp. 289–300, Wiley-VCH Verlag GmbH & Co. KGaA, Weinheim, Germany
351. Danoff, E. J., and Fleming, K. G. (2017) Novel kinetic intermediates populated along the folding pathway of the transmembrane β-barrel OmpA. *Biochemistry* **56,** 47–60 CrossRef Medline
352. Huysmans, G. H. M., Baldwin, S. A., Brockwell, D. J., and Radford, S. E. (2010) The transition state for folding of an outer membrane protein. *Proc. Natl. Acad. Sci. U. S. A.* **107,** 4099–4104 CrossRef Medline
353. Bond, P. J., and Sansom, M. S. P. (2006) Insertion and assembly of membrane proteins via simulation. *J. Am. Chem. Soc.* **128,** 2697–2704 CrossRef Medline
354. Moon, C. P., Zaccai, N. R., Fleming, P. J., Gessmann, D., and Fleming, K. G. (2013) Membrane protein thermodynamic stability may serve as the energy sink for sorting in the periplasm. *Proc. Natl. Acad. Sci. U. S. A.* **110,** 4285–4290 CrossRef Medline
355. Noinaj, N., Kuszak, A. J., Gumbart, J. C., Lukacik, P., Chang, H., Easley, N. C., Lithgow, T., and Buchanan, S. K. (2013) Structural insight into the biogenesis of β-barrel membrane proteins. *Nature* **501,** 385–390 CrossRef Medline
356. Noinaj, N., Kuszak, A. J., Balusek, C., Gumbart, J. C., and Buchanan, S. K. (2014) Lateral opening and exit pore formation are required for BamA function. *Structure* **22,** 1055–1062 CrossRef Medline
357. Gu, Y., Li, H., Dong, H., Zeng, Y., Zhang, Z., Paterson, N. G., Stansfeld, P. J., Wang, Z., Zhang, Y., Wang, W., and Dong, C. (2016) Structural basis of outer membrane protein insertion by the BAM complex. *Nature* **531,** 64–69 CrossRef Medline
358. Fleming, P. J., Patel, D. S., Wu, E. L., Qi, Y., Yeom, M. S., Sousa, M. C., Fleming, K. G., and Im, W. (2016) BamA POTRA domain interacts with a native lipid membrane surface. *Biophys. J.* **110,** 2698–2709 CrossRef Medline
359. Schiffrin, B., Calabrese, A. N., Higgins, A. J., Humes, J. R., Ashcroft, A. E., Kalli, A. C., Brockwell, D. J., and Radford, S. E. (2017) Effects of periplasmic chaperones and membrane thickness on BamA-catalyzed outer-membrane protein folding. *J. Mol. Biol.* **429,** 3776–3792 CrossRef Medline
360. Lundquist, K., Bakelar, J., Noinaj, N., and Gumbart, J. C. (2018) C-terminal kink formation is required for lateral gating in BamA. *Proc. Natl. Acad. Sci. U. S. A.* **115,** E7942–E7949 CrossRef Medline
361. Ellena, J. F., Lackowicz, P., Mongomery, H., and Cafiso, D. S. (2011) Membrane thickness varies around the circumference of the transmembrane protein BtuB. *Biophys. J.* **100,** 1280–1287 CrossRef Medline
362. Holdbrook, D. A., Huber, R. G., Piggot, T. J., Bond, P. J., and Khalid, S. (2016) Dynamics of crowded vesicles: local and global responses to membrane composition. *PLoS ONE* **11,** e0156963 CrossRef Medline
363. Ramakrishnan, M., Pocanschi, C. L., Kleinschmidt, J. H., and Marsh, D. (2004) Association of spin-labeled lipids with β-barrel proteins from the outer membrane of *Escherichia coli*. *Biochemistry* **43,** 11630–11636 CrossRef Medline
364. Anbazhagan, V., Qu, J., Kleinschmidt, J. H., and Marsh, D. (2008) Incorporation of outer membrane protein OmpG in lipid membranes: protein-lipid interactions and beta-barrel orientation. *Biochemistry* **47,** 6189–6198 CrossRef Medline
365. Anbazhagan, V., Vijay, N., Kleinschmidt, J. H., and Marsh, D. (2008) Protein-lipid interactions with *Fusobacterium nucleatum* major outer membrane protein FomA: spin-label EPR and polarized infrared spectroscopy. *Biochemistry* **47,** 8414–8423 CrossRef Medline

366. Ni, D., Wang, Y., Yang, X., Zhou, H., Hou, X., Cao, B., Lu, Z., Zhao, X., Yang, K., and Huang, Y. (2014) Structural and functional analysis of the β-barrel domain of BamA from *Escherichia coli*. *FASEB J.* **28,** 2677–2685 CrossRef Medline
367. Albrecht, R., Schütz, M., Oberhettinger, P., Faulstich, M., Bermejo, I., Rudel, T., Diederichs, K., and Zeth, K. (2014) Structure of BamA, an essential factor in outer membrane protein biogenesis. *Acta Crystallogr. D Biol. Crystallogr.* **70,** 1779–1789 CrossRef Medline
368. Bakelar, J., Buchanan, S. K., and Noinaj, N. (2016) The structure of the β-barrel assembly machinery complex. *Science* **351,** 180–186 CrossRef Medline
369. Han, L., Zheng, J., Wang, Y., Yang, X., Liu, Y., Sun, C., Cao, B., Zhou, H., Ni, D., Lou, J., Zhao, Y., and Huang, Y. (2016) Structure of the BAM complex and its implications for biogenesis of outer-membrane proteins. *Nat. Struct. Mol. Biol.* **23,** 192–196 CrossRef Medline
370. Gu, Y., Zeng, Y., Wang, Z., and Dong, C. (2017) BamA β16C strand and periplasmic turns are critical for outer membrane protein insertion and assembly. *Biochem. J.* **474,** 3951–3961 CrossRef Medline
371. Hartmann, J.-B., Zahn, M., Burmann, I. M., Bibow, S., and Hiller, S. (2018) Sequence-specific solution NMR assignments of the β-barrel insertase BamA to monitor its conformational ensemble at the atomic level. *J. Am. Chem. Soc.* **140,** 11252–11260 CrossRef Medline
372. Lessen, H. J., Majumdar, A., and Fleming, K. G. (2020) Backbone hydrogen bond energies in membrane proteins are insensitive to large changes in local water concentration. *J. Am. Chem. Soc.* **142,** 6227–6235 CrossRef Medline
373. Doerner, P. A., and Sousa, M. C. (2017) Extreme dynamics in the BamA β-barrel seam. *Biochemistry* **56,** 3142–3149 CrossRef Medline
374. Marsh, D. (2008) Energetics of hydrophobic matching in lipid-protein interactions. *Biophys. J.* **94,** 3996–4013 CrossRef Medline
375. Yin, F., and Kindt, J. T. (2012) Hydrophobic mismatch and lipid sorting near OmpA in mixed bilayers: atomistic and coarse-grained simulations. *Biophys. J.* **102,** 2279–2287 CrossRef Medline
376. Katira, S., Mandadapu, K. K., Vaikuntanathan, S., Smit, B., and Chandler, D. (2016) Pre-transition effects mediate forces of assembly between transmembrane proteins. *Elife.* **5,** e13150 CrossRef Medline
377. Ricci, D. P., Hagan, C. L., Kahne, D., and Silhavy, T. J. (2012) Activation of the *Escherichia coli* β-barrel assembly machine (Bam) is required for essential components to interact properly with substrate. *Proc. Natl. Acad. Sci. U. S. A.* **109,** 3487–3491 CrossRef Medline
378. Rigel, N. W., Schwalm, J., Ricci, D. P., and Silhavy, T. J. (2012) BamE modulates the *Escherichia coli* β-barrel assembly machine component BamA. *J. Bacteriol.* **194,** 1002–1008 CrossRef Medline
379. Rigel, N. W., Ricci, D. P., and Silhavy, T. J. (2013) Conformation-specific labeling of BamA and suppressor analysis suggest a cyclic mechanism for β-barrel assembly in *Escherichia coli*. *Proc. Natl. Acad. Sci. U. S. A.* **110,** 5151–5156 CrossRef Medline
380. McCabe, A. L., Ricci, D., Adetunji, M., and Silhavy, T. J. (2017) Conformational changes that coordinate the activity of BamA and BamD allowing β-barrel assembly. *J. Bacteriol.* **199,** 1–11 CrossRef Medline
381. Hart, E. M., Gupta, M., Wühr, M., and Silhavy, T. J. (2019) The synthetic phenotype of ΔbamB ΔbamE double mutants results from a lethal jamming of the Bam complex by the lipoprotein RcsF. *MBio* **10,** 1–12 CrossRef Medline
382. Tata, M., and Konovalova, A. (2019) Improper coordination of BamA and BamD results in Bam complex jamming by a lipoprotein substrate. *MBio* **10,** e00660-19 CrossRef Medline
383. Warner, L. R., Gatzeva-Topalova, P. Z., Doerner, P. A., Pardi, A., and Sousa, M. C. (2017) Flexibility in the periplasmic domain of BamA is important for function. *Structure* **25,** 94–106 CrossRef Medline
384. Höhr, A. I. C., Lindau, C., Wirth, C., Qiu, J., Stroud, D. A., Kutik, S., Guiard, B., Hunte, C., Becker, T., Pfanner, N., and Wiedemann, N. (2018) Membrane protein insertion through a mitochondrial β-barrel gate. *Science* **359,** eaah6834 CrossRef Medline
385. Kutik, S., Stojanovski, D., Becker, L., Becker, T., Meinecke, M., Krüger, V., Prinz, C., Meisinger, C., Guiard, B., Wagner, R., Pfanner, N., and Wiedemann, N. (2008) Dissecting membrane insertion of mitochondrial β-barrel proteins. *Cell* **132,** 1011–1024 CrossRef Medline
386. Paramasivam, N., Habeck, M., and Linke, D. (2012) Is the C-terminal insertional signal in Gram-negative bacterial outer membrane proteins species-specific or not? *BMC Genomics* **13,** 510 CrossRef Medline
387. Gruss, F., Zähringer, F., Jakob, R. P., Burmann, B. M., Hiller, S., and Maier, T. (2013) The structural basis of autotransporter translocation by TamA. *Nat. Struct. Mol. Biol.* **20,** 1318–1320 CrossRef Medline
388. Noinaj, N., Rollauer, S. E., and Buchanan, S. K. (2015) The β-barrel membrane protein insertase machinery from Gram-negative bacteria. *Curr. Opin. Struct. Biol.* **31,** 35–42 CrossRef Medline
389. Schiffrin, B., Brockwell, D. J., and Radford, S. E. (2017) Outer membrane protein folding from an energy landscape perspective. *BMC Biol.* **15,** 123 CrossRef Medline
390. Wang, Y., Wang, R., Jin, F., Liu, Y., Yu, J., Fu, X., and Chang, Z. (2016) A supercomplex spanning the inner and outer membranes mediates the biogenesis of β-barrel outer membrane proteins in bacteria. *J. Biol. Chem.* **291,** 16720–16729 CrossRef Medline
391. Alvira, S., Watkins, D. W., Troman, L., Lorriman, J., Daum, B., Gold, V. A. M., and Collinson, I. (2019) Trans-membrane association of the Sec and BAM complexes for bacterial outer-membrane biogenesis. *bioRxiv* CrossRef CrossRef
392. Carlson, M. L., Stacey, R. G., Young, J. W., Wason, I. S., Zhao, Z., Rattray, D. G., Scott, N., Kerr, C. H., Babu, M., Foster, L. J., and Duong Van Hoa, F. (2019) Profiling the *Escherichia coli* membrane protein interactome captured in Peptidisc libraries. *Elife* **8,** e46615 CrossRef Medline
393. Thoma, J., Manioglu, S., Kalbermatter, D., Bosshart, P. D., Fotiadis, D., and Müller, D. J. (2018) Protein-enriched outer membrane vesicles as a native platform for outer membrane protein studies. *Commun. Biol.* **1,** 23 CrossRef Medline
394. Thoma, J., Sun, Y., Ritzmann, N., and Müller, D. J. (2018) POTRA domains, extracellular lid, and membrane composition modulate the conformational stability of the β-barrel assembly factor BamA. *Structure* **26,** 987–996.e3 CrossRef Medline
395. Thoma, J., and Burmann, B. M. (2020) High-resolution *in situ* NMR spectroscopy of bacterial envelope proteins in outer membrane vesicles. *Biochemistry* **59,** 1656–1660 CrossRef Medline
396. Yang, J., and Zhang, Y. (2015) I-TASSER server: new development for protein structure and function predictions. *Nucleic Acids Res.* **43,** W174–W181 CrossRef Medline
397. Chorev, D. S., Baker, L. A., Wu, D., Beilsten-Edmands, V., Rouse, S. L., Zeev-Ben-Mordehai, T., Jiko, C., Samsudin, F., Gerle, C., Khalid, S., Stewart, A. G., Matthews, S. J., Grünewald, K., and Robinson, C. V. (2018) Protein assemblies ejected directly from native membranes yield complexes for mass spectrometry. *Science* **362,** 829–834 CrossRef Medline
398. Booth, P. J., and Curnow, P. (2009) Folding scene investigation: membrane proteins. *Curr. Opin. Struct. Biol.* **19,** 8–13 CrossRef Medline
399. Robert, V., Volokhina, E. B., Senf, F., Bos, M. P., Van Gelder, P., and Tommassen, J. (2006) Assembly factor Omp85 recognizes its outer membrane protein substrates by a species-specific C-terminal motif. *PLos Biol.* **4,** e377 CrossRef Medline
400. Arora, A., Abildgaard, F., Bushweller, J. H., and Tamm, L. K. (2001) Structure of outer membrane protein A transmembrane domain by NMR spectroscopy. *Nat. Struct. Biol.* **8,** 334–338 CrossRef Medline
401. Ishida, H., Garcia-Herrero, A., and Vogel, H. J. (2014) The periplasmic domain of *Escherichia coli* outer membrane protein A can undergo a localized temperature dependent structural transition. *Biochim. Biophys. Acta* **1838,** 3014–3024 CrossRef Medline
402. Baltoumas, F. A., Hamodrakas, S. J., and Iconomidou, V. A. (2019) The Gram-negative outer membrane modeler: automated building of lipopolysaccharide-rich bacterial outer membranes in four force fields. *J. Comput. Chem.* **40,** 1727–1734 CrossRef Medline
403. Tomasek, D., Rawson, S., and Lee, J., Wzorek, J. S., Harrison, S. C., Li, Z., and Kahne, D. (2020) Structure of a nascent membrane protein as it folds on the BAM complex. *Nature* CrossRef Medline